

Republic of Iraq  
Ministry of Higher Education and Scientific Research  
University of Technology  
Laser and Optoelectronics Engineering Department



# ***ENERGY DISTRIBUTION OF APODIZED LASER BEAM IN ANNULAR SYSTEM.***

A Thesis Submitted to the  
Laser and Optoelectronics Engineering Department, University of  
Technology in a Partial Fulfillment of the Requirements for the  
Degree of Master of Science in Optoelectronics Engineering

By

***Thanaa Hussein Abed Al-Bedary***

Supervisor

***Ass.Prof.Dr. Ali H.Al-Hamdani***



جمهورية العراق  
وزارة التعليم العالي والبحث العلمي  
الجامعة التكنولوجية  
قسم هندسة الليزر والبصريات الالكترونية

# توزيع طاقة حزمة الليزر المُحَسَّن

## في نظام بصري حلقي

رسالة مقدمة الى

قسم هندسة الليزر والبصريات الالكترونية الجامعة التكنولوجية  
كجزء من متطلبات نيل درجة الماجستير علوم في هندسة البصريات  
الالكترونية  
تقدم بها

ثناء حسين عبدالبديري

بإشراف

الدكتور علي هادي عبد المنعم

# Supervisor Certification

I certify that this thesis entitled (**Energy Distribution of Apodized Laser Beam in Annular System**) was prepared by (*Thanaa Hussein Abed Al-Bedary*) under my supervision at the Laser and Optoelectronics Engineering Department, University of Technology in a partial fulfillment of the requirements for the degree of Master of Science in Optoelectronics Engineering

Signature:

Supervisor: Assist Professor

**Dr. Ali H.Al-Hamdani**

Date:    /    /2007

In view of the available recommendation, I forward this thesis for debate the examination committee.

Signature:

Name: Dr.Sabah A.Dhahir

Title: Lecturer

Date:    /    /2007

Department of Laser and Optoelectronics Engineering

# **Certification of the Linguistic Supervisor**

I certify that this thesis entitled (**Energy Distribution of Apodized Laser Beam in Annular System**) was prepared under my linguistic supervision.

Its language was amended to meet the style of the English Language

Signature:

Name: Mohamed S. Ahmed

Title: Assist Professor

Date:    /    /2007

**Abstract**

Optical systems generally have a circular pupil and the imaging elements of such systems have a circular boundary. Hence they also represent circular pupil in fabrication and testing. Such that is not always, an example of system with non-circular pupil, is a Cassegranian telescope, which has an annular pupil.

For system with annular pupil the aberration, and the variance over annular is different from that of circular pupil. Also the amount of defocus that balances spherical aberration, which yields minimum variance over annular pupil, is different from that for circular aperture.

Although in many imaging applications the amplitude across pupil is uniform but this is not always the case, for example in system with an apodized pupil. An example of an apodized pupil is a Gaussian pupil when the amplitude across the pupil has the form of Gaussian due to either an amplitude filter placed at the pupil or the wave incident on the pupil being Gaussian as in the case of Gaussian beams. Also the variance and the balance, for Gaussian pupil have a form that is different from the corresponding balanced aberrations for a uniform pupil.

In this research various an apodized Gaussian filters are placed at the pupil of an annular system and different obstruction ratio ( $\epsilon$ ) of the secondary mirror ( $\epsilon = 0, 0.1, 0.2, 0.3, 0.4, 0.5, 0.6, 0.7, 0.8$ , and  $0.9$ ) are used.

A formula for the point spread function for the annular system was derived and numerically evaluated by using Gaussian quadrature method. A programme in Q.Basic language has been written to calculate the point spread function, for different obstruction ratio and different amount of aberrations. The results show the great dependence of the point spread function and Strehl ratio on the type of Gaussian filter and the amount of aberration in the annular optical systems.

# ***CONTENTS***

Seq.	<i>Contents</i>	Page
	Acknowledgment	I
	Abstract	II
	List of Symbols	III
	Creek symbols	IV
	Contents	V
<i>Chapter One: General Introduction</i>		
1.1	Introduction	1
1.2	Lens Testing	2
1.2.1	Qualitative Test	2
1.2.2	Quantitative Test	3
1.2.2.1	Visible Test	3
1.2.2.2	The Photometer Test	4
1.3	Diffraction	5
1.4	Aberration	7
1.4.1	Monochromatic Aberration	7
1.4.1.1	Spherical Aberration	8
1.4.1.2	Coma	9
1.4.1.3	Astigmatism	10
1.4.1.4	Field Curvature	11
1.4.1.5	Distortion	13
1.4.2	Chromatic Aberrations	13
1.5	Strehl Ratio	14
1.6	Aberration Balancing	17
1.7	Resolution of Optical System	18
1.8	Focus Error	19
1.9	Depth of Focus	20
1.10	Literature Survey	20
1.11	Aim of this Work	22

## *Chapter Two: Point Spread Function*

2.1	Introduction	23
2.2	Point Spread Function (PSF)	23
2.2.1	PSF for Circular Aperture	27
2.2.1.1	PSF for A Diffraction-Limited System	27
2.2.1.2	PSF with Focus Error	29
2.2.1.3	PSF with Third Order Spherical Aberration	31
2.3	Annular Aperture	32
2.3.1	PSF of Annular Aperture for a Diffraction-Limited System	33
2.3.2	PSF of Annular Aperture with Focus Error	35
2.3.3	PSF of Annular Aperture with Focus Error and Spherical Aberration	36
2.4	Apodization	37
2.4.1	Apodization of Annular Aperture for a Diffraction-Limited System	39
2.4.2	Apodization Of The Annular Aperture With Focus Error	40
2.4.3	Apodization Of The Annular Aperture With Focus Error and Spherical Aberration	41

## *Chapter Three: Numerical Evaluation*

3.1	Introduction	43
3.2	Gaussian Method	43
3.3	Numerical Evaluation of PSF	45
3.3.1	Numerical Evaluation of A Diffraction-Limited Optical System	45
3.3.2	Numerical Evaluation of PSF for Optical System Contained Focus Error	46
3.3.3	Numerical Evaluation of PSF for Optical System Contained Third Order Spherical Aberration	46
3.4	Numerical Evaluation of PSF for Optical System Contained Annular Aperture	46
3.4.1	Numerical Evaluation of PSF for a Diffraction-Limited Optical System Contained Annular Aperture	46
3.4.2	Numerical Evaluation of PSF for Annular Aperture Optical System with Focus Error	47

3.4.3	Numerical Evaluation of PSF for Annular Aperture Optical System Contained Third Order Spherical Aberration	47
3.5	Numerical Evaluation of PSF for Optical System Contain Apodized Annular Aperture	48
3.5.1	Numerical Evaluation of PSF for a Diffraction-Limited Optical System Contain Apodized Annular Aperture	48
3.5.2	Numerical Evaluation of PSF for Optical System Contained Apodized Annular Aperture with Focus Error	48
3.5.3.	Numerical Evaluation of PSF for Optical System Contained Apodized Annular Aperture with Third Order Spherical Aberration	49
3.6	The Programs	50
<b><i>Chapter Four: Results &amp; Discussions</i></b>		
4.1	Introduction	52
4.2	Effect of the Obstruction Ratio on the Free Optical System	52
4.3	Effect of the Obstruction on the Optical System Contained Focus Error ( $W_{20}=0.25, 0.5) \lambda$	53
4.4	Effect of the Width Factor of Super Gaussian Filter on Strehl Ratio for Free Optical System without an Obstruction	55
4.5	Effect of the Width Factor of Super Gaussian Filter on Resolution of the Free Optical System without an Obstruction	56
4.6	Effect of the Width Factor of Super Gaussian Filter on Strehl Ratio for the Optical System Contains Focus Error ( $W_{20}= 0.25, 0.5, \& 0.75) \lambda$	57
4.7	Effect of the Width Factor of Super Gaussian Filter on the Resolution of the Optical System Contained Focus Error ( $W_{20}= 0.25, 0.5, \& 0.75) \lambda$	60
4.8	Effect of the Width Factor of Super Gaussian Filter on the Resolution of the Optical System Contained Spherical Aberration ( $W_{40}=0.1, 0.3, 0.5, 0.7, \& 0.9) \lambda$	62
4.9	Effect of the Width Factor of Super Gaussian Filter on the Strehl Ratio for the Optical System Contained Spherical Aberration ( $W_{40}=0.1, 0.3, 0.5, 0.7, \& 0.9) \lambda$	65



4.10	Effect of the Width Factor of Super Gaussian Filter on Strehl Ratio for the Optical System Contained Optimum Balance Values ( $W_{20}=-1$ , $W_{40}=1$ ) $\lambda$	67
4.11	Effect of the Width Factor of Super Gaussian Filter on Strehl Ratio for the Obstructed Optical System Contained Optimum Balance Values	68
4.12	Effect of the Width Factor of Super Gaussian Filter on Strehl Ratio for the Free Optical System Contains Obstruction Ratio with Difference Values ( $\epsilon=0.2$ , 0.5, & 0.8)	70
4.13	Effect of the Width Factor of Super Gaussian Filter on Strehl Ratio for Obstructed Optical System ( $\epsilon=0.2$ ) Contains Focus Error ( $W_{20}=0.25$ , 0.5, & 0.75) $\lambda$	72
4.14	Effect of the Width Factor of Super Gaussian Filter on Strehl Ratio for the Obstructed Optical System ( $\epsilon=0.5$ ) Contains Focus Error ( $W_{20}=0.25$ , 0.5, & 0.75) $\lambda$	74
4.15	Effect of the Width Factor of Super Gaussian Filter on Strehl Ratio for the Obstructed Optical System ( $\epsilon=0.8$ ) Contains Focus Error ( $W_{20}=0.25$ , 0.5, & 0.75) $\lambda$	75
4.16	Effect of the Width Factor of Super Gaussian Filter on Strehl Ratio for the Obstructed Optical System ( $\epsilon=0.2$ ) Contains Spherical Aberration ( $W_{40}=0.1$ , 0.3, 0.5, 0.7, & 0.9) $\lambda$	77
4.17	Effect of the Width Factor of Super Gaussian Filter on Strehl Ratio for Obstructed Optical System ( $\epsilon=0.5$ ) Contains Spherical Aberration ( $W_{40}=0.1$ , 0.3, 0.5, 0.7, & 0.9) $\lambda$	79
4.18	Effect of the Width Factor of Super Gaussian Filter on Strehl Ratio for the Obstructed Optical System ( $\epsilon=0.8$ ) Contains Spherical Aberration ( $W_{40}=0.1$ , 0.3, 0.5, 0.7, & 0.9) $\lambda$	81
4.19	Conclusions	84
4.20	Suggestions for Future Work	85
<i>References</i>		86
<i>Appendixes</i>		
Appendix (A)		91
Appendix (B)		93

Program to calculate PSF for free optical system.

```

REM *****
CLS
PRINT "    POINT SPREAD FUNCTION PSF "
PRINT "    ANNULAR APERTURE "
PRINT "    FREE SYSTEM ABERATIONS "
PRINT
PRINT " BEGIN CALCULATIONS..."
' ***** DEFINE CONSTANT
  PI = 3.14159265#
  KK = 2 * PI
  A = SQR(PI) / 2
  N = 20
20  DIM T(N), W(N)
  RESTORE 80
  FOR I = 1 TO 20
  READ T(I), W(I)
  NEXT I
' ***** BEGIN
  INPUT "ENTER FILE NAME WITH [ *.DAT ] :", NA$
  OPEN NA$ FOR OUTPUT AS #1
  INPUT " Abscuration Ratio E :", E
  INPUT " Zmin , Zmax , STEP :", Z0, Z1, ST
  PRINT "Wait..."
  w20 = 0
  W40 = 0
  bz1 = 9.8708048#
  Z = Z0
36  SJ = 0: CJ = 0
  FOR J = 1 TO N
  YJ = T(J)
  RJ = SQR(1 - YJ ^ 2)
38  SI = 0: CI = 0
  FOR I = 1 TO N
  XI = T(I) * RJ
  R = XI ^ 2 + YJ ^ 2
  ARG = Z * XI + (2 * PI * (w20 * R + W40 * R ^ 2))
  CS = COS(ARG)
  SS = SIN(ARG)
  SI = SI + SS * W(I)
  CI = CI + CS * W(I)
  NEXT I
  SJ = SJ + SI * W(J) * RJ
  CJ = CJ + CI * W(J) * RJ
  NEXT J
  SQ = SJ: CQ = CJ
' *****
46  SJ = 0: CJ = 0
  FOR J = 1 TO N
  YJ = T(J) * E

```

```

RJ = SQR(E ^ 2 - YJ ^ 2)
48  SI = 0: CI = 0
FOR I = 1 TO N
  XI = T(I) * RJ
  R = XI ^ 2 + YJ ^ 2
  ARG = Z * XI + (2 * PI * (w20 * R + W40 * R ^ 2))
  CS = COS(ARG)
  SS = SIN(ARG)
  SI = SI + SS * W(I)
  CI = CI + CS * W(I)
NEXT I
SJ = SJ + SI * W(J) * RJ * E
CJ = CJ + CI * W(J) * RJ * E
NEXT J
SB = SJ: CB = CJ
49  PSF = ((SQ - SB) ^ 2 + (CQ - CB) ^ 2) / bz1
PRINT "Z="; Z; " G(Z)="; USING "#.#####"; PSF
PRINT #1, Z; " "; PSF
IF Z >= Z1 THEN 50
Z = Z + ST
GOTO 36
50  PRINT " _____"
PRINT " W20="; w20, "W40="; W40, "W60="; W60, "Norm="; NORM
FOR I = 1 TO 20
  PRINT #1, T(I), W(I)
NEXT I
CLOSE #1
END
' ***** GAUSS POINTS & WEIGHTS DATA

80  DATA 0.9931286, 0.01761401 ,0.9639719
DATA 0.04060143 , 0.9122344, 0.06267205
DATA 0.8391169,0.08327674 ,0.7463319
DATA 0.1019301, 0.6360536 , 0.1181945
DATA 0.510867, 0.1316886 , 0.3737061
DATA 0.1420961 , 0.2277858, 0.149173
DATA 0.07652652, 0.1527534 , -0.07652652
DATA 0.1527534 , -0.2277858, 0.149173
DATA -0.3737061, 0.1420961 , -0.510867
DATA 0.1316886, -0.6360536, 0.1181945
DATA -0.7463319, 0.1019301, -0.8391169
DATA 0.08327674, -0.9122344, 0.06267205
DATA -0.9639719, 0.04060143, -0.9931286
DATA 0.01761401

```

Program to calculate PSF for obstruction optical system with super Gaussian filter.

```
REM *****
CLS
PRINT "      POINT SPREAD FUNCTION PSF "
PRINT "      ANNULAR APERTURE "
PRINT "      FREE SYSTEM ABERATIONS "
PRINT
PRINT " BEGIN CALCULATIONS..."
' ***** DEFINE CONSTANT
  PI = 3.14159265#
  KK = 2 * PI
  a = SQR(PI) / 2
  N = 20
20 DIM T(N), W(N)
  RESTORE 80
  FOR I = 1 TO 20
    READ T(I), W(I)
  NEXT I
' ***** BEGIN
  INPUT "ENTER FILE NAME WITH [ *.DAT ] :", NA$
  OPEN NA$ FOR OUTPUT AS #1
  INPUT " Abscuration Ratio E :", E
  INPUT " a Factor : ", aa
  INPUT " Zmin , Zmax , STEP :", Z0, Z1, ST
  PRINT "Wait..."
  W20 = 0
  W40 = 0
  bz1 = 9.8708048#
  Z = Z0
36 SJ = 0: CJ = 0
  FOR J = 1 TO N
    YJ = T(J)
    RJ = SQR(1 - YJ ^ 2)
38 SI = 0: CI = 0
    FOR I = 1 TO N
      XI = T(I) * RJ
      filter = EXP(-XI * XI / (aa * aa))
      R = XI ^ 2 + YJ ^ 2
      ARG = Z * XI + (2 * PI * (W20 * R + W40 * R ^ 2))
      CS = COS(ARG) * filter
      SS = SIN(ARG) * filter
      SI = SI + SS * W(I)
      CI = CI + CS * W(I)
    NEXT I
    SJ = SJ + SI * W(J) * RJ
    CJ = CJ + CI * W(J) * RJ
  NEXT J
  SQ = SJ: CQ = CJ
  REM      PRINT SJ, CJ
```

```

' *****
46  SJ = 0: CJ = 0
    FOR J = 1 TO N

        YJ = T(J) * E
        RJ = SQR(E ^ 2 - YJ ^ 2)
48  SI = 0: CI = 0
    FOR I = 1 TO N
        XI = T(I) * RJ
        filter = EXP(-XI * XI / (aa * aa))
        R = XI ^ 2 + YJ ^ 2
        ARG = Z * XI + (2 * PI * (W20 * R + W40 * R ^ 2))
        CS = COS(ARG) * filter
        SS = SIN(ARG) * filter
        SI = SI + SS * W(I)
        CI = CI + CS * W(I)
    NEXT I
    SJ = SJ + SI * W(J) * RJ * E
    CJ = CJ + CI * W(J) * RJ * E
    NEXT J
    SB = SJ: CB = CJ
49  PSF = ((SQ - SB) ^ 2 + (CQ - CB) ^ 2) / bz1
    PRINT "Z ="; Z; " G(Z)="; USING "#.#####"; PSF
    PRINT #1, Z; " "; PSF
    IF Z >= Z1 THEN 50
    Z = Z + ST
    GOTO 36
50  PRINT " _____"
    PRINT " W20 ="; W20, "W40 ="; W40, "W60 ="; W60, "Norm="; NORM
    FOR I = 1 TO 20
        PRINT #1, T(I), W(I)
    NEXT I
    CLOSE #1
    END
' ***** GAUSS POINTS & WEIGHTS DATA

80  DATA 0.9931286, 0.01761401 ,0.9639719
    DATA 0.04060143 , 0.9122344, 0.06267205
    DATA 0.8391169,0.08327674 ,0.7463319
    DATA 0.1019301, 0.6360536 , 0.1181945
    DATA 0.510867, 0.1316886 , 0.3737061
    DATA 0.1420961 , 0.2277858, 0.149173
    DATA 0.07652652, 0.1527534 , -0.07652652
    DATA 0.1527534 , -0.2277858, 0.149173
    DATA -0.3737061, 0.1420961 , -0.510867
    DATA 0.1316886, -0.6360536, 0.1181945
    DATA -0.7463319, 0.1019301, -0.8391169
    DATA 0.08327674, -0.9122344, 0.06267205
    DATA -0.9639719, 0.04060143, -0.9931286
    DATA 0.01761401

```

# *Chapter one*

## *General Introduction*

### *1.1 Introduction*

The production and industrialization of the optical system pass through several stages, the optical design is the first one, after this stage is completed, the optical components industrialization will be the next stage and then, the evaluation and the testing of these components will be the last stage before the lens is being used.

The optical design include specification of the radii of the surfaces curvature, the thickness, the air spaces, the diameters of the various components, the type of glass to be used and the position of the stop. These parameters are known as "*degrees of freedom*" since the designer can change them to maintain the desired system.

The image that is formed by these optical systems will be approximately corrected from the aberrations. But there isn't ideal image correspond to the object dimensions because of the wave nature of the light, which almost affects with several factors like the type of illumination that be used (*incoherent, coherent and partial coherent*), the object shape (*Point, Line or Edge*) and the aperture shape [1].

There are several factors that affect the evaluation of the image quality which is formed by the optical system, from these important factors that effect on evaluation of the image quality, measured spread function (*Point, Line and Edge*) [1,2,3] which represents descriptions of the intensity distribution in image plane for an object (*Point, Line and Edge*). The spread function depends on diffraction that produces by the lens aperture and the amount of the aberrations and its type in lens or in the optical system. The point spread function is an important parameter that is used for identification the efficiency of the optical system, where several of the

other functions are derived from the point spread function or in differential relation or integral relation with it.

## **1.2 Lens Testing**

There are generally three basic reasons for carrying out series of test on lenses:

1. To determine if the lens is suitable for a given purpose.
2. To determine whether a lens which has been constructed fulfills the design characteristics.
3. To study the limitation on accuracy of optical imagery and the relation among various methods of assessing image quality [4].

There are two ways to test the lenses and optical systems.

### **1.2.1 Qualitative Test**

By the qualitative test we have the ability to know the type of aberrations in the tested lens, without measuring it, and the **star test** is classified under the qualitative test ways. In the **star test** a collimator used to produce plane waves and fall directly on the tested lens. The image formed by the tested lens is examined through a microscope as show in the figure (1-1). The lens rotates around it axis through the test. To examine the decentering aberrations and asymmetric aberrations in the point image. If the tested lens is perfect the observer sees bright circular surround by several ring rapidly diminishing brightness which called Airy pattern [5]. This process of examination managed us for deduction on some aberrations which reach to  $(1/10)$  from the wavelength that be used.

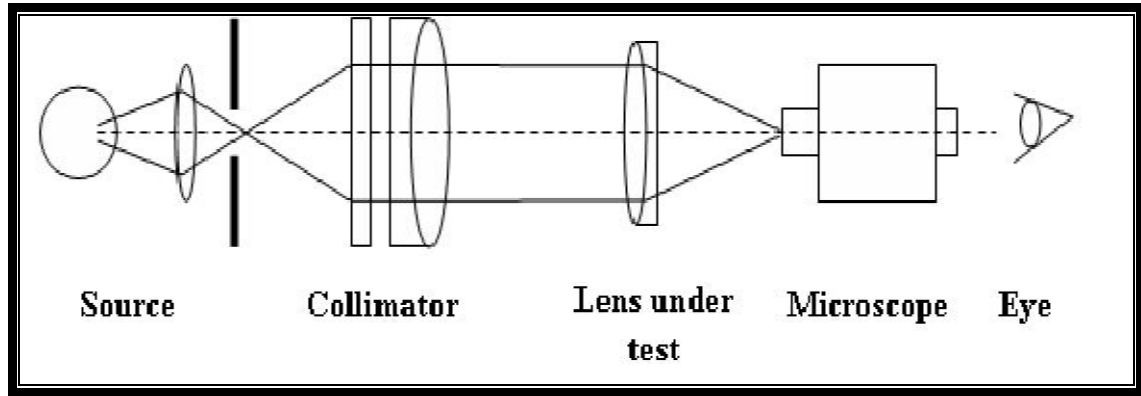


Figure (1-1), star test

In this process we use the human eye which is practically a good detector for asymmetric and for the change in the form, but it can not show us the exact difference value of the intensity and the distance between the fringes.

### 1.2.2 Quantitative Test

The Quantitative test is divided in two types:

#### 1.2.2.1 Visible Test

It is the test that contains all the required measurements that are designed on the basis principle of interference between the wave front coming from the lens through using ideal wave of mono wavelength from point source (the ideal wave is considered as a reference to the wave coming from the testing lens).

From the instruments that used for this purpose Twyman-Green interferometer [6] which is widely used in examination the lens and prisms, and the interferometer is a good instrument to know the amount of moving away from the ideal state, starting from  $(1/20) \lambda$  part from the wavelength until little wave length  $(3\lambda)$ . When the wavelength moving away for hundred wavelengths the interferometer will be useless. The Twyman-Green interferometer is essentially a variation of the Michelson



interferometer. It is an instrument of great importance in the domain of modern optical testing as shown in figure (1-2).

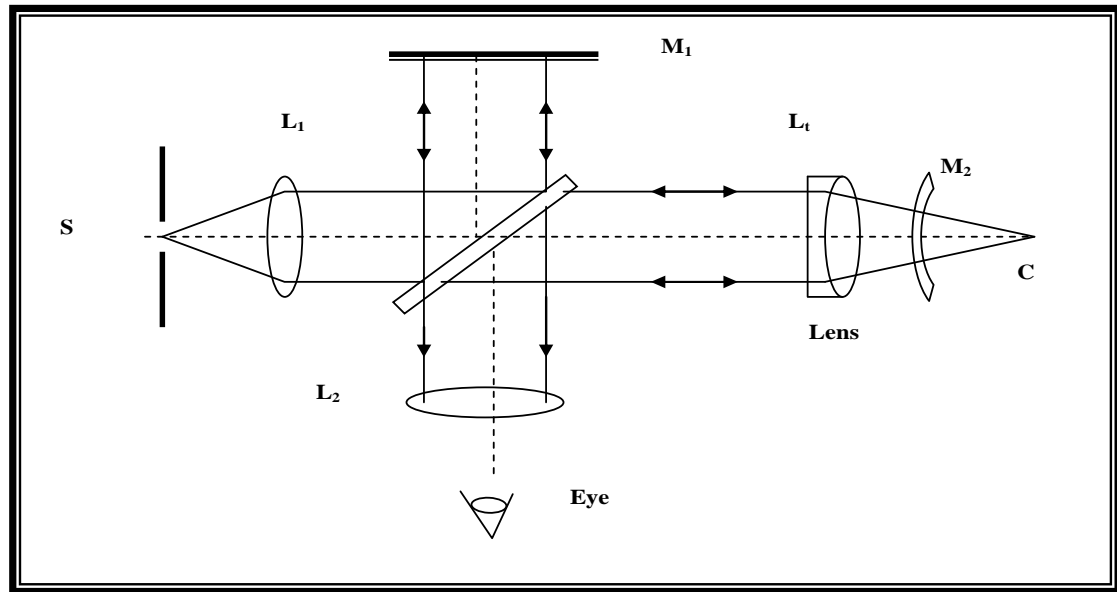


Figure (1-2): Twyman-Green interferometer [6]

This device is setup to examine lenses. This spherical mirror **M<sub>1</sub>** has its center of curvature tested is free of aberrations (which is usually plane mirror), the emerging reflected light returning to the beam splitter will again be plane wave. In case, an astigmatism, coma, or spherical aberrations deform, the waveform, fringe pattern will manifest these distortions and can be seen and photographed. When **M<sub>2</sub>** is replaced by plane mirror, a number of other elements (*primes, optical flats*) can be equally tested as well [7].

### 1.2.2.2 The Photometer Test

This way of examination includes the measurement of special function that explains the lens efficiency, its ideality, and the amount of aberrations that is present in it.

Some of these functions e.g. point spread functions (**PSF**), line spread function(**LSF**) , disk spread function (**DSF**)and other spread function that give good description of the intensity distribution in the image plane of an object by the optical system that be wanted to be examined. The spread

function depends on the aperture lens diffraction and the aberrations type and the amount of aberrations in the lens or in the optical components.

There is another important function which is used to examine the optical system like the optical transfer function (**OTF**). We can define the **OTF** as the ability of the optical system to transfer the different frequency from the object plane to the image plane as shown in figure (1-3) [8]. One of the other important functions used to evaluate the image specificity is the contrast transfer function (**MTF**):

$$MTF = \frac{I_{MAX} - I_{MIN}}{I_{MAX} + I_{MIN}} \quad (1-1)$$

where:

$I_{MAX}$  : represents the maximum intensity.

$I_{MIN}$  : represents the minimum intensity.

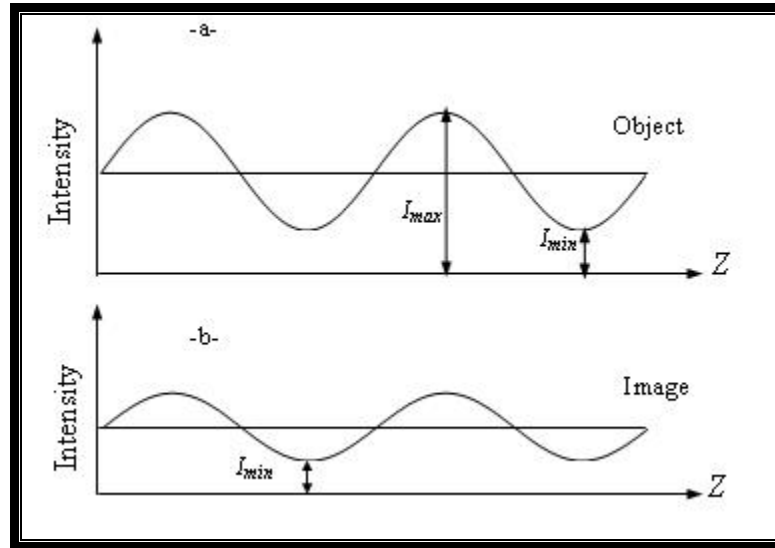


Figure (1-3): The optical transfer function [5]

### 1.3 Diffraction

Diffraction is a phenomena or effect resulting from the interaction of the radiation wave with the limiting edges of the aperture stop of optical system [5, 9]. Diffraction is a natural property of light arising from its wave nature, possesses fundamental limitation on any optical system. Diffraction is always present, although its effects may be made if the system has

significant aberrations. When an optical system is essentially free from aberrations, its performance is limited solely by diffraction, and it is referred to as diffraction-limited. The image of a point source formed by diffraction-limited optics is blurring, which appears as a bright central disk surrounded by several alternately bright dark rings [5,10,11]. This diffraction blur or Airy disk, named in honor of Lord George Biddell Airy; is one of those who analyzed the diffraction process. The energy distribution and the appearance of Airy disk are shown in figure (1-4).

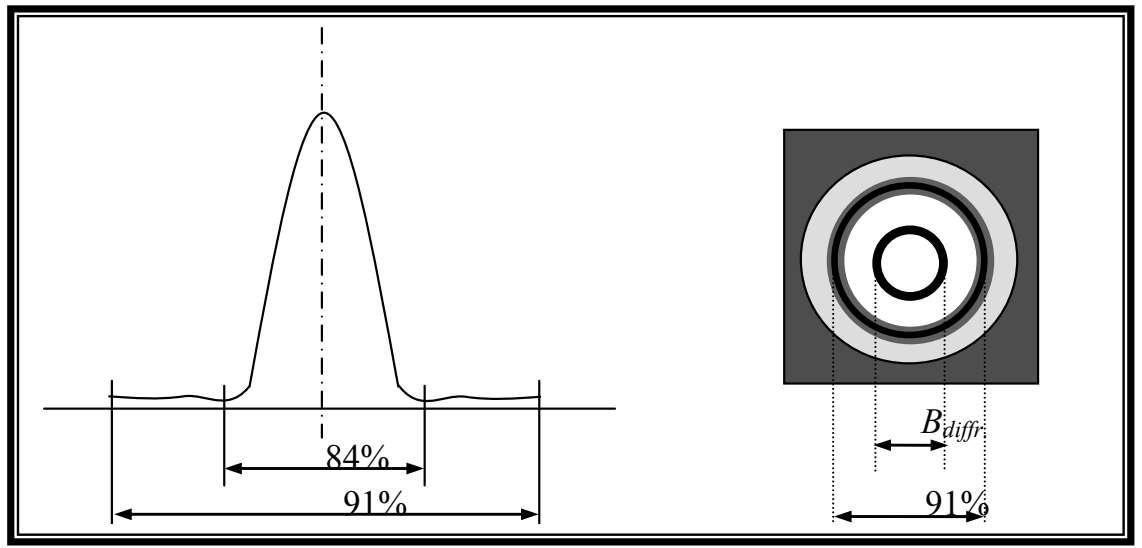


Figure (1-4): Airy disk, energy distribution and appearance [5].

If the aperture of the lens is circular, approximately (84%) of the energy from an image point energy is spread over the central disk and the rest is surrounding rings of the Airy pattern [5]. The angular diameter of Airy disk ( $B_{ang}$ ) which is assumed to be the diameter of the first dark ring is [5,10,12].

$$B_{ang} = 2.44 \lambda / D \quad (1-2)$$

The Airy disk diameter  $B_{diff}$  is then:

$$B_{diff} = B_{ang} f = 2.44 \lambda f / D = 2.44 \lambda (f / \#) \quad (1-3)$$

Where  $\lambda$  is light wavelength that is used. The angular diameter is expressed in radians if  $\lambda$  and  $D$  are in the same units. Since the blur size is

proportional to the wavelength as indicated in equation (1-3) the diffraction effect can often become the limiting factor for optical system.

### 1.4 Aberration

For a perfect lens and monochromatic point source the wave aberrations ( $Wa$ ) measure the optical path difference (OPD) of each ray compared with that of the principle ray [13].

The wave aberration polynomial in polar coordinates is [14]

$$Wa = W(\sigma^2, r^2, r \cos \phi) \quad (1-4)$$

$$Wa = \sum_i \sum_m \sum_j W_{mj} \sigma^i \cdot r^m \cdot \cos \phi \quad (1-5)$$

Where (i,m,j) represent the power of ( $\sigma$ ,  $r$ ,  $\cos \phi$ ) respectively [14]

Where

$r$ : represent the radius distance  $B'$ ,  $E'$  in exit plane

$\phi$ : the angle between the two variable  $x$ ,  $r$ .

$\sigma$ : represent the amount of principle ray high on the optical axis in the image plane.

#### 1.4.1 Monochromatic Aberration

The most important aberrations in the majority of application are **Seidel** aberrations [15]. The aberrations of any ray are expressed in terms of five sums  $S_1$  to  $S_5$  called **Seidel** sums [16]. **Seidel** was the first one who studied this type of aberration. If a lens is to be free of all defects all five of these sums would be of equal zero. No optical system can be made to satisfy all these conditions once. Therefore it is customary to treat each sum separately, and vanishing of certain once, thus, if for a given axial object point the **Seidel** sum  $S_1=0$ , there is no spherical aberration at the corresponding image point. If both  $S_1=0$  and  $S_2=0$ , the system will also be free of coma. If, in addition to  $S_1=0$  &  $S_2=0$  the sums  $S_3=0$  and  $S_4=0$  as well the images will be free of astigmatism and field curvature. If finally  $S_5$

could be made to vanish, there would be no distortion of the image. These aberrations are also known as the five monochromatic aberrations because they exist for any specified colour and refractive index. Additional image defects occur when the light contains various colours. We shall first discuss each of the monochromatic aberrations and then take up the chromatic effects.

#### ***1.4.1.1 Spherical Aberration***

In paraxial region (and with monochromatic light) all rays originating from an axial point again pass through a single point after traversing the system. This is not generally true for larger angle of divergence; different zones of the aperture have different focal length, depending on their distance from the axis. This difference called spherical aberration when the separation of these foci is taken as a measurement of the aberration, it is referred to as longitudinal, and where the accompanying spread in the image point is referred to as transverse aberration [4]. The primary spherical aberration seen in figure (1-5).

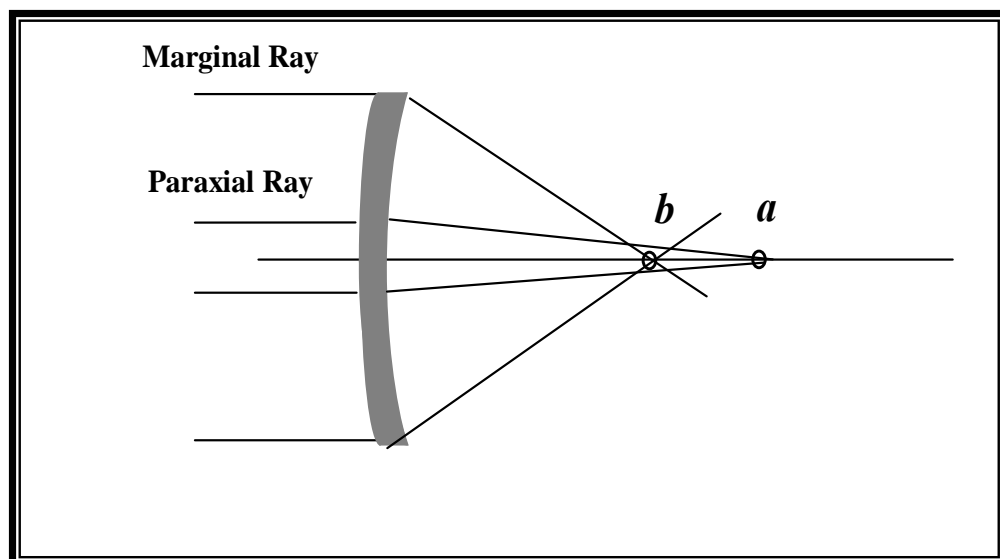


*Figure (1-5): Spherical aberration [5]*

The algebraic formulation of spherical aberration which is even and rotationally symmetric.

Figure (1-6): Coma aberration [5]

The ray at the upper edge of the lens has higher angle of incidence with the curved surface than the ray at the lower edge. The deflection of the upper ray will be greater, and it will intersect the chief ray closer to the lens than the ray from the lower edge [13].

Coma is un rotated axis and given as [14]:-

$$W = \sum_{m=odd} {}_1W_{m1} \sigma r^m \cos \phi = {}_1W_{31} \sigma r^3 \cos \phi + {}_1W_{51} \sigma r^5 \cos \phi + \dots \quad (1-9)$$

In cartesian coordinates the above equation will become as:

$$W(x', y') = {}_1W_{31} (x'^2 + y'^2) y' + {}_1W_{51} (x'^2 + y'^2)^2 y' + \dots \quad (1-10)$$

If the axis is rotated by angle  $\psi$  then the coordinates becomes [14]:

$$\begin{aligned} x' &= x \cos \psi - y \sin \psi \\ y' &= x \sin \psi + y \cos \psi \end{aligned} \quad (1-11)$$

then the equation (1-10) takes the form

$$W(x', y') = {}_1W_{31} (x'^2 + y'^2) (x' \sin \psi + y' \cos \psi) + {}_1W_{51} (x'^2 + y'^2)^2 (x' \sin \psi + y' \cos \psi) + \dots \quad (1-12)$$

Where:

$W(x', y')$ : represents the aberration polynomial.

Coma can be controlled by the lens curvature and for an object of no limits the condition to eliminate coma completely are given in [4, 19]:-

$$r_1 = \frac{(n^2 - 1)f}{n^2}, \quad r_2 = \frac{(n^2 - 1)f}{(n^2 - n - 1)} \quad (1-13)$$

### 1.4.1.3 Astigmatism

The word (Astigmatism) is derived from the Greek a-means not, and stigma means spot or point [12]. When a narrow beam of light is obliquely incident on reflecting surface, astigmatism is introduced and the image of the point source is formed by small lens aperture becomes a pair of focal lines. Astigmatism in Cartesian is given by [14]:

$$W(x', y') = W_{22}(x^2 \sin^2 \psi + y^2 \cos^2 \psi + xy \sin^2 \psi) \quad (1-14)$$

Astigmatism is off-axis and asymmetric aberration and it is controlled by lens curvature, by choosing the refractive indexes of the lens components, and by which the location of the iris and the refractive surfaces are selected, Astigmatism shown in figure (1-7).

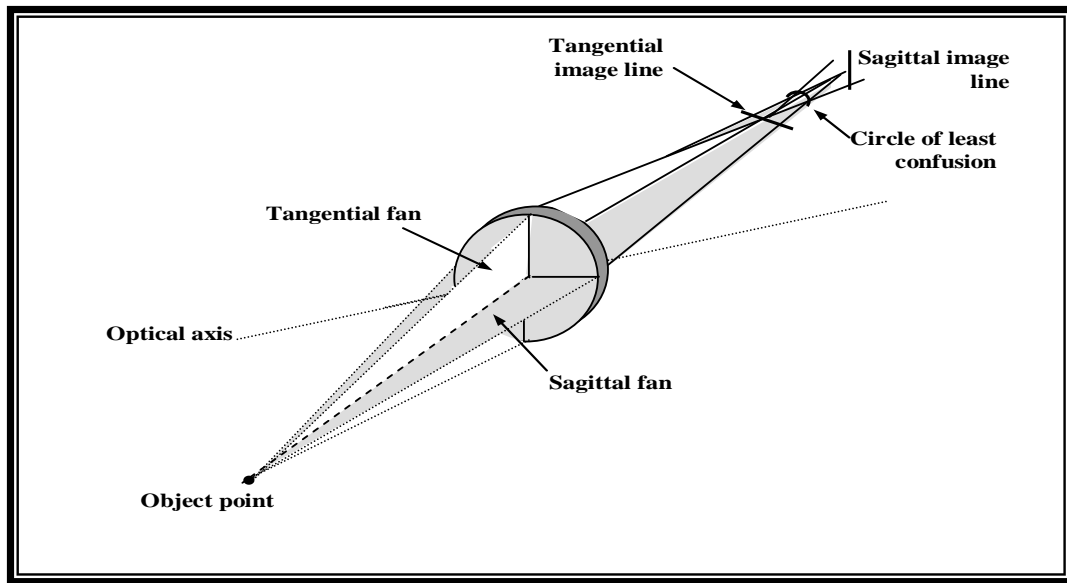


Figure (1-7): Astigmatism aberration [5].

#### 1.4.1.4 Field Curvature

When a plane surface, normal to the optical axis is imaged by a lens, in which all the above aberrations have been eliminated, the image will not be plane but will lie on curved surface, This image defect is known as curvature of the field, figure(1-8)[13].



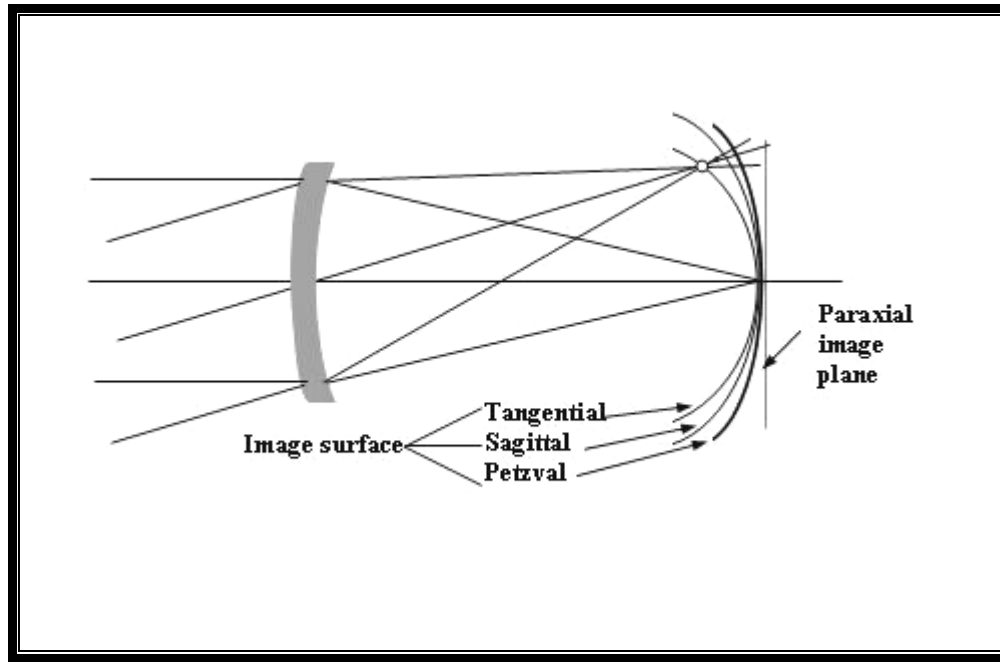


Figure (1-8): Field curvature aberration [5].

Field curvature is given by

$$W = W_2 W_{20} \sigma^2 r^2 + \dots \quad (1-15)$$

To minimize the aberration relatively strong negative element of low-index glass, it can be combined with positive elements of high-index glass. The positive and negative elements must be axially separated to provide the lens with useful amount of positive power.

### 1.4.15 Distortion

Distortion is produced when the chief rays intersect the image surface at heights different from those predicted by the paraxial approximation. The case of pincushion and barrel distortion is shown in figure (1-9) [4, 13].

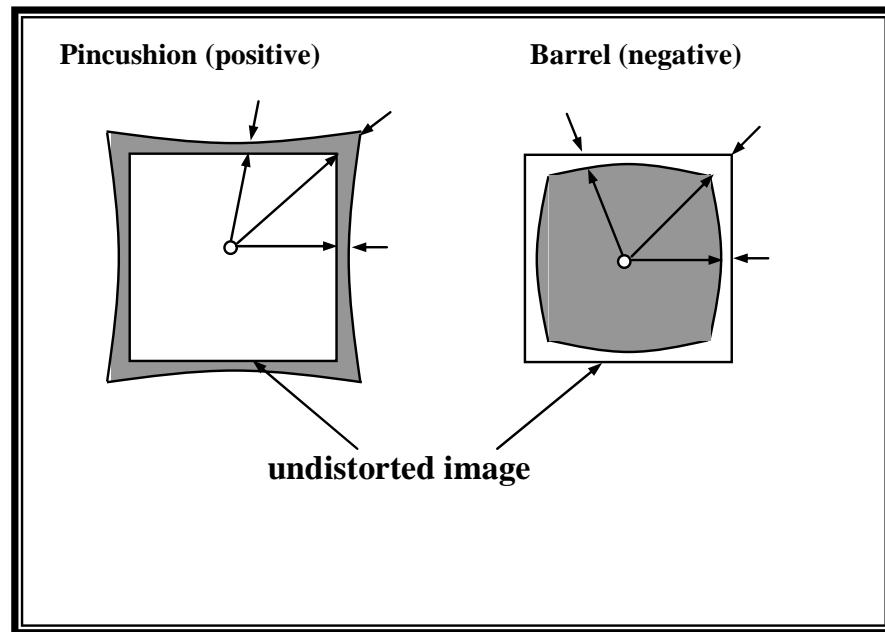


Figure (1-9): Distortion aberration [5].

Distortion is given by:

$$W = {}_3W_{11} \sigma^3 \cos \phi + \dots \quad (1-16)$$

Distortion is sensitive to lens shaping, spacing and iris position and its elimination may require skilful manipulation of these Parameters.

### 1.4.2 Chromatic Aberrations

The presence of material dispersion causes the refractive index to vary with wavelength [20]. The aberrations previously described are purely functional of the shape of the lens surface, and can be observed with monochromatic light. There are however other aberrations that arise when this optics is used to transform light containing multiple wavelengths. Chromatic aberrations caused by variation in the index of refraction of the lens material with wavelength. The first two chromatic errors are variation

of the paraxial image plane position and image height with wavelength. These are known respectively as longitudinal axial and lateral chromatic. Figure (1-10) illustrates these two types of aberrations.

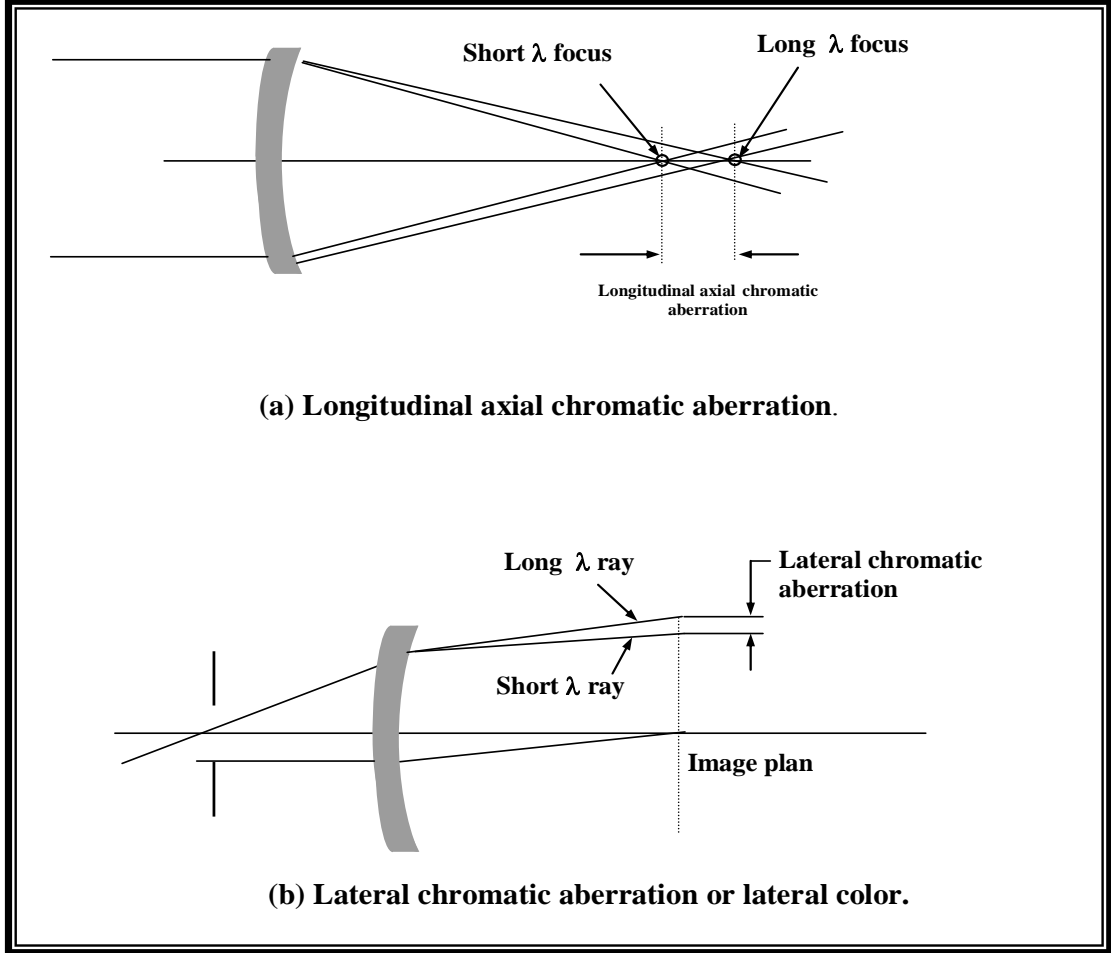


Figure (1-10): Chromatic aberration [5].

Chromatic aberration is given by [14]:

$$W = {}_1W_{11}B_r \cdot \cos \theta + {}_0W_{20}r^2 \quad (1-17)$$

### 1.5 Strehl Ratio

The ratio of the intensity at the Gaussian image point in the presence of aberration is divided by the intensity that would be obtained if no aberrations are present, is called, the **Strehl** definition, or **Strehl** intensity. **Strehl** ratio (**S.R**) is proportional to the on-axis intensity [21] .

**Strehl** ratio  $S.R$  is expressed as:

$$S.R = \frac{I(z)}{I_0} \quad (1-18)$$

Where  $I(z)$  is the misfocus intensity [22]. The intensity in the PSF can be expressed as Fourier transform for pupil function (we shall refer it in the second section).

$$F(u', v') = N \int_{-\infty}^{\infty} \int_{-\infty}^{\infty} e^{ikW(x', y')} e^{2\pi i (u'x' + v'y')} dx' dy' \quad (1-19)$$

where:

$(v', u')$  : represents the radius coordinates of the image.

$k$ : represents the wave number  $(k = \frac{2\pi}{\lambda})$

$N$ : represents the normalizing factor which is used to make  $F(0,0) = 1$ .

By using polar coordinates

$$\begin{aligned} x' &= r \sin \phi & y' &= r \cos \phi \\ u' &= p' \sin \psi & v' &= p' \cos \psi \end{aligned} \quad (1-20)$$

The equation (1-19), for circular aperture which its radius is  $r = 1$  and its area equals  $\pi$  in the image plane can be written as:

$$F(p', \psi) = \frac{1}{\pi} \int_0^{2\pi} \int_0^1 e^{ikW(r, \phi)} e^{2\pi i p' r \cos(\psi - \phi)} r dr d\phi \quad (1-21)$$

To calculate the axial intensity, put  $p'=0$  and  $W(r, \phi) = W_{20} r^2$ , then the equation (1-21) will be in the form:

$$F(0) = \frac{1}{\pi} \int_0^{2\pi} \int_0^1 e^{2\pi i W_{20} r^2 / \lambda} r dr d\phi \quad (1-22)$$

By solving the integral:

$$F(0) = \frac{-i\lambda}{2\pi W_{20}} (e^{i2\pi W_{20} / \lambda} - 1) \quad (1-23)$$

So that the intensity equals:

$$G(0) = |F(0)|^2 = \left| \frac{-i\lambda}{2\pi W_{20}} \left( e^{2\pi i W_{20}/\lambda} - 1 \right) \right|^2 \quad (1-24)$$

after long series of simplification occur on:

$$G(0) = \frac{\sin^2(\pi W_{20}/\lambda)}{(\pi W_{20}/\lambda)^2} = \text{sinc}^2(\pi W_{20}/\lambda) \quad (1-25)$$

When the focus coefficient  $W_{20} = \frac{\lambda}{4}$  the equation (1-25) abbreviates to:

$$G(0) = \frac{8}{\pi^2} \cong 0.8$$

**Strehl** intensity ratio of 0.8 is good tolerance which is equivalent to the **Rayleigh** quarter-wavelength criterion [23], for defocused system **Marshall** [24] has shown that decrees in the **Strehl** ratio resulting from presence of aberrations is determined by the total variance ( $V$ ) of the wave front aberration  $W$ , Let us define:

$$V = \overline{W^2} - \overline{W}^2 \quad (1-26)$$

Where the bars denote mean value over the pupil domain and for circular aperture of normalized area equal  $\pi$ , the variance is:

$$V = \frac{1}{\pi} \int_0^1 \int_0^{2\pi} [W(r, \phi)]^2 r dr d\phi - \frac{1}{\pi^2} \left[ \int_0^1 \int_0^{2\pi} W(r, \phi) r dr d\phi \right]^2 \quad (1-27)$$

**Marshall** shows that for small aberrations, (**S.R**) is given by:

$$S.R = \left( 1 - \frac{2\pi^2 V}{\lambda^2} \right)^2 \quad (1-28)$$

When the exit pupil contains annular aperture ( $\epsilon$ ), then the intensity equals to [25]:-

$$S.R = \left[ 1 - \left( \frac{2\pi^2}{\lambda^2} \right) V \right]^2 (1 - \epsilon^2)^2 \quad (1-29)$$

## 1.6 Aberration Balancing

To improve optical system performance, optical designers make sure that the total aberration contribution from all surfaces taken together sums to nearly zero. Normally, such process requires computerized analysis and optimization [26]. We will use the way that **Marshal** used it, by obtaining the minimum value to mean square derivation consequently, we get the maximum intensity central value according to **Strehl** criterion.

Let us take the primary spherical aberration for axial image:

$$W(r, \phi) = W_{20}r^2 + W_{40}r^4 \quad (1-30)$$

For circular pupil ( $x^2+y^2=1$ ) and area ( $A = \pi$ ) Substitution in equation of variance (1-27) is as follows:

$$V = \frac{1}{\pi} \int_0^1 \int_0^{2\pi} [W(r, \phi)]^2 r dr d\phi - \frac{1}{\pi^2} \left[ \int_0^1 \int_0^{2\pi} W(r, \phi) r dr d\phi \right]^2$$

by solving the above equation for primary spherical aberration we get:

$$V = \frac{4}{45} W_{40}^2 + \frac{1}{12} W_{20}^2 + \frac{1}{6} W_{20} W_{40} \quad (1-31)$$

The maximum Intensity value becomes maximum when the variance at minimum is:

$$\frac{\partial \varepsilon}{\partial W_{20}} = \frac{1}{6} W_{20} + \frac{1}{6} W_{40} \quad (1-32)$$

$$\frac{\partial \varepsilon}{\partial W_{20}} = 0 \text{ when } W_{20} = -W_{40} \quad (1-33)$$

Substitute  $W_{20} = -W_{40}$  in the equation (1-31) and entrance **Strehl** condition, then:

$$V = \frac{1}{180} W_{40}^2 \leq \frac{\lambda^2}{180}$$

Then we get the tolerance value for primary spherical aberration with focus error:

$$W_{20} \leq 1\lambda, \quad W_{40} \leq -1\lambda$$

We get best focus when there are optimum balance values (third order aberration and focus error) in the optical system.

### 1.7 Resolution of Optical System

Consider an optical system which images two equally bright point source of light, each point, is imaged as an Airy disk with the encircling rings, and if the points are close, the diffraction patterns will overlap. When the separation is such that it is just possible to determine that there are two points and not one, the points which are said to be resolved [27]. The most widely used value for the limiting resolution of an optical system is **Rayleigh's** criterion. **Rayleigh** suggested that the image formed by an aberration free system of two self luminous points of the same brightness may be regarded as resolved if the central maximum of one image falls on the first minimum of the other.

This minimum resolvable separation known as "limit of resolution" which is given by [28]

$$Z = \frac{0.61\lambda}{n' \sin u'} = 1.22\lambda(f/\#) \quad (1-34)$$

This represents Airy disk [27]. If slit aperture has been used **Rayleigh's** criterion for resolving power will be in the new form:

$$Z = 1.0 \lambda (f/\#) \quad (1-35)$$

Dawes criterion is used only for circular and annular aperture and gives the separation between point image centers for circular aperture:

$$Z = 1.02 \lambda (f/\#) \quad (1-36)$$

Both of Rayleigh's and Dawes criteria apply only for incoherent source. But Sparrow gives special criterion for resolving power. He seems that the second intensity derivation between half distance of point image center equal zero [29]. This criterion apply on coherent and incoherent source, according to that the separation distance for circular aperture:

38)

For slit aperture:-

$$Z=0.829\lambda (f/\#) \quad \text{Incoherent} \quad (1-39)$$

$$Z=1.325\lambda (f/\#) \quad \text{Coherent} \quad (1-40)$$

Therefore the resolution power of slit aperture performs more than the circular aperture for the two type of light source (coherent and incoherent), figure (1-11) represents the criterion discussed.

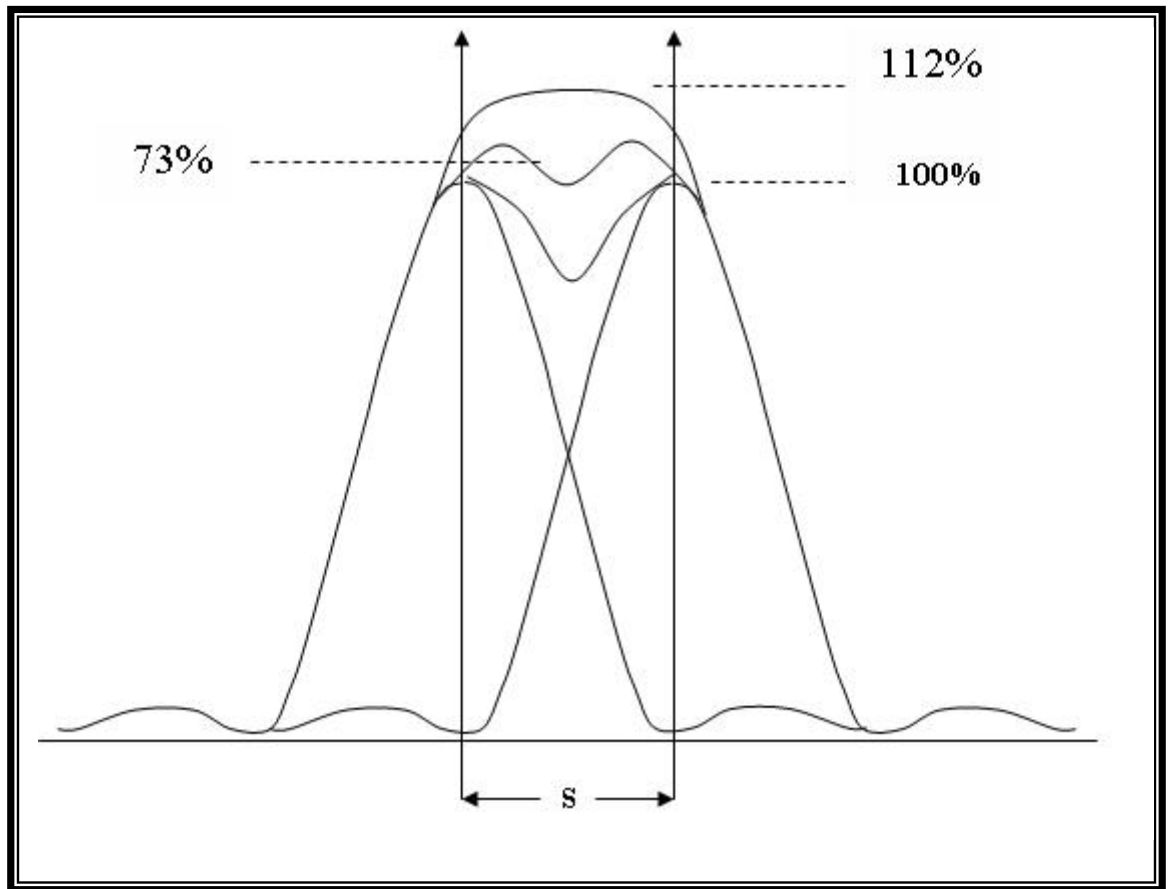


Figure (1-11): Raleigh's and Dawes criterions.

### 1.8 Focus Error

There are two types of focus error, longitudinal focus shift and transverse focus shift. The following equations represent the longitudinal focal shift and transverse focal respectively:

$$W(x', y') = W_{20} r^2 = {}_0W_{20} (x'^2 + y'^2) \quad (1-41)$$



$$W(x', y') = W_{11} \sigma r \cos \phi = W_{11} (x' \sin \psi + y' \cos \psi) \quad (1-42)$$

It is possible to reduce these two types of focus error through the search about a best image place; therefore this type of error is not affected.

### 1.9 Depth of Focus

The concept "depth of focus" rests on the assumption that for an optical system, there exists blur (due to defocusing) of small enough size such that it will not adversely affect that performance of the system. The depth of focus is the amount by which the image may be shifted longitudinally with respect to some reference plane and introduces no more than the acceptable blur. This is amount of the shifted image which is corresponding to being out of focus by one quarter wavelength. The depth of focus ( $\delta$ ) which is corresponding to an optical path difference of  $\pm \frac{1}{4} \lambda$  is

[30]

$$\delta = \pm 2\lambda (f/\#)^2 \quad (1-43)$$

### 1.10 Literature Survey

Many scientists and researchers are interested in the study of the intensity of the image that is formed by the optical system and find the ways and instruments which work on improving the image of optical system and specifying the qualification of the optical systems through specifying goodness of image that is formed by the optical system. **Lord George Biddel Airy** [31] studied the intensity distribution in image plane of a point source for free optical system. **Airy** [31] is the first to analyze the diffraction process using circular aperture. **Rayleigh** [32] studied the effect of wave front on the point spread function (**PSF**). **Barakat** [33] counts from the researchers who made their researches on point spread function because it is one of the important criterion that evaluates image quality. There are another researchers who made their researches on optical systems

contained aberrations. **O'Neill** [34] and **Hopkins** [35] were the first of them. **Sutton** [36], **Mahajan** [37], **Linfoot** and **Wolf** [38] study the effect of focus error on the intensity distribution in image plane. **Hopkins** [35] and **Wolf** [28] studied the effect of object illumination (coherent, incoherent illumination) on the intensity distribution of the image that is formed. **Mahajan** [26] works on the creation and development of simple pattern to calculate **PSF** for optical systems that contain asymmetric aberrations and illuminated with incoherent source. **O'Neill** [40] explains a process which evaluates the intensity distribution of a point image for annular aperture by using 2D-fourier transform. **Poon** [41] uses Fourier approximation in calculation the intensity distribution around the geometric focus. **Gauss** [42] was the first to give equivalence between the  $1^{st}$  orders spherical aberration and the  $2^{nd}$  orders spherical aberration in presence of the focus error. **Strehl** [43] studied the effect of the  $1^{st}$  orders aberrations on the image of a point source and evaluate the optimum balance values. **Dufieux** [3] studied Fourier transforms technique for optical systems. **Hopkins** [44] used the simple canonical coordinates in calculation the diffraction pattern in image plane. **Barakat** [45] calculates the intensity for optical systems contains circular aperture in presence of the spherical aberration and he uses **Gauss rule** in the numerical analysis. And in another research **Barakat** [46] calculates the **PSF** for optical systems contains aberrations.

There are many researches in the field of image apodization by using different kinds of filters. **O'Neil** [34] and **Marechal** [47] made their researches on the filters that used coherent light. **Luneburg** [48] used the optical systems with circular exit pupil and concluded that homogeneous energy distribution on the circular exit pupil in limits of the paraxial rays gives perfect results. There are other researches [49, 50] who used only the paraxial rays. **Forskin** [51] studied the non-paraxial state. **RAO** [52] studies the effect of filters forms (pupil's transparency form) on the edge spread

function (*ESF*). *Reddy* [53] indicates that the resolution limits increased with presence *LANCZOS* filters. *RAO* [54] notices that if the optical systems contain *BARTLETT* filters the secondary peaks will be disappeared.

In 1997 *RAO* [55] studied the modulation transfer function (*MTF*) by using different filters types. *J.campos, J.C.Escalerd* and *M.J, Yzuel* [56] studied the effect of aperture form on characteristic's symmetric image. In the field of calculation the total object energy in image plane *Wolf* [28] gives a study for calculating the total illumination by using *Lommel function*. *Mahajan* [57] calculates the total illumination function for obstruction diffraction- limited system.

### ***1.11 Aim of this Work***

This research, aims to study an obstructed optical system with or without different aberration. Also study the effect of the Gaussian form of the filter, on the annular optical system and circular optical system (with and without aberration).

## ***Chapter two***

### ***Point Spread Function***

#### ***2.1 Introduction***

For the importance of the point spread function (***PSF***) in testing and evaluating optical systems, it becomes the dependent measurement to know the optical systems efficiency. It has been studied for optical systems with circular aperture and also for annular aperture with Gaussian filter, where that function could evaluate the image efficiency for point object in image plane.

#### ***2.2 Point Spread Function (PSF)***

The image of point source formed by a lens system is known as the point spread function (***PSF***) of the lens. Other names for the ***PSF*** include "***impulse response***", "***Green's function***", and "***Fraunhofer diffraction pattern***" it is one of the most completed functions for describing the performance of an optical system and can be extended to include the effects of an obstructed aperture, apodization and any factor external to the optical system [4]. The most fundamental type of objects used in the testing of optical components is point source of light which is effectively of negligibly small dimensions. The ***PSF*** is a characteristic of the system under test. When the system contains less aberration, the image of a bright point is a finite disk of light surrounded by a series of weak diffraction rings; only the first is usually bright enough to be visible to the eye. This phenomenon was early expanded by Airy [5], who was the first one to calculate the intensity in the image of a point source as a formed by a diffraction-limited system, seen in figure (1-4) [17]. To calculate the intensity in the image plane for monochromatic point source, suppose that we have an optical system contains a lens forming an image for a point

source, and we know that all optical systems have aperture in some place in the optical system and it form an image in object space called "*Entrance pupil*" and it's image in image space called "*Exit pupil*" as in figure (2-1).

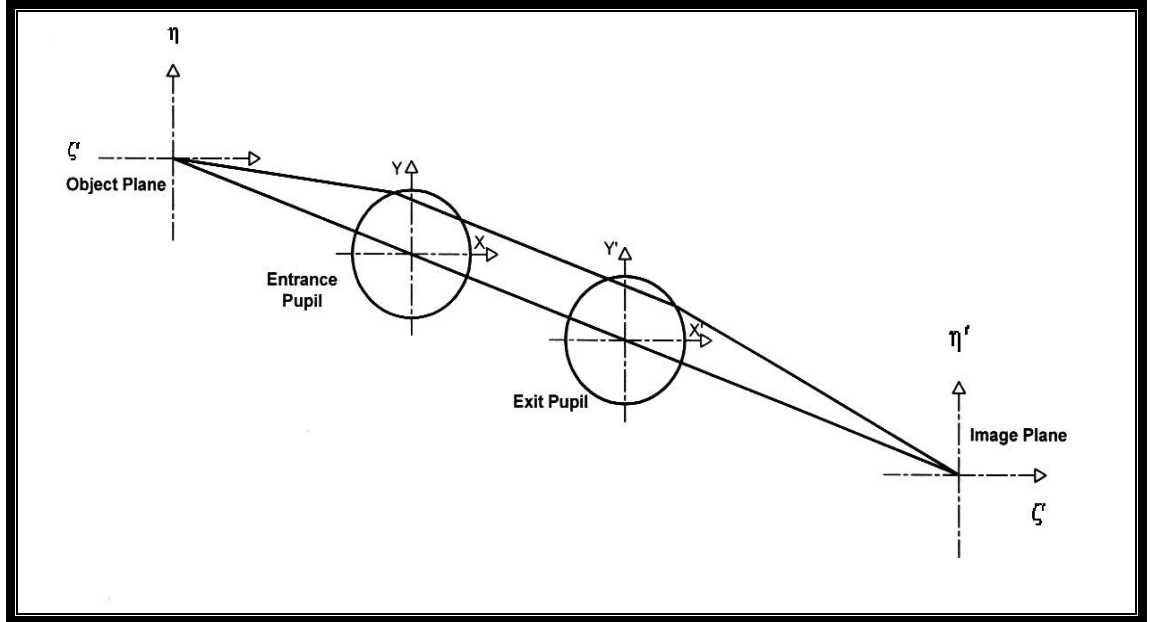


Figure (2-1): Optical axes, object plane, entrance pupil, exit pupil, image plane

The ray which comes from the point source is spherical and of less aberration and its spherical center in the point source like in figure (2-2)

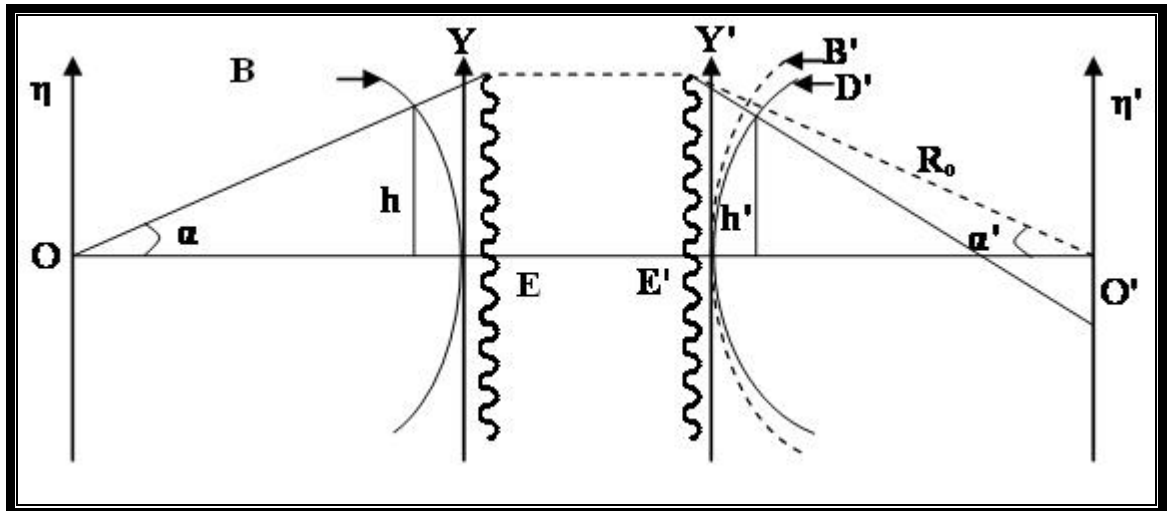


Figure (2-2): Diffraction image of a point source [10].

The wave (*E*) passes through Entrance pupil and the wave (*E'*) passes through exit pupil. The complex amplitude function distributed on the front (*EB*) is  $u_0(x, y)$  and The complex amplitude function distributed on the front spherical reference (*E'B'*) for the center (*o'*) in the image

space is  $u_0(\mathbf{x}', \mathbf{y}')$ , therefore we can define the pupil function for the optical system as [28].

$$f(x, y) = \frac{u_o(x', y')}{u_o(x, y)} \quad (2-1)$$

The coordinates  $(X, Y)$ ,  $(X', Y')$  are real space coordinates for entrance and exit pupil respectively. The ray heights that pass through the edges of entrance pupil and exit pupil are  $(h, h')$  respectively, for aberration less system:

$$h = y_{\max}, h' = y'_{\max}$$

We can use the reduced coordinate to describe the pupil function [28]

$$\begin{aligned} x &= \frac{X}{h}, y = \frac{Y}{h} \\ x' &= \frac{X'}{h}, y' = \frac{Y'}{h} \end{aligned} \quad (2-2)$$

The spherical wave  $(EB)$  is empty of aberration and diffraction, it is an ideal and it could be  $u_0(\mathbf{x}, \mathbf{y})=1$  and on the other side the wave  $(E'D')$  represents the real wave that suffers from the aberrations and diffraction. The wave  $(E'B')$  will be represented as spherical reference and the phase difference between the two waves  $(E'D', E'B')$  in the aperture  $B'$  is  $k(B'D')$  where  $(k = \text{the wave number})$  and equals :-

Where the path difference  $(B'D')$  between the two waves represents the aberration function for coordinates  $(\mathbf{x}', \mathbf{y}')$  at the exit pupil therefore:-

$$W(\mathbf{x}', \mathbf{y}') = B'D' \quad (2-3)$$

We can right the pupil function as:-

$$f(x, y) = \tau(x, y) e^{ikW(x, y)} \quad (2-4)$$

When we use the polar coordinates

$$\begin{aligned} r &= \sqrt{x'^2 + y'^2}, \quad \phi = \tan^{-1}\left(\frac{y'}{x'}\right) \\ y' &= r' \sin \phi, \quad x' = r' \cos \phi \end{aligned}$$

Then the equation (2-4) will take the new form as:

$$f(x, y) = \tau(r', \phi') e^{ik(r', \phi')} \quad (2-5)$$

$\tau(r', \theta')$  and  $\tau(x', y')$  represents the real amplitude function distributed in exit pupil and it is called "**pupil transparency**" or called "**Transmission function**" and it taken different values according to its use, and when we use the reduced coordinates of the object, it is defined as [28]

$$u = \left\{ \frac{n \sin \alpha}{\lambda} \right\} \xi, v = \left\{ \frac{n \sin \alpha}{\lambda} \right\} \eta \quad (2-6)$$

and the reduced coordinates of the image:

$$u' = \left\{ \frac{n \sin \alpha}{\lambda} \right\} \xi', v' = \left\{ \frac{n \sin \alpha}{\lambda} \right\} \eta' \quad (2-7)$$

Where  $\eta'$ ,  $\xi'$ ,  $\eta$ ,  $\xi$  represent the coordinates in the image space and object space respectively where:

$$\sin \alpha = \frac{h}{R} \text{ and } \sin \alpha' = \frac{h'}{R'}$$

$R$ ,  $R'$  represent the radii of spherical waves in the entrance and exit pupil respectively, therefore we can express **PSF** in its integral form as [28]

$$F(u', v') = \frac{1}{A'} \int_y \int_x f(x, y) e^{i2\pi(u'x + v'y)} dx dy \quad (2-8)$$

Where  $A'$  represents the area of exit pupil and  $F(u', v')$  represents the complex amplitude function.

The equation's limit can be defined from the circular aperture of normalized area ( $\pi$ ) and radii equal ( $1$ ) therefore:-

$$f(x, y) = \begin{cases} \tau(x, y) e^{iW(x, y)} & x^2 + y^2 \leq 1 \\ 0 & x^2 + y^2 > 1 \end{cases} \quad (2-9)$$

Let  $m' = 2\pi v'$ ,  $z' = 2\pi u'$  equation (2-7) takes the new form [28]

$$F(u', v') = \frac{1}{A'} \int_y \int_x f(x, y) e^{i2\pi(u'x + v'y)} dx dy \quad (2-10)$$

The intensity  $G(u', v')$  can be expressed as:

$$G(u', v') = F(u', v') \cdot F^*(u', v') \quad (2-11)$$

where  $F^*(u', v')$  the complex conjugate.

$$G(u', v') = N \left| \int_y \int_x f(x, y) e^{2\pi i(u'x + v'y)} dx dy \right|^2 \quad (2-12)$$

or

$$G(z', m') = N \left| \int_{-1-\sqrt{1-y^2}}^1 \int_{-1-\sqrt{1-y^2}}^{\sqrt{1-y^2}} f(x, y) e^{i(z'x + m'y)} dx dy \right|^2 \quad (2-13)$$

The intensity distribution on the two axis  $(z', m')$  are symmetric, so we can reduce it to one axis only.

Let  $m' = 0$  therefore equation (2-13) will take the form:-

$$G(z') = N \left| \int_{-1-\sqrt{1-y^2}}^1 \int_{-1-\sqrt{1-y^2}}^{\sqrt{1-y^2}} f(x, y) e^{iz'x} dx dy \right|^2 \quad (2-14)$$

### 2.2.1 PSF for Circular Aperture.

#### 2.2.1.1 PSF for a Diffraction-Limited System

If the optical system is of less aberration it is called "diffraction-limited system". For more simplification let  $\tau(x, y) = 1$ , therefore  $f(x, y) = 1$ , then the intensity function is as follows:

$$G(z') = N \left| \int_{-1-\sqrt{1-y^2}}^1 \int_{-1-\sqrt{1-y^2}}^{\sqrt{1-y^2}} e^{iz'x} dx dy \right|^2 \quad (2-15)$$

To find the normalization factor that made  $G(z') = 1$  when  $z' \rightarrow 0$  we must simplify the above equation (2-15)

$$1 = N \left| \int_{-1-\sqrt{1-y^2}}^1 \int_{-1-\sqrt{1-y^2}}^{\sqrt{1-y^2}} e^{iz'x} dx dy \right|^2 \quad (2-16)$$

When  $z' \rightarrow 0$ ,  $e^{iz'x} = 1$



$$1 = N \left| \int_{-1-\sqrt{1-y^2}}^1 \int_{-\sqrt{1-y^2}}^{\sqrt{1-y^2}} dx dy \right|^2 \quad (2-17)$$

$$N = \frac{1}{\pi^2}$$

In substituting the normalization factor (N) in equation (2-14) the equation will take the new form:

$$G(z') = \frac{1}{\pi^2} \left| \int_{-1-\sqrt{1-y^2}}^1 \int_{-\sqrt{1-y^2}}^{\sqrt{1-y^2}} f(x, y) e^{iz'x} dx dy \right|^2 \quad (2-18)$$

For a diffraction-limited system:

$$G(z') = \frac{1}{\pi^2} \left| \int_{-1-\sqrt{1-y^2}}^1 \int_{-\sqrt{1-y^2}}^{\sqrt{1-y^2}} \tau(x, y) e^{iz'x} dx dy \right|^2 \implies$$

$$G(z') = \frac{1}{\pi^2} \left| \int_{-1-\sqrt{1-y^2}}^1 \int_{-\sqrt{1-y^2}}^{\sqrt{1-y^2}} \tau(x, y) [\cos(z'x) + j \sin(z'x)] dx dy \right|^2 \quad (2-19)$$

$$G(z') = \frac{1}{\pi^2} \left| \int_{-1-\sqrt{1-y^2}}^1 \int_{-\sqrt{1-y^2}}^{\sqrt{1-y^2}} \tau(x, y) \cos(z'x) dx dy \right|^2 + \frac{1}{\pi^2} \left| \int_{-1-\sqrt{1-y^2}}^1 \int_{-\sqrt{1-y^2}}^{\sqrt{1-y^2}} \tau(x, y) j \sin(z'x) dx dy \right|^2 \quad (2-20)$$

$\sin(z'x)$  is odd function, therefore  $(2^{nd})$  part of the integral will be negligible, and the equation will be:

$$G(z') = \frac{1}{\pi^2} \left[ \int_{-1-\sqrt{1-y^2}}^1 \int_{-\sqrt{1-y^2}}^{\sqrt{1-y^2}} \tau(x, y) \cos(z'x) dx dy \right]^2 \quad (2-21)$$

Equation (2-21) represents PSF for a diffraction-limited system.

We can use the polar conditions where:

$$\begin{aligned} y &= r \cos \phi & , & & x &= r \sin \phi \\ v &= p \cos \psi & , & & u &= p \sin \psi \\ p &= \sqrt{u^2 + v^2} & , & & \psi &= \tan^{-1} \left( \frac{v}{u} \right) \end{aligned}$$

Where

$\Psi$ = the angle in polar coordinates.

$P$ = polar distance from the plane center.

Equation (2-8) takes the new form:-

$$F(p, \psi) = N \int_0^1 \int_0^{2\pi} \tau(r, \phi) e^{ikW(r, \phi)} e^{i2\pi pr \cos(\psi - \phi)} r dr d\phi \quad (2-22)$$

For a less aberration system and  $\tau(x, y) = 1$  equation (2-22) is solved as:-

$$F(p, \psi) = \frac{2 J_1(2\pi p)}{2\pi p} \quad (2-23)$$

where  $J_1(2\pi p)$  = **1st** order Bessel function and the intensity is given as:

$$G(p, \psi) = |F(p, \psi)|^2 = \left[ \frac{2 J_1(2\pi p)}{2\pi p} \right]^2 \quad (2-24)$$

Equation (2-24) represents the intensity in Airy diffraction.

### 2.2.1.2 PSF with Focus Error

The spherical aberrations polynomial is:-

$$W(x, y) = W_{20}(x^2 + y^2) + W_{40}(x^2 + y^2)^2 + W_{60}(x^2 + y^2)^3 + \dots \quad (2-25)$$

If the optical system does not contain spherical aberration and when axial focus is moved from focus plane to another therefore the equation of spherical aberration gives inductively the focus error  $W_{20}(x^2 + y^2)$ . When pupil function  $f(x, y) = \tau(x, y) e^{ikw(x, y)}$  is substituted in equation (2-14) we shall get:

$$G(z') = \frac{1}{\pi^2} \left| \int_{-1-\sqrt{1-y^2}}^1 \int_{-1-\sqrt{1-y^2}}^{\sqrt{1-y^2}} \tau(x, y) e^{ikW(x, y)} e^{iz'x} dx dy \right|^2 \quad (2-26)$$

$$G(z') = \frac{1}{\pi^2} \left| \int_{-1-\sqrt{1-y^2}}^1 \int_{-1-\sqrt{1-y^2}}^{\sqrt{1-y^2}} \tau(x, y) [\cos(kW(x, y) + z'x) + j \sin(kW(x, y) + z'x)] dx dy \right|^2 \quad (2-27)$$

where  $\sin(kW(x, y) + z'x)$  is an odd function therefore

$$G(z') = \left[ \frac{1}{\pi^2} \left| \int_{-1-\sqrt{1-y^2}}^1 \int_{-\sqrt{1-y^2}}^{\sqrt{1-y^2}} \tau(x, y) \cos(kW(x, y) + z'x) dx dy \right|^2 \right] \quad (2-28)$$

In substitution the value of the wave number  $(k = \frac{2\pi}{\lambda})$  and regarding the aberrations function measured in unit of wave number we shall get:

$$G(z') = \frac{1}{\pi^2} \left[ \int_{-1-\sqrt{1-y^2}}^1 \int_{-\sqrt{1-y^2}}^{\sqrt{1-y^2}} \tau(x, y) \cos(2\pi W_{20}(x^2 + y^2) + z'x) dx dy \right]^2 \quad (2-29)$$

By using equation (2-22) and substituting the value of focus error  $(W_{20}r^2)$  we shall get:-

$$F(p, \psi) = \frac{1}{\pi} \int_0^1 \int_0^{2\pi} \tau(r, \phi) e^{ikW_{20}r^2} e^{i2\pi pr \cdot \cos(\psi - \phi)} r dr d\phi \quad (2-30)$$

Let  $\mathbf{p} = \mathbf{0}$  along the optical axis then we get:-

$$F(0, 0) = \frac{1}{\pi} \int_{r=0}^1 \int_{\phi=0}^{2\pi} \tau(r, \phi) e^{ikW_{20}r^2} r dr d\phi \quad (2-31)$$

For more simplification  $\tau(r, \phi) = 1$

$$F(0, 0) = e^{i\pi W_{20} / \lambda} \frac{\sin\left(\frac{\pi W_{20}}{\lambda}\right)}{\left(\frac{\pi W_{20}}{\lambda}\right)} \quad (2-32)$$

the intensity will be:

$$G(0, 0) = \left[ \frac{\sin\left(\frac{\pi W_{20}}{\lambda}\right)}{\left(\frac{\pi W_{20}}{\lambda}\right)} \right]^2 \longrightarrow G(0, 0) = \text{sinc}^2\left(\frac{\pi W_{20}}{\lambda}\right) \quad (2-33)$$

The axial intensity go to zero when the focus error takes the values

$$(W_{20} = \pm\lambda, \pm2\lambda, \pm3\lambda)$$

The intensity in the center of the PSF counts as a function of focus plane position[44]. We can observe it in the figure (2-3), which represents the intensity in image plane or PSF for different values of focus error.

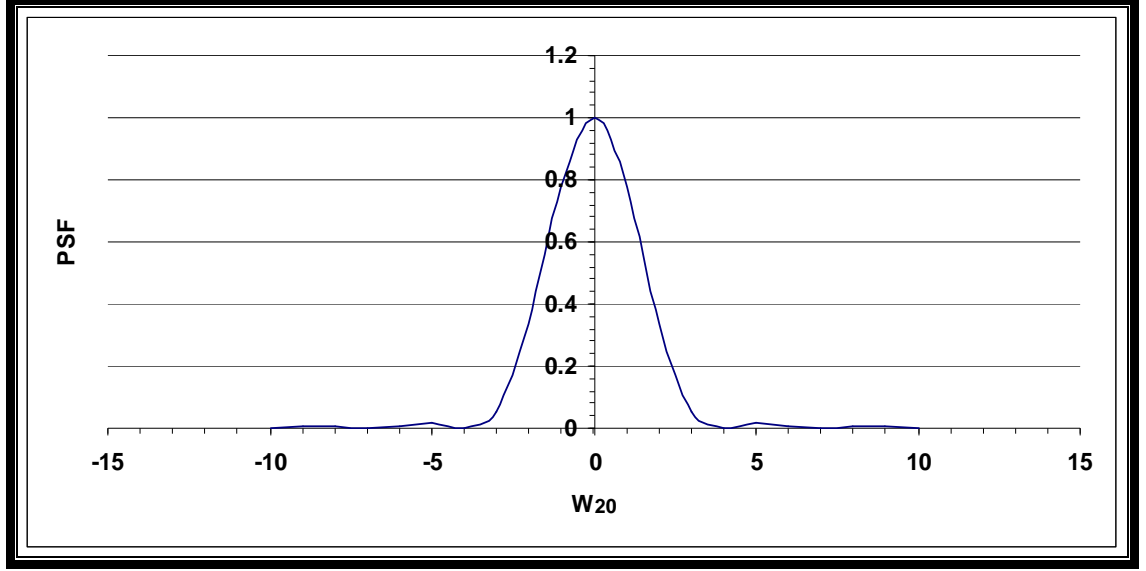


Figure (2-3): The intensity in image plane.

### 2.2.1.3 PSF with Third Order Spherical Aberration

When we enter the factor of third order spherical aberration  $(W_{20}(x^2 + y^2) + W_{40}(x^2 + y^2)^2)$ , the intensity equation will contain the focus error and spherical aberration, then equation (2-14) will take the new form:

$$G(z') = \left[ \frac{1}{\pi^2} \left| \int_{-1-\sqrt{1-y^2}}^1 \int_{-1-\sqrt{1-y^2}}^{\sqrt{1-y^2}} \tau(x, y) \cos(2\pi(W_{20}(x^2 + y^2) + W_{40}(x^2 + y^2)^2) + z'x) dx dy \right|^2 \right. \\ \left. + \frac{1}{\pi^2} \left| \int_{-1-\sqrt{1-y^2}}^1 \int_{-1-\sqrt{1-y^2}}^{\sqrt{1-y^2}} \tau(x, y) j \sin(2\pi(W_{20}(x^2 + y^2) + W_{40}(x^2 + y^2)^2) + z'x) dx dy \right|^2 \right] \quad (2-34)$$

Where  $\sin(2\pi(W_{20}(x^2 + y^2) + W_{40}(x^2 + y^2)^2) + z'x)$  is an odd function therefore:

$$G(z') = \frac{1}{\pi^2} \left| \int_{-1-\sqrt{1-y^2}}^1 \int_{-1-\sqrt{1-y^2}}^1 \tau(x, y) \cos(2\pi(W_{20}(x^2 + y^2) + W_{40}(x^2 + y^2)^2) + z'x) dx dy \right|^2 \quad (2-35)$$

Equation (2-35) represent PSF with 3<sup>rd</sup> spherical aberration.

### 2.3 Annular Aperture

Annular aperture is of a considerable practical importance and usually encountered when using control stop in the optical system with circular aperture. Considerable work in this direction done by **Steel** [58], **O'Neill** [34]. They evaluated independently the **(OTF)** for different values of annular aperture. **Welford** [59] published a theoretical study on increasing the focus depth of photographic object using annular aperture. The transfer function of an annular aperture in the presence of spherical aberrations and defocusing is evaluated by **Richard Barakat** [46] **Mahjan** [37] has shown that for symmetric pupils, a noncentral obstruction always produces a higher concentration of energy image center obstruction. **Tschunko** [60] investigates the image of infinity thin incoherent bright lines generated by annular aperture of central obstruction ratio approaching (1). **Jorge Ojeda–Castaneda** [61] calculates Strehl ratio for annular aperture system in the presence of focus error and primary spherical aberration. In the present work a formula is derived to determine the intensity in the image of coherently of illuminated point object using annular aperture. A new formula is derived to determine the intensity in image illuminated point object using apodization annular aperture. This formula is of finite limits and can be expanded for any kind of aberrations. The annular aperture is illustrated in the figure (2-4) where (p) represents the circular aperture and its radius ( $r_2$ , p') represents the central obstruction with radius ( $r_1$ ), where ( $\epsilon$ ) represents the

obstruction ratio ( $\epsilon = r_2 / r_1$ ). We can express the annular aperture by using pupil function where:

$$f(x, y) = \tau(x, y)e^{ikW(x, y)} \quad \text{With in Q}$$

$$f(x, y) = 0 \quad \text{Out side Q}$$

Then image intensity for annular aperture =

Image intensity for outer circle Image - Intensity for inner circle.

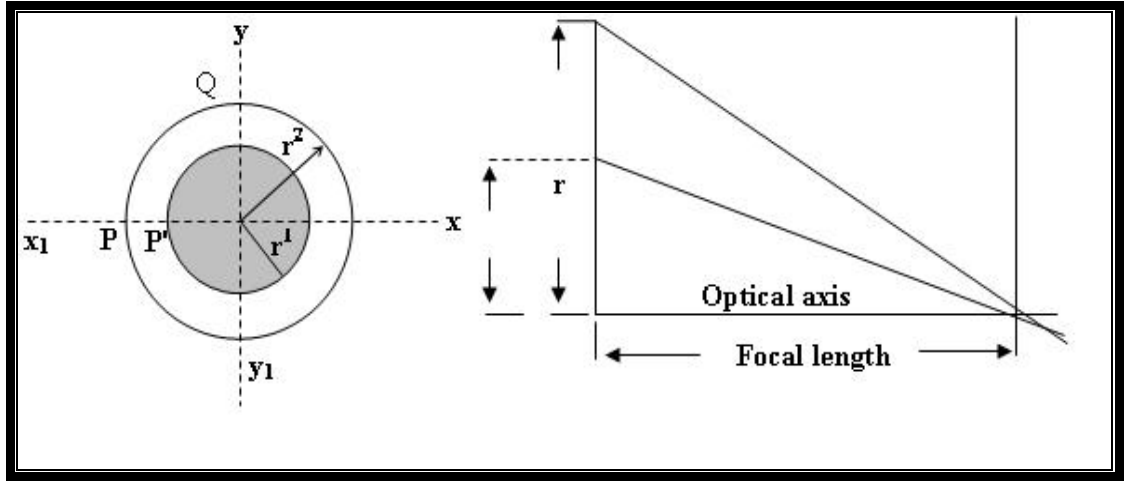


Figure (2-4): Annular aperture.

By using equation (2-14), the **PSF** for annular aperture can be calculated.

$$G(z') = N \left| \int_{-1-\sqrt{1-y^2}}^1 \int_{-1-\sqrt{1-y^2}}^{\sqrt{1-y^2}} f(x, y) e^{iz'x} dx dy - \int_{-\epsilon-\sqrt{\epsilon-y^2}}^{\epsilon} \int_{-\epsilon-\sqrt{\epsilon-y^2}}^{\sqrt{\epsilon-y^2}} f(x', y') e^{iz'x'} dx' dy' \right|^2 \quad (2-36)$$

Where  $(x, y)$  represented the coordinates of the central obstruction ( $0 < \epsilon \leq 1$ ) the intensity  $I_\epsilon = (1 - \epsilon^2)$  (2-37)

Where  $I$  = Intensity for circular aperture.

### 2.3.1 PSF of Annular Aperture for a Diffraction-Limited System

When the system is a diffraction-limited  $W(x, y) = 0$  therefore  $f(x, y) = 1$ . To find the normalized factor that makes  $G(z') = 1$  when  $z' \Rightarrow 0$ , we shall integrate equation (2-39):

$$G(0) = 1 = N \left| \int_{-1-\sqrt{1-y^2}}^1 \int_{-\sqrt{1-y^2}}^{\sqrt{1-y^2}} dx dy - \int_{-\varepsilon-\sqrt{\varepsilon-y'^2}}^{\varepsilon} \int_{-\sqrt{\varepsilon-y'^2}}^{\sqrt{\varepsilon-y'^2}} dx' dy' \right|^2 \quad (2-38)$$

$$1 = N \left| \int_{-1}^1 dy \cdot x \Big|_{-\sqrt{1-y^2}}^{\sqrt{1-y^2}} - \int_{-\varepsilon}^{\varepsilon} dy' \cdot x' \Big|_{-\sqrt{\varepsilon-y'^2}}^{\sqrt{\varepsilon-y'^2}} \right|^2 \quad (2-39)$$

$$1 = N \left| \int_{-1}^1 2\sqrt{1-y^2} dy - \int_{-\varepsilon}^{\varepsilon} 2\sqrt{\varepsilon-y'^2} dy' \right|^2 \quad (2-40)$$

Let  $y = \sin \theta$ ,  $y' = \varepsilon \sin \theta$

$$1 = N \left| 4 \int_0^{\frac{\pi}{2}} \cos^2 \theta d\theta - 4 \int_0^{\frac{\pi}{2}} \varepsilon^2 \cos^2 \theta d\theta \right|^2 \quad (2-41)$$

$$N = \frac{1}{\pi^2 (1 - \varepsilon^2)^2} \quad (2-42)$$

In substituting the normalized factor (N) in equation (2-36):

$$G(z') = \frac{1}{\pi^2 (1 - \varepsilon^2)^2} \left| \int_{-1-\sqrt{1-y^2}}^1 \int_{-\sqrt{1-y^2}}^{\sqrt{1-y^2}} f(x, y) e^{iz'x} dx dy - \int_{-\varepsilon-\sqrt{\varepsilon-y'^2}}^{\varepsilon} \int_{-\sqrt{\varepsilon-y'^2}}^{\sqrt{\varepsilon-y'^2}} f(x', y') e^{iz'x'} dx' dy' \right|^2 \quad (2-43)$$

For a diffraction-limited system  $f(x, y) = 1$  therefore equation (2-43) will be:

$$G(z') = \frac{1}{\pi^2 (1 - \varepsilon^2)^2} \left| \int_{-1-\sqrt{1-y^2}}^1 \int_{-\sqrt{1-y^2}}^{\sqrt{1-y^2}} \cos(z'x) + j \sin(z'x) dx dy - \int_{-\varepsilon-\sqrt{\varepsilon-y'^2}}^{\varepsilon} \int_{-\sqrt{\varepsilon-y'^2}}^{\sqrt{\varepsilon-y'^2}} \cos(z'x') + j \sin(z'x') dx' dy' \right|^2 \quad (2-44)$$

$\sin(z'x)$  is an odd function and this part of equation will be neglected, we shall write equation (2-44) in a new form:

$$G(z') = \frac{1}{\pi^2 (1 - \varepsilon^2)^2} \left| \int_{-1-\sqrt{1-y^2}}^1 \int_{-\sqrt{1-y^2}}^{\sqrt{1-y^2}} \cos(z'x) dx dy - \int_{-\varepsilon-\sqrt{\varepsilon-y'^2}}^{\varepsilon} \int_{-\sqrt{\varepsilon-y'^2}}^{\sqrt{\varepsilon-y'^2}} \cos(z'x') dx' dy' \right|^2 \quad (2-45)$$

Equation (2-45) represents function of the intensity of annular aperture with obstruction ( $\varepsilon$ ) for a free system.

### 2.3.2 PSF of Annular Aperture with Focus Error

If the aberration polynomial  $W_{20}(x^2 + y^2)$  which represents the focus error is substituted in equation of pupil function, equation (2-43) will be:

$$G(z') = \frac{1}{\pi^2(1-\varepsilon^2)^2} \left| \int_{-1-\sqrt{1-y^2}}^1 \int_{-\sqrt{1-y^2}}^{\sqrt{1-y^2}} e^{ikW_{20}(x^2+y^2)} e^{iz'x} dx dy - \int_{-\varepsilon-\sqrt{\varepsilon-y'^2}}^{\varepsilon} \int_{-\sqrt{\varepsilon-y'^2}}^{\sqrt{\varepsilon-y'^2}} e^{ikW_{20}(x'^2+y'^2)} e^{iz'x'} dx' dy' \right|^2 \quad (2-46)$$

Substituting the wave number  $k = \frac{2\pi}{\lambda}$  and regarding the aberrations function measured in unit of wave number. Then equation (2-46) takes the new form:-

$$G(z') = \frac{1}{\pi^2(1-\varepsilon^2)^2} \left| \int_{-1-\sqrt{1-y^2}}^1 \int_{-\sqrt{1-y^2}}^{\sqrt{1-y^2}} e^{i2\pi W_{20}(x^2+y^2)+z'x} dx dy - \int_{-\varepsilon-\sqrt{\varepsilon-y'^2}}^{\varepsilon} \int_{-\sqrt{\varepsilon-y'^2}}^{\sqrt{\varepsilon-y'^2}} e^{i2\pi W_{20}(x'^2+y'^2)+z'x'} dx' dy' \right|^2 \quad (2-47)$$

$$G(z') = \frac{1}{\pi^2(1-\varepsilon^2)^2} \left[ \begin{aligned} & \left| \int_{-1-\sqrt{1-y^2}}^1 \int_{-\sqrt{1-y^2}}^{\sqrt{1-y^2}} \cos(2\pi W_{20}(x^2+y^2)+z'x) dx dy \right|^2 \\ & + \left| \int_{-1-\sqrt{1-y^2}}^1 \int_{-\sqrt{1-y^2}}^{\sqrt{1-y^2}} j \sin(2\pi W_{20}(x^2+y^2)+z'x) dx dy \right|^2 \\ & - \left| \int_{-\varepsilon-\sqrt{\varepsilon-y'^2}}^{\varepsilon} \int_{-\sqrt{\varepsilon-y'^2}}^{\sqrt{\varepsilon-y'^2}} \cos(2\pi W_{20}(x'^2+y'^2)+z'x') dx' dy' \right|^2 \\ & - \left| \int_{-\varepsilon-\sqrt{\varepsilon-y'^2}}^{\varepsilon} \int_{-\sqrt{\varepsilon-y'^2}}^{\sqrt{\varepsilon-y'^2}} j \sin(2\pi W_{20}(x'^2+y'^2)+z'x') dx' dy' \right|^2 \end{aligned} \right] \quad (2-48)$$

$\sin(2\pi W_{20}(x^2+y^2)+z'x)$  is an odd function therefore equation (2-48) will be:

$$G(z') = \frac{1}{\pi^2(1-\varepsilon^2)^2} \left[ \begin{aligned} & \left| \int_{-1-\sqrt{1-y^2}}^1 \int_{-\sqrt{1-y^2}}^{\sqrt{1-y^2}} \cos(2\pi W_{20}(x^2+y^2)+z'x) dx dy \right|^2 \\ & - \left| \int_{-\varepsilon-\sqrt{\varepsilon-y'^2}}^{\varepsilon} \int_{-\sqrt{\varepsilon-y'^2}}^{\sqrt{\varepsilon-y'^2}} \cos(2\pi W_{20}(x'^2+y'^2)+z'x') dx' dy' \right|^2 \end{aligned} \right] \quad (2-49)$$

Equation (2-49) represents PSF for annular system with focus error. The axial intensity for perfect system with annular aperture is given as:



$$G(0) = \left( \frac{\sin \left( \frac{\pi W_{20}(1 - \varepsilon^2)}{\lambda} \right)}{\frac{\pi W_{20}(1 - \varepsilon^2)}{\lambda}} \right)^2 \quad (2-50)$$

If  $\varepsilon=0$  then one has:

$$G(0) = \left( \frac{\sin \frac{\pi W_{20}}{\lambda}}{\frac{\pi W_{20}}{\lambda}} \right)^2 \quad (2-51)$$

$G(0)$  represents the axial intensity of annular aperture with focus error.

### 2.3.3 PSF of Annular Aperture with Focus Error and Spherical Aberration

If the polynomial of spherical aberration which contains the focus error and spherical aberration  $(W_{20}(x^2 + y^2) + W_{40}(x^2 + y^2)^2)$  is substituted in equation of pupil function. Equation (2-43) will be:

$$G(z') = \frac{1}{\pi^2 (1 - \varepsilon^2)^2} \left| \int_{-1-\sqrt{1-y^2}}^1 \int_{-1-\sqrt{1-y^2}}^{\sqrt{1-y^2}} e^{ik(W_{20}(x^2+y^2)+W_{40}(x^2+y^2)^2)} e^{iz'x} dx dy - \int_{-\varepsilon-\sqrt{\varepsilon-y'^2}}^{\varepsilon} \int_{-\varepsilon-\sqrt{\varepsilon-y'^2}}^{\sqrt{\varepsilon-y'^2}} e^{ik(W_{20}(x'^2+y'^2)+W_{40}(x'^2+y'^2)^2)} e^{iz'x'} dx' dy' \right|^2 \quad (2-52)$$

$$G(z') = \frac{1}{\pi^2(1-\varepsilon^2)^2} \left[ \begin{aligned} & \left| \int_{-1-\sqrt{1-y^2}}^1 \int_{-\sqrt{1-y^2}}^{\sqrt{1-y^2}} \cos\left(2\pi\left(W_{20}(x^2+y^2)+W_{40}(x^2+y^2)^2\right)+z'x\right) dx dy \right|^2 \\ & + \left| \int_{-1-\sqrt{1-y^2}}^1 \int_{-\sqrt{1-y^2}}^{\sqrt{1-y^2}} j \sin\left(2\pi\left(W_{20}(x^2+y^2)+W_{40}(x^2+y^2)^2\right)+z'x\right) dx dy \right|^2 \\ & - \left| \int_{-\varepsilon-\sqrt{\varepsilon-y'^2}}^{\varepsilon} \int_{-\sqrt{\varepsilon-y'^2}}^{\sqrt{\varepsilon-y'^2}} \cos\left(2\pi\left(W_{20}(x'^2+y'^2)+W_{40}(x'^2+y'^2)^2\right)+z'x'\right) dx' dy' \right|^2 \\ & - \left| \int_{-\varepsilon-\sqrt{\varepsilon-y'^2}}^{\varepsilon} \int_{-\sqrt{\varepsilon-y'^2}}^{\sqrt{\varepsilon-y'^2}} j \sin\left(2\pi\left(W_{20}(x'^2+y'^2)+W_{40}(x'^2+y'^2)^2\right)+z'x'\right) dx' dy' \right|^2 \end{aligned} \right] \quad (2-53)$$

Where  $\sin\left(2\pi\left(W_{20}(x^2+y^2)+W_{40}(x^2+y^2)^2\right)+z'x\right)$  is an odd function therefore the equation will be:-

$$G(z') = \frac{1}{\pi^2(1-\varepsilon^2)^2} \left[ \begin{aligned} & \left| \int_{-1-\sqrt{1-y^2}}^1 \int_{-\sqrt{1-y^2}}^{\sqrt{1-y^2}} \cos\left(2\pi\left(W_{20}(x^2+y^2)+W_{40}(x^2+y^2)^2\right)+z'x\right) dx dy \right|^2 \\ & - \left| \int_{-\varepsilon-\sqrt{\varepsilon-y'^2}}^{\varepsilon} \int_{-\sqrt{\varepsilon-y'^2}}^{\sqrt{\varepsilon-y'^2}} \cos\left(2\pi\left(W_{20}(x'^2+y'^2)+W_{40}(x'^2+y'^2)^2\right)+z'x'\right) dx' dy' \right|^2 \end{aligned} \right] \quad (2-54)$$

Equation (2-54) represents the **PSF** of annular aperture with focus error and spherical aberration.

## 2.4 Apodization

Apodization is a complicated word for the simple process of shading part of the aperture usually the out side. "Apod" means "without feet" and, judging from the name. The process of apodization is to reduce the intensity of the diffraction rings [4,12,17].

The meaning of the term "Apodization" has been extended by usage to include all terms of modifying the **PSF** through the amplitude transmittance pupil function  $\tau(x,y)$  [4]. A considerable amount of our work has been done taking into account the use of filter to improve the image qualities, such as a resolving power, depth of focus and energy

distribution in the image. Five-level classification of the apodization function is given bellow.

Class-1:  $\tau(x, y) = 1$  at all point in the pupil.

Class-2:  $\tau(x, y) = 1 \text{ or } 0$  at all point in the pupil.

Class-3:  $\tau(x, y) = r^2$  increases monotonically from center to edge

Class-4:  $\tau(x, y) = 1 - r$  decreases monotonically from center to edge.

Class-5:  $\tau(x, y) = e^{-r^2/a^2}$  super Gaussian filter with various width (a).

In this research a super Gaussian filter has been used with various width ( $a=0.1, 0.2, 0.3-1$ ). The super Gaussian filter is important in laser application because it is making us to use the center spot of laser beam ( $\text{TEM}_{00}$ ) central mod only. Figure (2-5) illustrates super Gaussian filter function according to its width which is used in this research, the super Gaussian filter works on specification area of entering rays to the optical system.

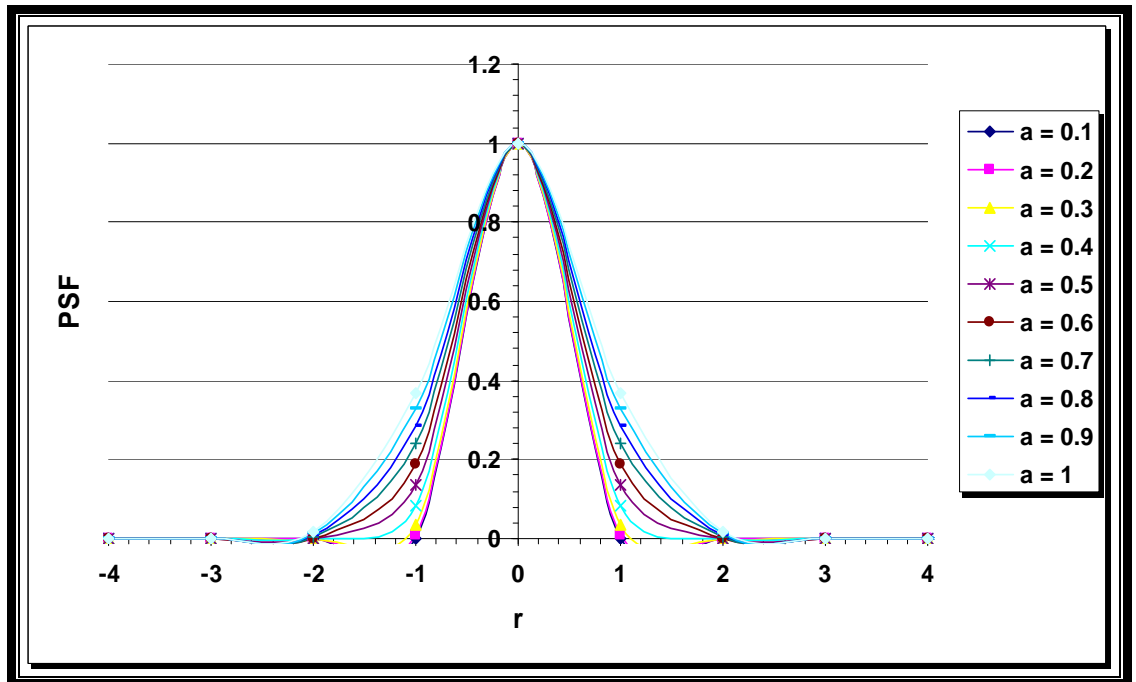


Figure (2-5): Super Gaussian filter with various widths.

### 2.4.1 Apodization of Annular Aperture for a Diffraction-Limited System

Equation (2-43) of annular aperture will be used to express the apodization of annular aperture in substitution with  $e^{-r^2/a^2} e^{iW(x,y)}$  where  $e^{iW(x,y)}$  will be negligible because there is no aberration and  $e^{-r^2/a^2}$  represents the super Gaussian filter that is used to apodize the annular aperture with a width factor (**a**).

$$G(z') = \frac{1}{\pi^2(1-\varepsilon^2)^2} \left| \int_{-1-\sqrt{1-y^2}}^1 \int_{-1-\sqrt{1-y^2}}^{\sqrt{1-y^2}} f(x,y) e^{iz'x} dx dy - \int_{-\varepsilon-\sqrt{\varepsilon-y'^2}}^{\varepsilon-\sqrt{\varepsilon-y'^2}} \int_{-\varepsilon-\sqrt{\varepsilon-y'^2}}^{\varepsilon-\sqrt{\varepsilon-y'^2}} f(x',y') e^{iz'x'} dx' dy' \right|^2$$

where is  $f(x,y) = e^{-r^2/a^2}$ . Therefore equation (2-43) will be:

$$G(z') = \frac{1}{\pi^2(1-\varepsilon^2)^2} \left| \int_{-1-\sqrt{1-y^2}}^1 \int_{-1-\sqrt{1-y^2}}^{\sqrt{1-y^2}} e^{-r^2/a^2} e^{iz'x} dx dy - \int_{-\varepsilon-\sqrt{\varepsilon-y'^2}}^{\varepsilon-\sqrt{\varepsilon-y'^2}} \int_{-\varepsilon-\sqrt{\varepsilon-y'^2}}^{\varepsilon-\sqrt{\varepsilon-y'^2}} e^{-r^2/a^2} e^{iz'x'} dx' dy' \right|^2 \quad (2-55)$$

$$G(z') = \frac{1}{\pi^2(1-\varepsilon^2)^2} \left| \int_{-1-\sqrt{1-y^2}}^1 \int_{-1-\sqrt{1-y^2}}^{\sqrt{1-y^2}} e^{iz'x - (r^2/a^2)} dx dy - \int_{-\varepsilon-\sqrt{\varepsilon-y'^2}}^{\varepsilon-\sqrt{\varepsilon-y'^2}} \int_{-\varepsilon-\sqrt{\varepsilon-y'^2}}^{\varepsilon-\sqrt{\varepsilon-y'^2}} e^{iz'x' - (r^2/a^2)} dx' dy' \right|^2 \quad (2-56)$$

$$G(z') = \frac{1}{\pi^2(1-\varepsilon^2)^2} \left[ \int_{-1-\sqrt{1-y^2}}^1 \int_{-1-\sqrt{1-y^2}}^{\sqrt{1-y^2}} \cos(z'x - (r^2/a^2)) + j \sin(z'x - (r^2/a^2)) dx dy - \int_{-\varepsilon-\sqrt{\varepsilon-y'^2}}^{\varepsilon-\sqrt{\varepsilon-y'^2}} \int_{-\varepsilon-\sqrt{\varepsilon-y'^2}}^{\varepsilon-\sqrt{\varepsilon-y'^2}} \cos(z'x' - (r^2/a^2)) + j \sin(z'x' - (r^2/a^2)) dx' dy' \right]^2 \quad (2-57)$$

$\sin(z'x - (r^2/a^2))$  is an odd function therefore the equation will be in the new form:

$$G(z') = \frac{1}{\pi^2(1-\varepsilon^2)^2} \left[ \int_{-1-\sqrt{1-y^2}}^1 \int_{-1-\sqrt{1-y^2}}^{\sqrt{1-y^2}} \cos(z'x - (r^2/a^2)) dx dy - \int_{-\varepsilon-\sqrt{\varepsilon-y'^2}}^{\varepsilon-\sqrt{\varepsilon-y'^2}} \int_{-\varepsilon-\sqrt{\varepsilon-y'^2}}^{\varepsilon-\sqrt{\varepsilon-y'^2}} \cos(z'x' - (r^2/a^2)) dx' dy' \right]^2 \quad (2-58)$$

where equation (2-58) represents the apodized annular aperture for a diffraction-limited system.

### 2.4.2 Apodization of the Annular Aperture with Focus Error

In substituting the super Gaussian filter with the focus error in pupil function, we shall get:

$$f(x, y) = e^{ikW_{20}(x^2+y^2)} e^{-r^2/a^2} \quad (2-59)$$

in substituting equation (2-59) in equation (2-43), we shall get:

$$G(z') = \frac{1}{\pi^2(1-\varepsilon^2)^2} \left| \int_{-1}^1 \int_{-\sqrt{1-y^2}}^{\sqrt{1-y^2}} e^{ikW_{20}(x^2+y^2)} \frac{r^2}{a^2} e^{iz'x} dx dy - \int_{-\varepsilon}^{\varepsilon} \int_{-\sqrt{\varepsilon-y'^2}}^{\sqrt{\varepsilon-y'^2}} e^{ikW_{20}(x'^2+y'^2)} \frac{r^2}{a^2} e^{iz'x'} dx' dy' \right|^2 \quad (2-60)$$

$$G(z') = \frac{1}{\pi^2(1-\varepsilon^2)^2} \left| \int_{-1}^1 \int_{-\sqrt{1-y^2}}^{\sqrt{1-y^2}} e^{i(kW_{20}(x^2+y^2)+(z'x))-(\frac{r^2}{a^2})} dx dy - \int_{-\varepsilon}^{\varepsilon} \int_{-\sqrt{\varepsilon-y'^2}}^{\sqrt{\varepsilon-y'^2}} e^{i(kW_{20}(x'^2+y'^2)+(z'x'))-(\frac{r^2}{a^2})} dx' dy' \right|^2 \quad (2-61)$$

(by substituting the value of the wave number  $k = 2\pi/\lambda$ )

$$G(z') = \frac{1}{\pi^2(1-\varepsilon^2)^2} \left| \int_{-1}^1 \int_{-\sqrt{1-y^2}}^{\sqrt{1-y^2}} e^{i(2\pi W_{20}(x^2+y^2)+(z'x))-(\frac{r^2}{a^2})} dx dy - \int_{-\varepsilon}^{\varepsilon} \int_{-\sqrt{\varepsilon-y'^2}}^{\sqrt{\varepsilon-y'^2}} e^{i(2\pi W_{20}(x'^2+y'^2)+(z'x'))-(\frac{r^2}{a^2})} dx' dy' \right|^2 \quad (2-62)$$

$$G(z') = \frac{1}{\pi^2(1-\varepsilon^2)^2} \left[ \left| \int_{-1}^1 \int_{-\sqrt{1-y^2}}^{\sqrt{1-y^2}} \cos\left(2\pi W_{20}(x^2+y^2) + z'x - \frac{r^2}{a^2}\right) dx dy \right|^2 + \left| \int_{-1}^1 \int_{-\sqrt{1-y'^2}}^{\sqrt{1-y'^2}} j \sin\left(2\pi W_{20}(x^2+y^2) + z'x - \frac{r^2}{a^2}\right) dx dy \right|^2 - \left| \int_{-\varepsilon}^{\varepsilon} \int_{-\sqrt{\varepsilon-y'^2}}^{\sqrt{\varepsilon-y'^2}} \cos\left(2\pi W_{20}(x'^2+y'^2) + z'x' - \frac{r^2}{a^2}\right) dx' dy' \right|^2 - \left| \int_{-\varepsilon}^{\varepsilon} \int_{-\sqrt{\varepsilon-y'^2}}^{\sqrt{\varepsilon-y'^2}} j \sin\left(2\pi W_{20}(x'^2+y'^2) + z'x' - \frac{r^2}{a^2}\right) dx' dy' \right|^2 \right] \quad (2-63)$$

Where  $\sin\left(2\pi W_{20}(x^2+y^2) + z'x - \frac{r^2}{a^2}\right)$  is an odd function therefore

equation (2-63) will be in new form:

$$G(z') = \frac{1}{\pi^2 (1 - \varepsilon^2)^2} \left[ \int_{-1-\sqrt{1-y^2}}^1 \int_{-\sqrt{1-y^2}}^{\sqrt{1-y^2}} \cos \left( 2\pi W_{20}(x^2 + y^2) + z'x - \frac{r^2}{a^2} \right) dx dy \right]^2 - \left[ \int_{-\varepsilon-\sqrt{\varepsilon-y'^2}}^{\varepsilon} \int_{-\sqrt{\varepsilon-y'^2}}^{\sqrt{\varepsilon-y'^2}} \cos \left( 2\pi W_{20}(x'^2 + y'^2) + z'x' - \frac{r^2}{a^2} \right) dx' dy' \right]^2 \quad (2-64)$$

Equation (2-64) represents the apodization of annular aperture with focus error.

### 2.4.3 Apodization of the Annular Aperture with Focus Error and Spherical Aberration

In substituting the super Gaussian filter with the focus error and spherical aberration in pupil function we shall get:

$$f(x, y) = e^{i \left( kW_{20}(x^2 + y^2) + W_{40}(x^2 + y^2)^2 \right)} e^{-r^2/a^2} \quad (2-65)$$

then equation (2-43) will be:

$$G(z') = \frac{1}{\pi^2 (1 - \varepsilon^2)^2} \left[ \int_{-1-\sqrt{1-y^2}}^1 \int_{-\sqrt{1-y^2}}^{\sqrt{1-y^2}} e^{ik \left( W_{20}(x^2 + y^2) + W_{40}(x^2 + y^2)^2 \right) - \frac{r^2}{a^2}} e^{iz'x} dx dy \right]^2 - \left[ \int_{-\varepsilon-\sqrt{\varepsilon-y'^2}}^{\varepsilon} \int_{-\sqrt{\varepsilon-y'^2}}^{\sqrt{\varepsilon-y'^2}} e^{ik \left( W_{20}(x'^2 + y'^2) + W_{40}(x'^2 + y'^2)^2 \right) - \frac{r^2}{a^2}} e^{iz'x'} dx' dy' \right]^2 \quad (2-66)$$

(by substituting the value of the wave number  $k = 2\pi/\lambda$ )

$$G(z') = \frac{1}{\pi^2 (1 - \varepsilon^2)^2} \left[ \int_{-1-\sqrt{1-y^2}}^1 \int_{-\sqrt{1-y^2}}^{\sqrt{1-y^2}} e^{2\pi i \left( W_{20}(x^2 + y^2) + W_{40}(x^2 + y^2)^2 \right) + iz'x - \frac{r^2}{a^2}} dx dy \right]^2 - \left[ \int_{-\varepsilon-\sqrt{\varepsilon-y'^2}}^{\varepsilon} \int_{-\sqrt{\varepsilon-y'^2}}^{\sqrt{\varepsilon-y'^2}} e^{2\pi i \left( W_{20}(x'^2 + y'^2) + W_{40}(x'^2 + y'^2)^2 \right) + iz'x' - \frac{r^2}{a^2}} dx' dy' \right]^2 \quad (2-67)$$

$$G(z') = \frac{1}{\pi^2(1-\varepsilon^2)^2} \left[ \begin{aligned} & \left| \int_{-1}^1 \int_{-\sqrt{1-y^2}}^{\sqrt{1-y^2}} \cos \left( 2\pi \left( W_{20}(x^2+y^2) + w_{40}(x^2+y^2)^2 \right) + z'x - \frac{r^2}{a^2} \right) dx dy \right|^2 \\ & + \left| \int_{-1}^1 \int_{-\sqrt{1-y^2}}^{\sqrt{1-y^2}} j \sin \left( 2\pi \left( W_{20}(x^2+y^2) + w_{40}(x^2+y^2)^2 \right) + z'x - \frac{r^2}{a^2} \right) dx dy \right|^2 \\ & - \left| \int_{-\varepsilon}^{\varepsilon} \int_{-\sqrt{\varepsilon-y'^2}}^{\sqrt{\varepsilon-y'^2}} \cos \left( 2\pi \left( W_{20}(x'^2+y'^2) + w_{40}(x'^2+y'^2)^2 \right) + z'x' - \frac{r'^2}{a^2} \right) dx' dy' \right|^2 \\ & - \left| \int_{-\varepsilon}^{\varepsilon} \int_{-\sqrt{\varepsilon-y'^2}}^{\sqrt{\varepsilon-y'^2}} j \sin \left( 2\pi \left( W_{20}(x'^2+y'^2) + w_{40}(x'^2+y'^2)^2 \right) + z'x' - \frac{r'^2}{a^2} \right) dx' dy' \right|^2 \end{aligned} \right] \quad (2-68)$$

Where  $\sin \left( 2\pi \left( W_{20}(x^2+y^2) + W_{40}(x^2+y^2)^2 \right) + z'x - \frac{r^2}{a^2} \right)$  is an odd function.

Therefore equation (2-68) will be in new form:-

$$G(z') = \frac{1}{\pi^2(1-\varepsilon^2)^2} \left[ \begin{aligned} & \left| \int_{-1}^1 \int_{-\sqrt{1-y^2}}^{\sqrt{1-y^2}} \cos \left( 2\pi \left( W_{20}(x^2+y^2) + W_{40}(x^2+y^2)^2 \right) + z'x - \frac{r^2}{a^2} \right) dx dy \right|^2 \\ & - \left| \int_{-\varepsilon}^{\varepsilon} \int_{-\sqrt{\varepsilon-y'^2}}^{\sqrt{\varepsilon-y'^2}} \cos \left( 2\pi \left( W_{20}(x'^2+y'^2) + W_{40}(x'^2+y'^2)^2 \right) + z'x' - \frac{r'^2}{a^2} \right) dx' dy' \right|^2 \end{aligned} \right] \quad (2-69)$$

Equation (2-69) represents the apodization of annular aperture with focus error and spherical aberration.

## Chapter three

### Numerical Evaluation

#### 3.1 Introduction

The equations which contain triangle functions and aberrations can not be solved analytically, therefore numerical integration method used to solve these equations. From these numerical integration methods, **Trapezoidal rule** and **Simpson rule** where the points distribute homogenous over the integration interval. In **Gaussian quadrature** the points distribute non homogenous over the integration interval. There are two types of numerical integration methods classified according to their point's distribution.

1. Numerical integration ways which have points distance equally and its point's distribution is homogenous over the integration interval. Form these methods (**Trapezoidal rule**, **simpson rule** and **filon rule**) [62].
2. Numerical integral methods that have non homogenous points distribution which have difference weight values, these point values and weight coefficient given in special tables depend on number of points over integration interval from these numerical integration **Gauss rule**. In spite of complexity which **Gauss rule** contain in comparison with integration methods which have a non homogenous points distribution, but it is the best way to solve the equation which contains oscillating function like **((sin, cos) functions)** and it gives high accuracy in solving these equations.

#### 3.2 Gaussian Method

Gauss rule in numerical integration is regarded an application for **Legendre** polynomials( $P_N(X)$ ). Gauss proved that  $f(t)$  represents polynomial of  $(2N - 1)$  order or less, so we can say:



$$\int_{-1}^1 f(t)dt = \sum_{i=1}^{20} W_i f(t_i) \quad (3-1)$$

where:

$W_i$ : represents Gaussian weight values which have numerical values that depend on number of points ( $\bar{N}$ ) used.

$t_i$ : represents **Legendr** polynomial roots of order( $\bar{N}$ ) that make  $P_{\bar{N}}(t_i) = 0$ .

Reference [63] included weight values, and the points used in the method reach to  $\bar{N}96$ .

**Al-Hamdani**[4] indicates the optimal **Gauss** number which gives more accurate results in comparison with **Simpson rule**. Also **Al-Hamdani** [4] indicates the effect of points distribution process in exit pupil and on results accuracy and he suggested the optimal points distributions for annular aperture. Figure (3-1) illustrate integral limits for circular aperture with optimal Gauss points distribution in exit pupil, where the short distance on x-axis contains less number of points and the longitudinal distance contains large number of points, that for reduction computing-time which increases with the increasing number of Gauss points. Also the accuracy increases with increase **Gauss** point; therefore we make a balance between, the accuracy and computing-time when choosing the optimal number of Gaussian points

When the integration limits of  $f(x)$  are (a,b) the next expression can be used:

$$\begin{aligned} x_i &= \frac{b-a}{2} t_j + \frac{b+a}{2} \\ y_j &= \frac{b-a}{2} t_i + \frac{b+a}{2} \end{aligned} \quad (3-2)$$

Therefore equation (3-1) can be written as:

$$\int_a^b f(x)dx = \frac{b-a}{2} \sum_{i=1}^{\bar{N}} W_i f(x_i) \quad (3-3)$$

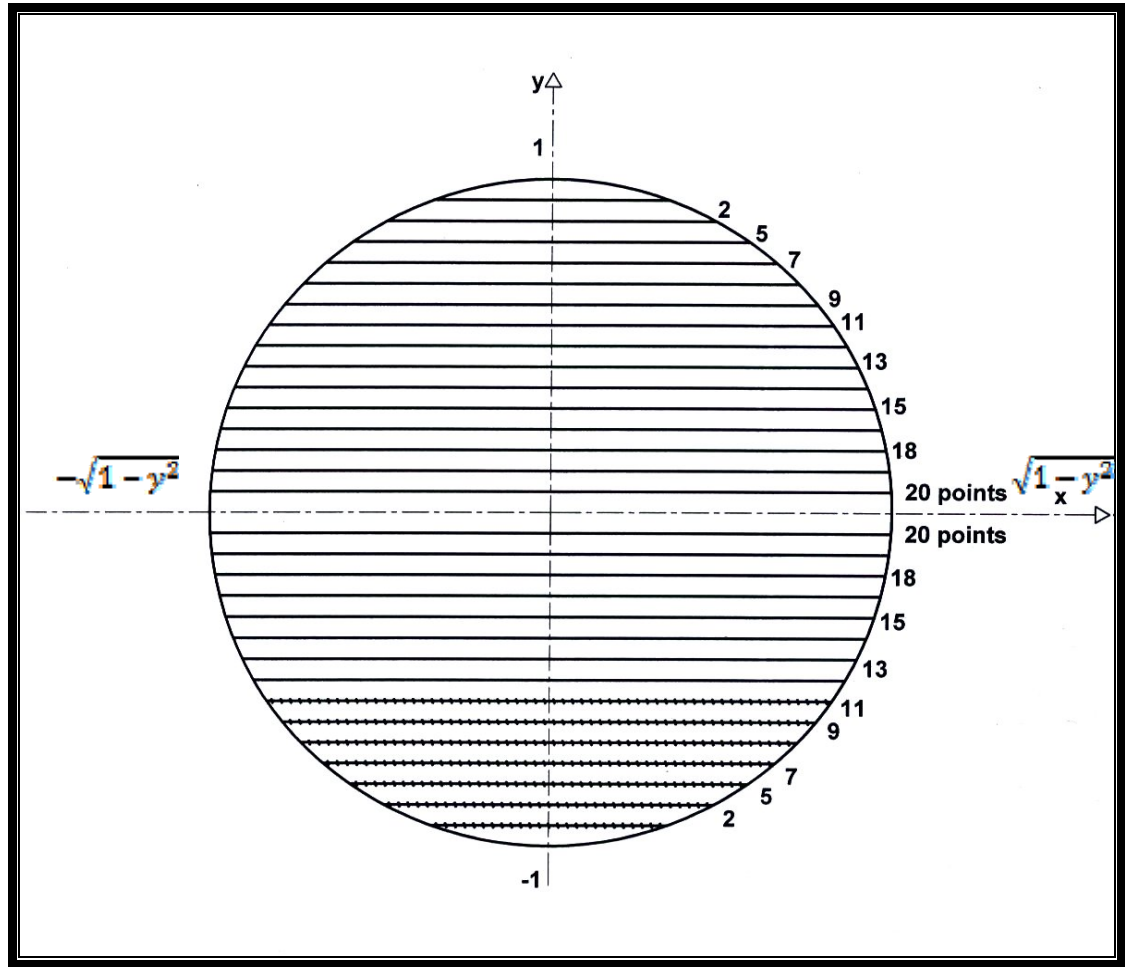


Figure (3-1): Integral limits for circular aperture with optimal Gauss point's distribution in exit pupil

### 3.3 Numerical Evaluation of PSF

#### 3.3.1 Numerical Evaluation of a Diffraction-Limited Optical System

Equation (2-21) (which represent the **PSF** for a diffraction-limited optical system) can be written according to **Gaussian formula**.

$$G(z') = \frac{1}{\pi^2} \left| \int_{-1-\sqrt{1-y^2}}^1 \int_{-1-\sqrt{1-y^2}}^{\sqrt{1-y^2}} \tau(x, y) \cos(z'x) dx dy \right|^2$$

where:

$$y_j = t_i$$

$$x_i = \sqrt{1 - y_j^2} \cdot t_j$$

By using equation (2-21) we get:

$$G(z') = \frac{1}{\pi^2} \left| \tau(x, y) \sum_{j=1}^{20} W_j \sqrt{1 - y_j^2} \sum_{i=1}^{20} W_i \cos(z'x_i) \right|^2 \quad (3-4)$$

### 3.3.2 Numerical Evaluation of PSF for Optical System Contained Focus Error.

Equation (2-29) can be writing *in Gaussian formula*:

$$G(z') = \frac{1}{\pi^2} \left| \tau(x, y) \sum_{j=1}^{20} W_j \sqrt{1 - y_j^2} \sum_{i=1}^{20} W_i \cos(2\pi(W_{20}(x_i^2 + y_j^2)) + z'x_i) \right|^2 \quad (3-5)$$

### 3.3.3. Numerical Evaluation of PSF for Optical System Contained Third Order Spherical Aberration.

According to *Gaussian formula* equation (2-35) is written as follows:

$$G(z') = \frac{1}{\pi^2} \left| \tau(x, y) \sum_{j=1}^{20} W_j \sqrt{1 - y_j^2} \sum_{i=1}^{20} W_i \cos(2\pi(W_{20}(x_i^2 + y_j^2) + W_{40}(x_i^2 + y_j^2)) + z'x_i) \right|^2 \quad (3-6)$$

## 3.4. Numerical Evaluation of PSF for Optical System Contained Annular Aperture

### 3.4.1. Numerical Evaluation of PSF for a Diffraction-Limited Optical System Contained Annular Aperture.

Equation (2-45) (which represents the *PSF* for a diffraction-limited optical system with annular aperture) can be written according to *Gaussian formula*.

$$G(z') = \frac{1}{\pi^2(1 - \varepsilon^2)^2} \left| \int_{-1-\sqrt{1-y^2}}^1 \int_{-1-\sqrt{1-y^2}}^{\sqrt{1-y^2}} \tau(x, y) \cos(z'x) dx dy - \int_{-\varepsilon-\sqrt{\varepsilon-y^2}}^{\varepsilon} \int_{-\varepsilon-\sqrt{\varepsilon-y^2}}^{\sqrt{\varepsilon-y^2}} \cos(z'x) dx dy \right|^2 \quad (3-7)$$

where:

$$\begin{aligned} y_j &= t_i & y'_j &= \varepsilon t_i \\ x_i &= \sqrt{1 - y_j^2} \cdot t_j & x'_i &= \sqrt{\varepsilon - y_j^2} \cdot t_j \end{aligned}$$

therefore:

$$G(z') = \frac{1}{\pi^2(1 - \varepsilon^2)^2} \left| \begin{aligned} &\tau(x, y) \sum_{j=1}^{20} W_j \sqrt{1 - y_j^2} \sum_{i=1}^{20} W_i \cos(z'x_i) \\ &- \tau(x, y) \varepsilon \sum_{j=1}^{20} W_j \sqrt{\varepsilon - y_j^2} \sum_{i=1}^{20} W_i \cos(z'x'_i) \end{aligned} \right|^2 \quad (3-8)$$

### 3.4.2. Numerical Evaluation of PSF for Annular Aperture Optical System with Focus Error.

When the focus error is present equation (2-49) will take the new form according to *Gaussian formula*.

$$G(z') = \frac{1}{\pi^2(1 - \varepsilon^2)^2} \left| \begin{aligned} &\tau(x, y) \sum_{j=1}^{20} W_j \sqrt{1 - y_j^2} \sum_{i=1}^{20} w_i \cos(2\pi(W_{20}(x_i^2 + y_j^2)) + z'x_i) \\ &- \tau(x, y) \varepsilon \sum_{j=1}^{20} W_j \sqrt{\varepsilon - y_j^2} \sum_{i=1}^{20} w_i \cos(2\pi(W_{20}(x_i'^2 + y_j'^2)) + z'x'_i) \end{aligned} \right|^2 \quad (3-9)$$

### 3.4.3. Numerical Evaluation of PSF for Annular Aperture Optical System Contained Third Order Spherical Aberration.

Equation (2-54) will take the new form according to *Gaussian formula*:

$$G(z') = \frac{1}{\pi^2(1 - \varepsilon^2)^2} \left| \begin{aligned} &\tau(x, y) \sum_{j=1}^{20} W_j \sqrt{1 - y_j^2} \sum_{i=1}^{20} W_i \cos(2\pi(W_{20}(x_i^2 + y_j^2) + W_{40}(x_i^2 + y_j^2)^2) + z'x_i) \\ &- \tau(x, y) \varepsilon \sum_{j=1}^{20} W_j \sqrt{\varepsilon - y_j'^2} \sum_{i=1}^{20} W_i \cos(2\pi(W_{20}(x_i'^2 + y_j'^2) + W_{40}(x_i'^2 + y_j'^2)^2) + z'x'_i) \end{aligned} \right|^2 \quad (3-10)$$

### 3.5 Numerical Evaluation of PSF for Optical System Contain Apodized Annular Aperture:

#### 3.5.1 Numerical Evaluation of PSF for a Diffraction-Limited Optical System Contain Apodized Annular Aperture.

Equation (2-58) can be written according to **Gaussian formula** as follows.

$$G(z') = \frac{1}{\pi^2 (1 - \varepsilon^2)^2} \left| \sum_{j=1}^{20} W_j \sqrt{1 - y_j^2} \sum_{i=1}^{20} W_i \cos(z'x_i - \frac{r^2}{a^2}) - \varepsilon \sum_{j=1}^{20} W_j \sqrt{\varepsilon - y_j'^2} \sum_{i=1}^{20} W_i \cos(z'x'_i - \frac{r^2}{a^2}) \right|^2 \quad (3-11)$$

#### 3.5.2. Numerical Evaluation of PSF for Optical System Contained Apodized Annular Aperture with Focus Error

Equation (2-64) (which represents the **PSF** of apodized annular aperture contained focus error) will take the new form according to **Gaussian formula**:

$$G(z') = \frac{1}{\pi^2 (1 - \varepsilon^2)^2} \left| \sum_{j=1}^{20} W_j \sqrt{1 - y_j^2} \sum_{i=1}^{20} W_i \cos\left(2\pi W_{20}(x_i^2 + y_j^2) + z'x_i - \frac{r^2}{a^2}\right) - \varepsilon \sum_{j=1}^{20} W_j \sqrt{\varepsilon - y_j'^2} \sum_{i=1}^{20} W_i \cos\left(2\pi W_{20}(x_i'^2 + y_j'^2) + z'x'_i - \frac{r^2}{a^2}\right) \right|^2 \quad (3-12)$$

### 3.5.3. Numerical Evaluation of PSF for Optical System Contained Apodized Annular Aperture with Third Order Spherical Aberration

In the presence of the aberrations (third order spherical aberration) equation (2-69) will take the new form according to **Gauss formula**:

$$G(z) = \frac{1}{\pi^2(1-\varepsilon^2)^2} \left| \frac{\sum_{j=1}^{20} W_j \sqrt{1-y_j^2} \sum_{i=1}^{20} W_i \cos \left( 2\pi \left( W_{20}(x_i^2 + y_j^2) + W_{40}(x_i^2 + y_j^2)^2 \right) + z'x_i - \frac{r^2}{a^2} \right)}{-\varepsilon \sum_{j=1}^{20} W_j \sqrt{\varepsilon - y_j^2} \sum_{i=1}^{20} W_i \cos \left( 2\pi \left( W_{20}(x_i^2 + y_j^2) + W_{40}(x_i^2 + y_j^2)^2 \right) + z'x_i - \frac{r^2}{a^2} \right)} \right|^2 \quad (3-13)$$

### 3.6. The Programs

After writing the last equations for **PSF** according to Gaussian formula in numerical integration for each state of aberrations present in the optical system and after choice the optimum number and the optimum distribution for Gaussian's points, program in **Q.Basic** language version 4.5 has been written to calculate the results of these functions that contain focus error and spherical aberrations with obstruction and super Gaussian filter.

**Appendix (A)** explains a program to calculate **PSF** for free optical system. This program help us to change the focus error values ( $W_{20}=0.25, 0.5 \text{ and } 0.75\lambda$ ) and spherical aberrations values ( $W_{40}=0.1, 0.3, 0.5, 0.7 \text{ and } 0.9\lambda$ ) or width factor of the super Gaussian filter ( $a=0.1-0.9$ ).

**Appendix (B)** explains a program to calculate **PSF** for obstruction optical system with super Gaussian filter. This program help us to change the obstruction ratio ( $\epsilon$ ) and focus error values ( $W_{20}=0.25, 0.5 \text{ and } 0.75\lambda$ ) and spherical aberrations values ( $W_{40}=0.1, 0.3, 0.5, 0.7 \text{ and } 0.9\lambda$ ) or width factor of the super Gaussian filter ( $a=0.1-0.9$ ).

Table (3-1) explains the comparison between the extracted results by using the programs placed to calculate **PSF** in this research and Hopkins results [57] also calculated results from Airy pattern for a limited-diffraction optical system equation (2-24).

The programs that are used to compute the PSF were correct because the values of free aberration PSF of annular aperture were in agreement with the numerical analytical values.

Table (3-1) comparison between the written program results and Hopkins results and the results calculated from the equation (2-24).

Z	The current research	Hopkins results	The results calculated from Airy pattern Equation(2-24)
0	1	1	1
1.25	0.6675	0.6645	0.6645
2.5	0.1581	0.1543	0.1544
3.75	0.0003	0.0002	0.0002
5	0.0171	0.017	0.017
6.25	0.0049	0.0046	0.0046
7.5	0.0013	0.0015	0.0015
8.75	0.0037	0.0036	0.0036
10	0	0	0



## Chapter four

### Results and Discussions

#### 4.1 Introduction

This chapter is containing of results and discussions. Where the different obstruction ratio effect has studied on the optical system with or without aberrations. Also the Gaussian filter with different width factor on the annular optical system with or without aberrations, to know it is effect on *PSF* and *Strehl* ratio.

#### 4.2 Effect of the Obstruction Ratio on the Free Optical System

The central tops of the *PSF* effected with the increase of the obstruction ratio in the optical system which clearly appears through the data that is calculated from equation (3-8) and is given in table (4-1) and according to figure (4-1). The first curve represents optical system without obstruction. The intensity in the *PSF* is almost containing under the curve with few intensity distributions on the secondary tops. The first curve contained on (84%) from total intensity , and the remaining intensity(16%) distributed on the secondary tops . The first curve represents Airy disk .When the obstruction increases, the intensity will decrease about original value and equals to zero when the obstruction is completed.

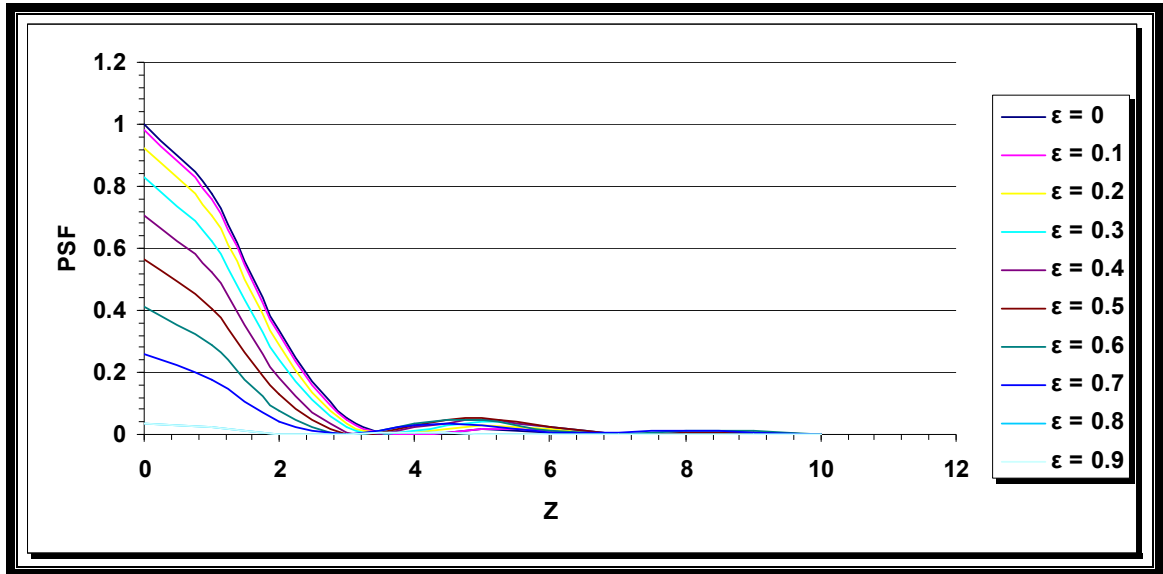


Figure (4-1): Effect of the obstruction ratio on the free optical system.

Table (4-1): Effect of the obstruction ratio on the free optical system.

z	$\varepsilon = 0$	$\varepsilon = 0.1$	$\varepsilon = 0.2$	$\varepsilon = 0.3$	$\varepsilon = 0.4$	$\varepsilon = 0.5$	$\varepsilon = 0.6$	$\varepsilon = 0.7$	$\varepsilon = 0.8$	$\varepsilon = 0.9$
0	1.00012	0.98022	0.92171	0.8282	0.70569	0.56257	0.40965	0.26013	0.0361	0.0361
1	0.77469	0.7572	0.7062	0.62594	0.52321	0.40689	0.2874	0.17601	0.02232	0.02232
2	0.33268	0.3213	0.28899	0.24086	0.18425	0.12727	0.07717	0.03896	0.00285	0.00285
3	0.05112	0.04675	0.0353	0.021	0.00869	0.00161	4.3E-05	0.00153	0.00151	0.00151
4	0.00109	0.00183	0.00488	0.0116	0.02159	0.03138	0.03574	0.03111	0.00577	0.00577
5	0.01715	0.01979	0.02761	0.03917	0.04984	0.05309	0.0451	0.02872	0.00229	0.00229
6	0.00849	0.01035	0.01572	0.0226	0.02609	0.02211	0.01238	0.00358	0.00013	0.00013
7	1.6E-06	0.00011	0.00104	0.0025	0.00231	0.00044	0.00051	0.0038	0.00272	0.00272
8	0.00345	0.00245	0.00091	0.00039	0.00106	0.00448	0.01071	0.01374	0.00216	0.00216
9	0.00298	0.00208	0.00083	0.00063	0.00212	0.00644	0.01012	0.00755	2.5E-05	2.5E-05
10	7.7E-05	0	0.0002	0.00013	0.0002	0.00172	0.00176	8.8E-05	0.00126	0.00126

### 4.3 Effect of the Obstruction on the Optical System Contained Focus Error ( $W_{20}=0.25, 0.5$ ) $\lambda$ .

The central tops of the **PSF** effect in the presence of the focus error in the optical system which clearly appears through the data that is calculated from equation (3-9) and is given in the tables (4-2), (4-3) where the maximum intensity of the **PSF** in figure (4-2) equals to (0.810646) when the focus error equals ( $W_{20}=0.25\lambda$ ). The intensity ratio reduced with obstruction increases like in figure (4-2). When the focus error equals to ( $W_{20}=0.5\lambda$ ), the maximum intensity will reduce to (0.405283) from its value, and this value will be reduced with increase the obstruction like in figure (4-3).

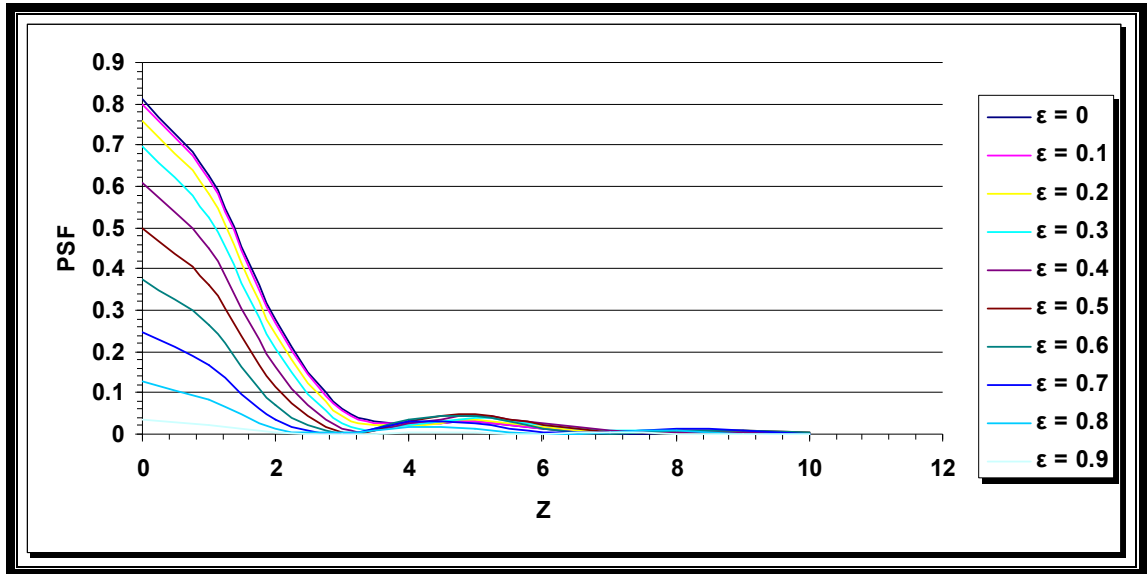


Figure (4-2): Effect of the obstruction on the optical system contains focus error ( $W_{20}=0.25$ )  $\lambda$ .

Table (4-2): Effect of the obstruction on the optical system contains focus error ( $W_{20}=0.25$ )  $\lambda$ .

z	$\varepsilon = 0$	$\varepsilon = 0.1$	$\varepsilon = 0.2$	$\varepsilon = 0.3$	$\varepsilon = 0.4$	$\varepsilon = 0.5$	$\varepsilon = 0.6$	$\varepsilon = 0.7$	$\varepsilon = 0.8$	$\varepsilon = 0.9$
0	0.81064	0.79791	0.75974	0.69642	0.60905	0.50043	0.37628	0.24651	0.12619	0.03583
1	0.62859	0.61700	0.58263	0.52673	0.45180	0.36206	0.26404	0.16680	0.08187	0.02215
2	0.27725	0.26868	0.24409	0.20674	0.16156	0.11446	0.07134	0.03703	0.01422	0.00282
3	0.06226	0.05746	0.04474	0.02843	0.01369	0.00427	0.00100	0.00166	0.00259	0.00150
4	0.02692	0.02544	0.02257	0.02170	0.02489	0.03047	0.03358	0.02963	0.01843	0.00572
5	0.03061	0.03117	0.03379	0.03952	0.04628	0.04863	0.04195	0.02736	0.01177	0.00227
6	0.01210	0.01329	0.01714	0.02268	0.02571	0.02198	0.01255	0.00374	0.0002	0.0001
7	0.00183	0.00268	0.00531	0.00813	0.00782	0.00421	0.00205	0.00396	0.00552	0.00270
8	0.00508	0.00532	0.00628	0.00705	0.00638	0.00685	0.01075	0.01319	0.00881	0.00214
9	0.00369	0.00351	0.00356	0.00363	0.00393	0.00676	0.00986	0.00742	0.00201	2.6E-05
10	0.00035	0.00012	7.5E-05	5.8E-05	0.00063	0.00274	0.00279	0.00055	0.00086	0.00124

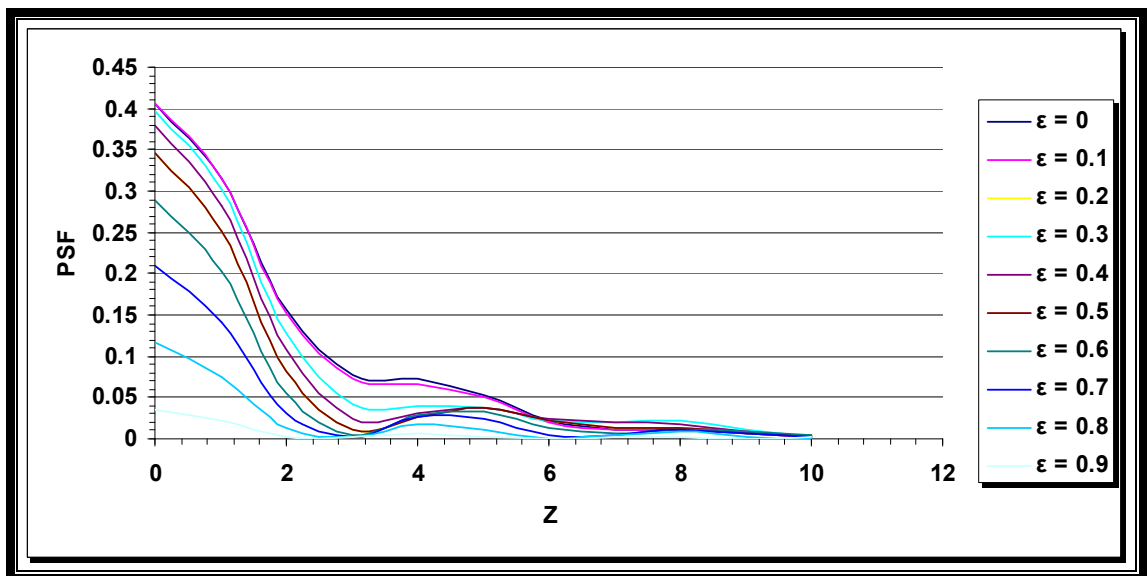


Figure (4-3): Effect of the obstruction on the optical system contains focus error ( $W_{20}=0.5$ )  $\lambda$ .

Table (4-3): Effect of the obstruction on the optical system contains focus error ( $W_{20}=0.25$ )  $\lambda$ .

$z$	$\varepsilon = 0$	$\varepsilon = 0.1$	$\varepsilon = 0.2$	$\varepsilon = 0.3$	$\varepsilon = 0.4$	$\varepsilon = 0.5$	$\varepsilon = 0.6$	$\varepsilon = 0.7$	$\varepsilon = 0.8$	$\varepsilon = 0.9$
0	0.40528	0.40518	0.34595	0.39724	0.38023	0.34595	0.28894	0.20902	0.11637	0.03504
1	0.31579	0.31477	0.25061	0.30137	0.28265	0.25061	0.20287	0.14147	0.07550	0.02166
2	0.15582	0.15268	0.08235	0.12794	0.10715	0.08235	0.05603	0.03172	0.01315	0.00276
3	0.07796	0.07307	0.01019	0.04167	0.02368	0.01019	0.00335	0.00200	0.00245	0.00147
4	0.07187	0.06689	0.02748	0.04035	0.03064	0.02748	0.02779	0.02552	0.01703	0.00560
5	0.05382	0.05062	0.03709	0.03803	0.03672	0.03709	0.03359	0.02362	0.01092	0.00222
6	0.02131	0.02074	0.02114	0.02235	0.02407	0.02114	0.01279	0.00416	0.00031	0.00012
7	0.01002	0.01151	0.01281	0.02016	0.01962	0.01281	0.00584	0.00438	0.00519	0.00264
8	0.01139	0.01344	0.01217	0.02113	0.01792	0.01217	0.01071	0.01169	0.00818	0.00209
9	0.00632	0.00757	0.00755	0.01086	0.00839	0.00755	0.00909	0.00704	0.00200	2.9E-05
10	0.00167	0.00166	0.00531	0.00188	0.00259	0.00531	0.00534	0.00177	0.00097	0.00122

#### 4.4 Effect of the Width Factor of Super Gaussian Filter on Strehl Ratio for Free Optical System without an Obstruction.

The effect of the super Gaussian filter on the free optical system is shown in figure (4-4). This figure is drawn from the data that is calculated from equation (3-8) and is given in table (4-4). The upper curve in the figure (4-4) represents the intensity distribution for a diffraction-limited system contains super Gaussian filter with width factor  $a=1$ , where the *Strehl* ratio equals to (0.642352) and it is decreased with decreasing the width of super Gaussian filter, and the same think is done in the other curves.

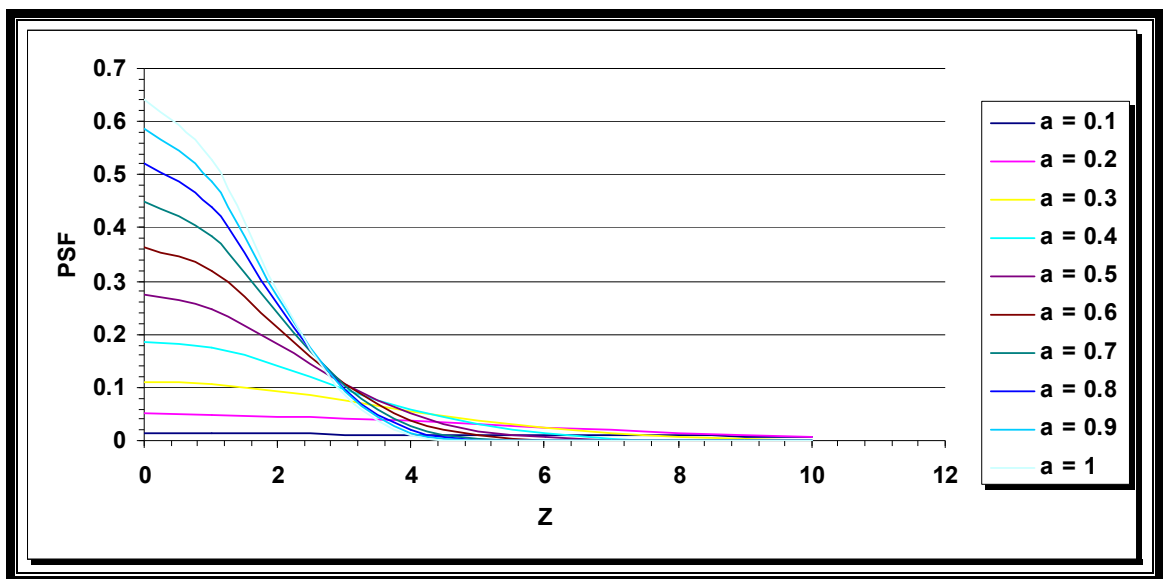


Figure (4-4): Strehl ratio for the free optical system contains super Gaussian filter & ( $\varepsilon = 0$ ).

Table (4-4): Strehl ratio for the free optical system contains super Gaussian filter & ( $\varepsilon = 0$ ).

z	$\varepsilon = 0$	$\varepsilon = 0.1$	$\varepsilon = 0.2$	$\varepsilon = 0.3$	$\varepsilon = 0.4$	$\varepsilon = 0.5$	$\varepsilon = 0.6$	$\varepsilon = 0.7$	$\varepsilon = 0.8$	$\varepsilon = 0.9$
0	1.2E-02	4.9E-02	0.10932	0.18651	0.27437	0.36401	0.44820	0.52310	0.58764	0.64235
1	1.2E-02	4.9E-02	0.10475	0.17355	0.24753	0.31935	0.38425	0.44036	0.48769	0.52716
2	1.2E-02	4.6E-02	9.2E-02	0.13974	0.18129	0.21413	0.23894	0.25747	0.27137	0.28194
3	1.1E-02	4.1E-02	7.4E-02	9.7E-02	0.10697	0.10725	0.10288	9.7E-02	9.1E-02	8.5E-02
4	1.1E-02	3.6E-02	0.05513	5.8E-02	5.0E-02	0.03837	2.7E-02	1.9E-02	1.3E-02	8.8E-03
5	1.0E-02	3.0E-02	3.7E-02	3.0E-02	0.01841	9.0E-03	3.4E-03	7.9E-04	1.1E-05	2.8E-04
6	1.0E-02	2.4E-02	2.3E-02	1.3E-02	5.2E-03	1.2E-03	5.0E-05	1.8E-04	8.4E-04	1.6E-03
7	9.4E-03	1.9E-02	1.3E-02	5.0E-03	1.1E-03	9.2E-05	1.5E-05	1.1E-04	1.9E-04	2.2E-04
8	8.6E-03	1.4E-02	7.0E-03	0.00165	2.0E-04	1.2E-05	4.5E-06	2.5E-05	9.2E-05	2.1E-04
9	7.8E-03	1.0E-02	3.3E-03	4.6E-04	3.4E-05	1.2E-05	4.8E-05	1.4E-04	3.0E-04	4.9E-04
10	6.9E-03	7.0E-03	1.4E-03	1.1E-04	5.9E-06	6.5E-06	2.1E-05	4.2E-05	6.3E-05	7.8E-05

#### 4.5 Effect of the Width Factor of Super Gaussian Filter on Resolution of the Free Optical System without an Obstruction.

The width factor of the super Gaussian filter will affect on the resolution of the free optical system without obstruction ratio. The effect will be shown in the figure (4-5) that is drawn from the data which is extracted from equation (3-8) and is given in table (4-5). The lower curve of figure (4-5) represents the resolution of the optical system which contain super Gaussian filter with  $a = 1$ . Also, it is noticed clearly that in the same figure that the resolution ability of the optical system increases with the increase of the width factors of the super Gaussian filter, where the resolution is better when  $a = 1$ .

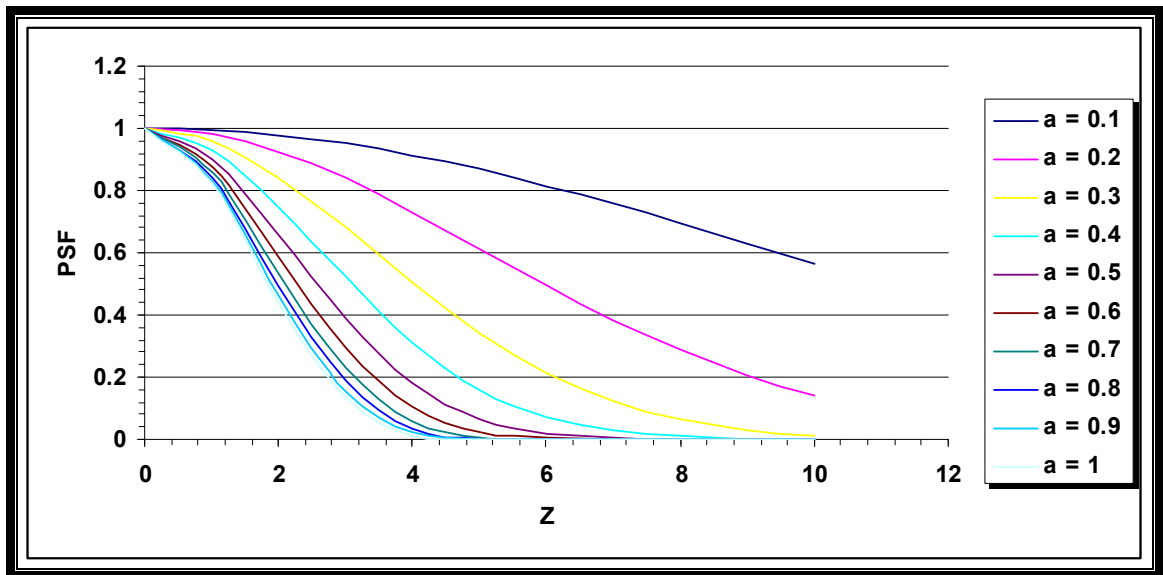


Figure (4-5): Point spread function for the free optical system contains super Gaussian filter & ( $\varepsilon = 0$ ).

Table (4-5): Point spread function for the free optical system contains super Gaussian filter & ( $\varepsilon = 0$ ).

<b>z</b>	$\varepsilon = 0$	$\varepsilon = 0.1$	$\varepsilon = 0.2$	$\varepsilon = 0.3$	$\varepsilon = 0.4$	$\varepsilon = 0.5$	$\varepsilon = 0.6$	$\varepsilon = 0.7$	$\varepsilon = 0.8$	$\varepsilon = 0.9$
<b>0</b>	1	1	1	1	1	1	1	1	1	1
<b>1</b>	9.9E-01	9.8E-01	0.95815	0.93047	0.90217	0.87732	0.85733	0.84182	0.82990	0.82068
<b>2</b>	9.7E-01	9.2E-01	0.84243	0.74922	0.66076	0.58826	0.53311	0.49219	0.46179	0.43892
<b>3</b>	9.5E-01	8.4E-01	0.68053	0.52113	0.38987	0.29463	0.22955	0.18543	0.15502	0.13353
<b>4</b>	9.1E-01	7.3E-01	0.50429	0.31310	0.18296	0.10541	0.06135	0.03651	0.02229	0.01376
<b>5</b>	8.7E-01	6.1E-01	0.34301	0.16137	0.06713	0.02488	0.00769	0.00152	1.9E-05	0.00043
<b>6</b>	8.1E-01	4.9E-01	0.21403	0.07184	0.01895	0.00340	0.00011	0.00035	0.00143	0.00255
<b>7</b>	7.5E-01	3.8E-01	0.12256	0.02718	0.00411	0.00025	3.3E-05	0.00022	0.00033	0.00035
<b>8</b>	6.9E-01	2.8E-01	0.06421	0.00885	0.00073	3.4E-05	1.0E-05	4.8E-05	0.00015	0.0003
<b>9</b>	6.3E-01	2.0E-01	0.03091	0.00248	0.00012	3.4E-05	0.00010	0.00028	0.00051	0.00076
<b>10</b>	5.6E-01	1.4E-01	0.01362	0.00059	2.1E-05	1.7E-05	4.7E-05	8.1E-05	0.00010	0.00012

#### 4.6 Effect of the Width Factor of Super Gaussian Filter on *Strehl* Ratio for the Optical System Contains Focus Error ( $W_{20} = 0.25, 0.5, \text{ and } 0.75$ ) $\lambda$ .

From figure (4-6) which is drawn from the data that are calculated from equation (3-9) and given in table (4-6). We notice that the first curve appears of a maximum *Strehl* ratio which starts at (0.521329) when  $a=1$ , this value reduces with the decrease of the width factor of the super Gaussian filter, it is reduced to (9.93E-03) when  $a=0.1$ . When the focus error equals to ( $W_{20}=0.5 \lambda$ ), the *Strehl* ratio reduces to (0.262423) when  $a=1$ . Also it reduce with reduces ( $a$ ) for the other curves as it is shown in figure (4-7) that is drawn from the data given in table (4-7). Figure (4-8) shows the decrease in *Strehl* ratio with the increase of the focus error ( $W_{20}=0.75 \lambda$ ), the maximum value of the *Strehl* ratio equals to (6.10E-02) when  $a=1$ , and it decreases with the decrease of ( $a$ ). The energy distribution under the curves decreases with the increase of the focus error. Figure (4-8) drawn from the data given in table (4-8).

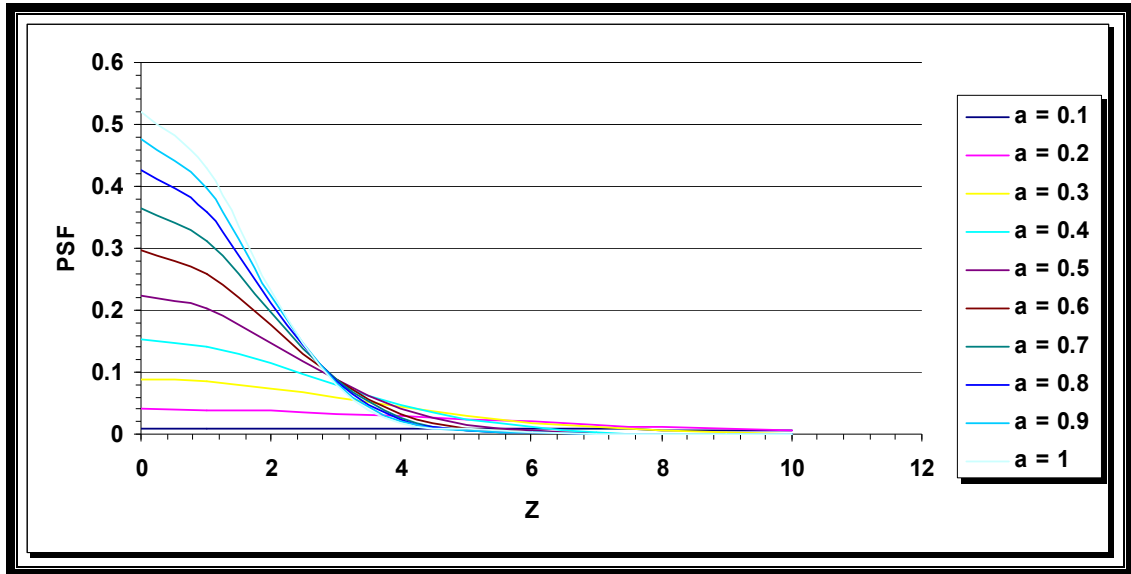


Figure (4-6): Strehl ratio for the optical system contains focus error ( $W_{20} = 0.25 \lambda$ ) with super Gaussian filter & ( $\varepsilon = 0$ ).

Table (4-6): Strehl ratio for the optical system contains focus error ( $W_{20} = 0.25 \lambda$ ) with super Gaussian filter & ( $\varepsilon = 0$ ).

z	$\varepsilon = 0$	$\varepsilon = 0.1$	$\varepsilon = 0.2$	$\varepsilon = 0.3$	$\varepsilon = 0.4$	$\varepsilon = 0.5$	$\varepsilon = 0.6$	$\varepsilon = 0.7$	$\varepsilon = 0.8$	$\varepsilon = 0.9$
0	9.9E-03	4.0E-02	8.8E-02	0.15191	0.22361	0.29640	0.36454	0.42505	0.47716	0.52132
1	9.8E-03	3.9E-02	8.5E-02	0.14130	0.20177	0.26024	0.31290	0.35834	0.39662	0.42853
2	9.7E-03	3.7E-02	7.4E-02	0.11367	0.14794	0.17524	0.19604	0.21171	0.22356	0.23263
3	9.4E-03	3.3E-02	6.0E-02	7.9E-02	0.08765	8.9E-02	8.7E-02	8.4E-02	8.1E-02	7.8E-02
4	9.0E-03	2.9E-02	4.4E-02	0.04732	4.1E-02	3.3E-02	2.7E-02	2.2E-02	0.01958	1.8E-02
5	8.6E-03	2.4E-02	3.0E-02	2.4E-02	1.5E-02	9.4E-03	6.4E-03	5.8E-03	6.5E-03	8.0E-03
6	8.1E-03	1.9E-02	1.8E-02	1.0E-02	4.7E-03	2.1E-03	1.7E-03	2.3E-03	3.3E-03	4.3E-03
7	7.5E-03	1.5E-02	1.0E-02	4.0E-03	1.1E-03	4.0E-04	4.2E-04	5.6E-04	7.0E-04	8.0E-04
8	6.9E-03	1.1E-02	5.5E-03	1.3E-03	2.0E-04	3.9E-05	4.4E-05	1.2E-04	2.9E-04	5.2E-04
9	6.2E-03	8.1E-03	2.6E-03	3.6E-04	2.4E-05	4.3E-06	6.9E-05	2.2E-04	4.4E-04	6.9E-04
10	5.5E-03	5.6E-03	0.00115	8.5E-05	1.4E-06	6.3E-06	3.3E-05	7.0E-05	1.0E-04	1.4E-04

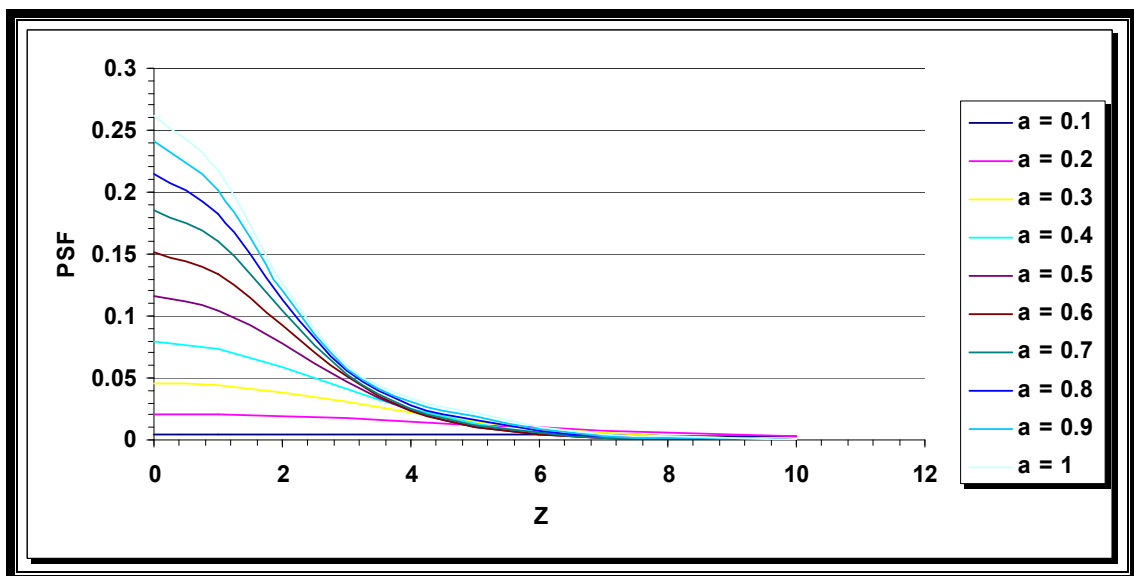


Figure (4 - 7): Strehl ratio for the optical system contains focus error ( $W_{20} = 0.5 \lambda$ ) with super Gaussian filter & ( $\varepsilon = 0$ ).

Table (4-7): Strehl ratio for the optical system contains focus error ( $W_{20} = 0.5 \lambda$ ) with super Gaussian filter & ( $\varepsilon = 0$ ).

z	$\varepsilon = 0$	$\varepsilon = 0.1$	$\varepsilon = 0.2$	$\varepsilon = 0.3$	$\varepsilon = 0.4$	$\varepsilon = 0.5$	$\varepsilon = 0.6$	$\varepsilon = 0.7$	$\varepsilon = 0.8$	$\varepsilon = 0.9$
0	4.9E-03	2.0E-02	4.5E-02	0.07881	0.11563	0.15211	0.18573	0.21537	0.24083	0.26242
1	4.8E-03	1.9E-02	4.3E-02	7.3E-02	0.10458	0.13421	0.16050	0.18297	0.20182	0.21749
2	4.8E-03	1.8E-02	3.8E-02	5.9E-02	7.7E-02	9.2E-02	0.10442	0.11361	0.12074	0.12632
3	4.6E-03	1.7E-02	3.0E-02	4.1E-02	4.7E-02	5.0E-02	5.3E-02	5.5E-02	5.8E-02	6.0E-02
4	4.4E-03	1.4E-02	2.2E-02	2.4E-02	0.02402	2.3E-02	2.5E-02	2.7E-02	0.03089	3.4E-02
5	4.2E-03	1.2E-02	0.01513	1.2E-02	1.0E-02	1.0E-02	1.2E-02	1.5E-02	1.9E-02	2.2E-02
6	4.0E-03	9.8E-03	9.3E-03	5.8E-03	4.0E-03	4.3E-03	5.6E-03	7.4E-03	9.1E-03	1.0E-02
7	3.7E-03	7.5E-03	5.2E-03	2.3E-03	1.4E-03	1.5E-03	2.0E-03	2.6E-03	3.2E-03	3.8E-03
8	3.4E-03	5.6E-03	2.6E-03	8.0E-04	4.2E-04	5.0E-04	7.9E-04	1.2E-03	1.9E-03	2.6E-03
9	3.0E-03	3.9E-03	1.2E-03	2.4E-04	1.1E-04	1.9E-04	4.3E-04	8.0E-04	1.2E-03	1.7E-03
10	2.7E-03	2.7E-03	5.4E-04	6.7E-05	3.1E-05	6.9E-05	1.5E-04	2.6E-04	3.8E-04	5.0E-04

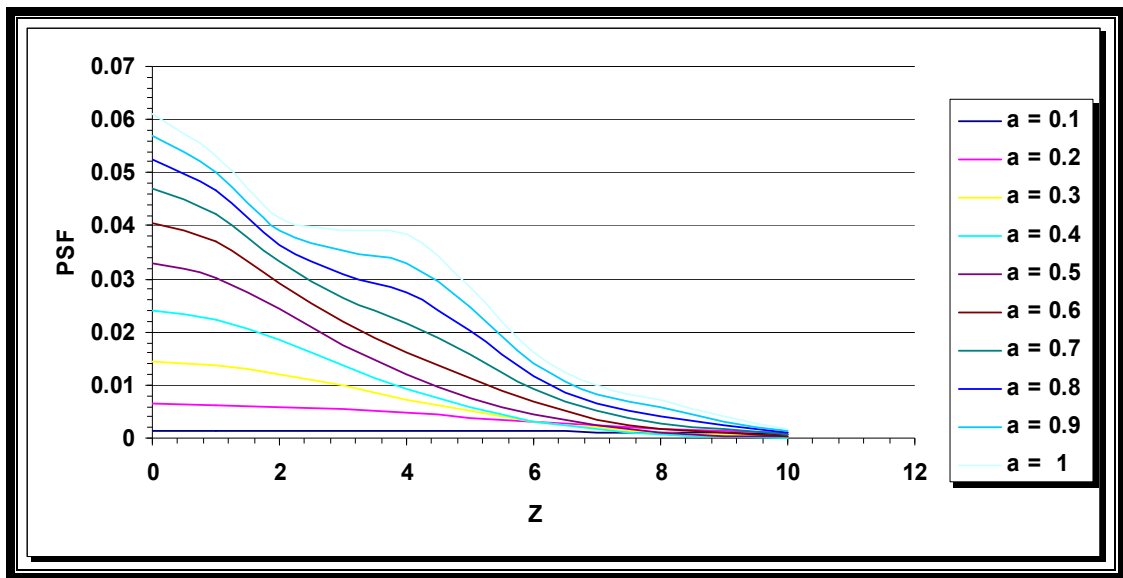


Figure (4-8): Strehl ratio for the optical system contains focus error ( $W_{20} = 0.75 \lambda$ ) with super Gaussian filter & ( $\varepsilon = 0$ ).

Table (4-8): Strehl ratio for the optical system contains focus error ( $W_{20} = 0.75 \lambda$ ) with super Gaussian filter & ( $\varepsilon = 0$ ).

z	$\varepsilon = 0$	$\varepsilon = 0.1$	$\varepsilon = 0.2$	$\varepsilon = 0.3$	$\varepsilon = 0.4$	$\varepsilon = 0.5$	$\varepsilon = 0.6$	$\varepsilon = 0.7$	$\varepsilon = 0.8$	$\varepsilon = 0.9$
0	1.5E-03	6.4E-03	1.4E-02	2.3E-02	3.2E-02	4.0E-02	4.6E-02	5.2E-02	5.7E-02	6.1E-02
1	1.5E-03	6.3E-03	0.01382	0.02240	3.0E-02	3.7E-02	4.2E-02	0.04664	5.0E-02	5.3E-02
2	1.4E-03	5.9E-03	1.2E-02	1.8E-02	2.4E-02	2.9E-02	3.3E-02	3.6E-02	3.9E-02	4.1E-02
3	1.4E-03	5.3E-03	9.8E-03	0.01377	1.7E-02	2.1E-02	2.6E-02	3.0E-02	3.5E-02	3.9E-02
4	1.3E-03	4.6E-03	7.3E-03	9.2E-03	1.1E-02	1.6E-02	2.1E-02	2.7E-02	3.3E-02	3.8E-02
5	1.3E-03	3.9E-03	5.0E-03	5.6E-03	7.6E-03	1.1E-02	1.5E-02	2.0E-02	2.4E-02	2.8E-02
6	1.2E-03	3.1E-03	3.2E-03	3.2E-03	4.4E-03	6.7E-03	9.2E-03	1.1E-02	1.4E-02	0.01615
7	1.1E-03	2.4E-03	1.9E-03	1.7E-03	2.3E-03	3.5E-03	5.0E-03	6.6E-03	8.2E-03	9.8E-03
8	1.0E-03	1.7E-03	1.0E-03	8.4E-04	1.1E-03	1.8E-03	2.8E-03	4.2E-03	5.7E-03	7.2E-03
9	9.0E-04	1.2E-03	5.5E-04	3.8E-04	5.0E-04	8.9E-04	1.5E-03	2.3E-03	3.2E-03	4.0E-03
10	7.9E-04	8.6E-04	2.6E-04	1.5E-04	1.9E-04	3.6E-04	6.5E-04	9.9E-04	1.3E-03	1.7E-03



#### 4.7 Effect of the Width Factor of Super Gaussian Filter on the Resolution of the Optical System Contains Focus Error ( $W_{20}=0.25, 0.5, \text{ and } 0.75) \lambda$ .

Figures (4-9-11) that are drawn from the data given in tables (4-9-11) respectively which show the effect of the width factor on the resolution of the optical system that contains focus error where ( $W_{20}=0.25, 0.5, \text{ \& } 0.75) \lambda$ . The band width of figures (4-9-11) increases with the increase of the value of the focus error where the curves of the figures contain distortion, this distortion in curves increases with the increase of the value of the focus error, that is clearly appears in figure (4-11) where the value of the focus error equals to ( $W_{20}=0.75 \lambda$ ). The resolution of the optical system increases with the width factor of the super Gaussian filters. For the three figures (4-9-11) the resolution decreases with the increase of the focus error. The normalized factor has been found for the three types of the systems in presence of the super Gaussian filter. Also these figures show that all the curves start from the same point but with different curve shapes.

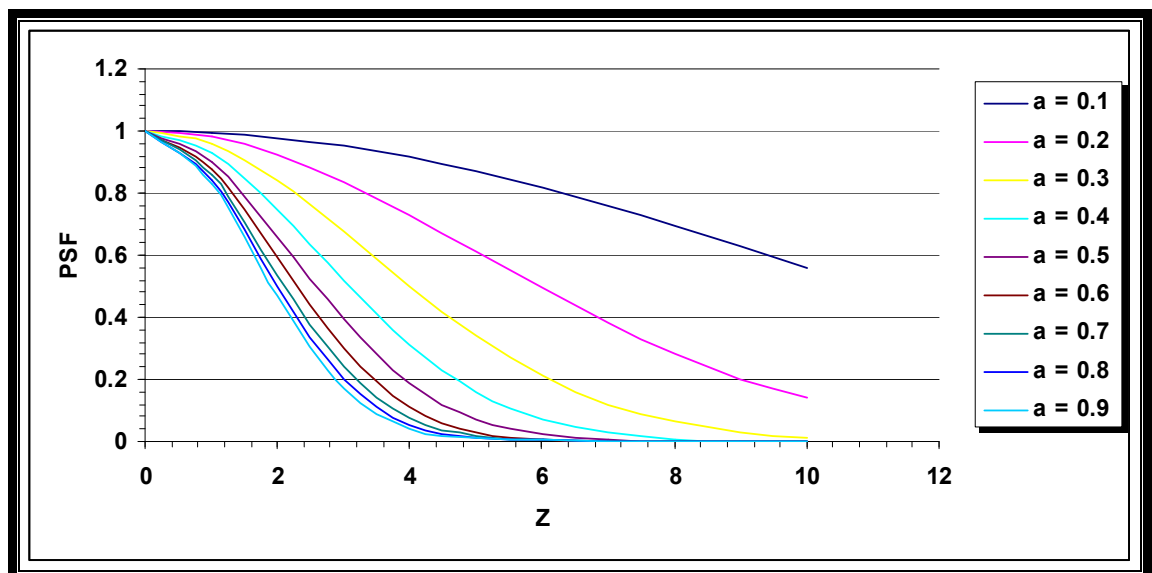


Figure (4 - 9): Point spread function for the optical system contains focus error ( $W_{20} = 0.25 \lambda$ ) with super Gaussian filter & ( $\varepsilon = 0$ ).

Table (4-9): Point spread function for the optical system contains focus error ( $W_{20} = 0.25 \lambda$ ) with super Gaussian filter & ( $\varepsilon = 0$ ).

z	$\varepsilon = 0$	$\varepsilon = 0.1$	$\varepsilon = 0.2$	$\varepsilon = 0.3$	$\varepsilon = 0.4$	$\varepsilon = 0.5$	$\varepsilon = 0.6$	$\varepsilon = 0.7$	$\varepsilon = 0.8$	$\varepsilon = 0.9$
0	1	1	1	1	1	1	1	1	1	1
1	9.9E-01	9.8E-01	9.5E-01	0.93017	0.90232	0.87798	0.85835	0.84304	0.83120	0.82201
2	9.7E-01	9.2E-01	8.4E-01	0.74829	0.66161	0.59121	0.53777	0.49807	0.46852	0.44624
3	9.5E-01	8.3E-01	6.7E-01	0.51997	0.39198	0.30090	0.23946	0.19824	0.17009	0.15036
4	9.1E-01	7.3E-01	5.0E-01	0.31152	0.18611	0.11359	0.07397	0.05260	0.04103	0.03473
5	8.7E-01	6.1E-01	3.4E-01	0.16054	0.07024	0.03183	0.01762	0.01366	0.01380	0.01545
6	8.1E-01	4.9E-01	2.1E-01	0.07099	0.02099	0.00714	0.00481	0.00561	0.00702	0.00836
7	7.5E-01	3.8E-01	1.2E-01	0.02688	0.00496	0.00137	0.00116	0.00133	0.00146	0.00154
8	6.9E-01	2.8E-01	6.2E-02	0.00869	0.00090	0.00013	0.00012	0.00029	0.00061	0.00101
9	6.2E-01	2.0E-01	2.9E-02	0.00239	0.00010	1.4E-05	0.00019	0.00052	0.00092	0.00133
10	5.6E-01	1.3E-01	1.3E-02	0.00055	6.3E-06	2.1E-05	9.0E-05	0.00016	0.00022	0.00026

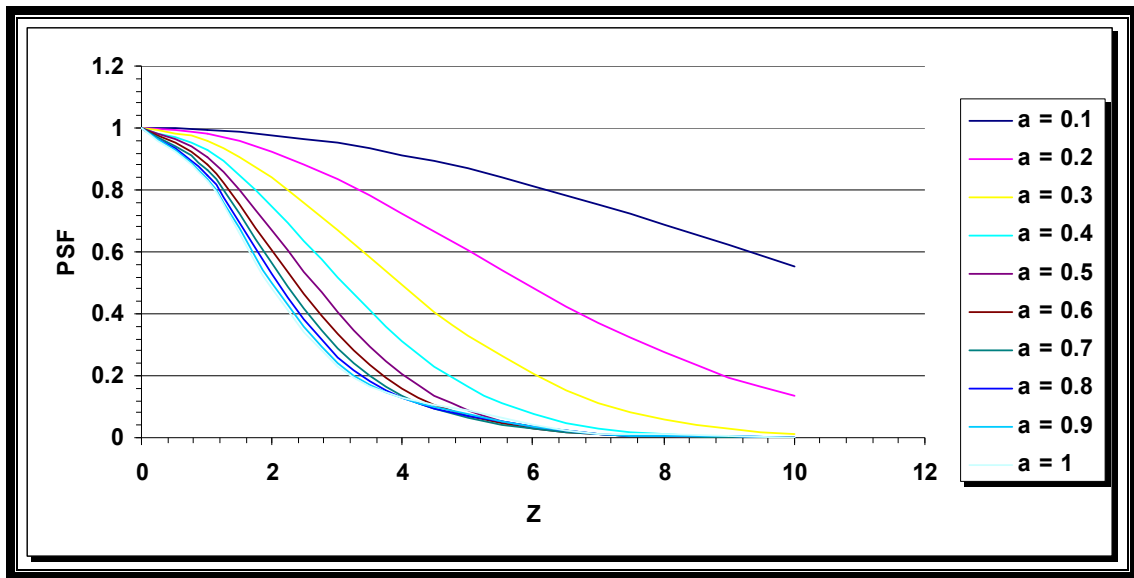


Figure (4 - 10): Point spread function for the optical system contains focus error ( $W_{20} = 0.5 \lambda$ ) with super Gaussian filter & ( $\varepsilon = 0$ ).

Table (4-10): Point spread function for the optical system contains focus error ( $W_{20} = 0.5 \lambda$ ) with super Gaussian filter & ( $\varepsilon = 0$ ).

z	$\varepsilon = 0$	$\varepsilon = 0.1$	$\varepsilon = 0.2$	$\varepsilon = 0.3$	$\varepsilon = 0.4$	$\varepsilon = 0.5$	$\varepsilon = 0.6$	$\varepsilon = 0.7$	$\varepsilon = 0.8$	$\varepsilon = 0.9$
0	1	1	1	1	1	1	1	1	1	1
1	9.9E-01	9.8E-01	9.5E-01	0.93000	0.90441	0.88232	0.86415	0.84957	0.83798	0.82878
2	9.7E-01	9.2E-01	8.3E-01	0.74807	0.66982	0.60851	0.56221	0.52751	0.50135	0.48138
3	9.5E-01	8.3E-01	6.7E-01	0.52054	0.40835	0.33488	0.28870	0.25964	0.24096	0.22860
4	9.1E-01	7.2E-01	4.9E-01	0.31355	0.20779	0.15620	0.13479	0.12817	0.12827	0.13117
5	8.6E-01	6.0E-01	3.3E-01	0.16373	0.09066	0.06805	0.06636	0.07187	0.07912	0.08615
6	8.1E-01	4.8E-01	2.0E-01	0.07432	0.03500	0.02839	0.03064	0.03441	0.03782	0.04055
7	7.5E-01	3.7E-01	1.1E-01	0.02943	0.01206	0.01026	0.0111	0.01228	0.01347	0.01459
8	6.9E-01	2.7E-01	5.8E-02	0.01021	0.00366	0.00329	0.00426	0.00593	0.00792	0.00995
9	6.2E-01	1.9E-01	2.7E-02	0.00313	0.00101	0.00126	0.00232	0.00374	0.00520	0.00654
10	5.5E-01	1.3E-01	1.1E-02	0.00085	0.00027	0.00045	0.00083	0.00123	0.00160	0.00191

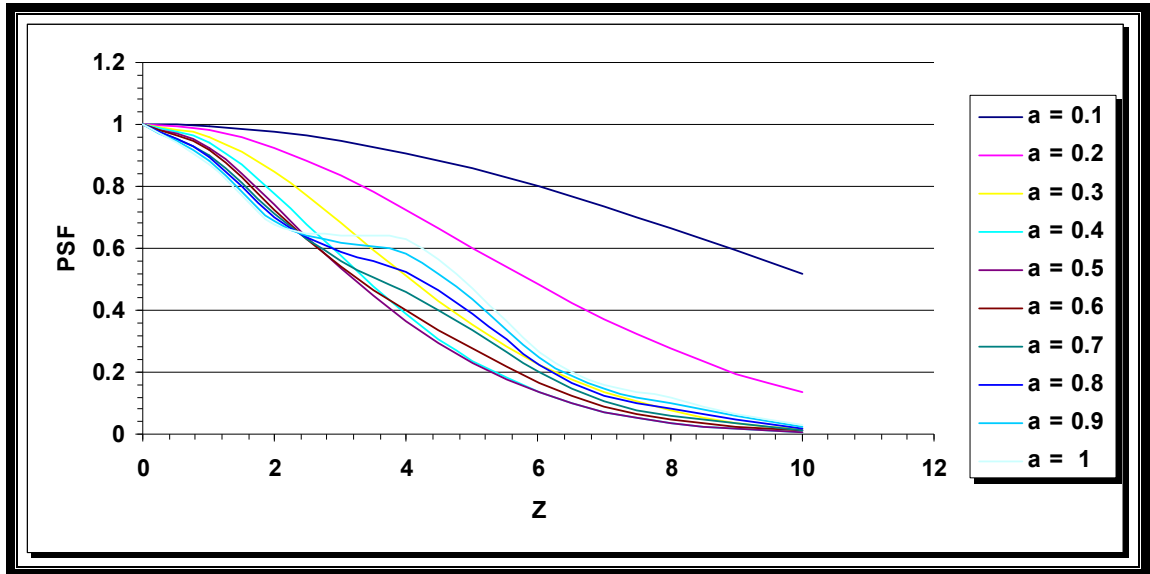


Figure (4 - 11): Point spread function for the optical system contains focus error ( $W_{20} = 0.75 \lambda$ ) with super Gaussian filter & ( $\varepsilon = 0$ ).

Table (4-11): Point spread function for optical system contains focus error ( $W_{20} = 0.75 \lambda$ ) with super Gaussian filter & ( $\varepsilon = 0$ ).

z	$\varepsilon = 0$	$\varepsilon = 0.1$	$\varepsilon = 0.2$	$\varepsilon = 0.3$	$\varepsilon = 0.4$	$\varepsilon = 0.5$	$\varepsilon = 0.6$	$\varepsilon = 0.7$	$\varepsilon = 0.8$	$\varepsilon = 0.9$
0	1	1	1	1	1	1	1	1	1	1
1	9.9E-01	9.8E-01	9.5E-01	9.3E-01	9.2E-01	9.1E-01	9.0E-01	8.9E-01	8.8E-01	8.7E-01
2	9.7E-01	9.2E-01	8.4E-01	7.7E-01	7.4E-01	7.2E-01	7.0E-01	6.9E-01	6.8E-01	6.7E-01
3	9.4E-01	8.3E-01	6.8E-01	5.7E-01	5.3E-01	5.4E-01	5.6E-01	5.9E-01	6.1E-01	6.4E-01
4	9.0E-01	7.2E-01	5.1E-01	3.8E-01	3.6E-01	3.9E-01	4.5E-01	5.2E-01	5.8E-01	6.2E-01
5	8.5E-01	6.0E-01	3.5E-01	2.3E-01	2.3E-01	2.7E-01	3.3E-01	3.8E-01	4.3E-01	4.6E-01
6	8.0E-01	4.8E-01	2.2E-01	1.3E-01	1.3E-01	1.6E-01	1.9E-01	2.2E-01	2.4E-01	2.6E-01
7	7.3E-01	3.7E-01	1.3E-01	7.2E-02	7.2E-02	8.7E-02	1.0E-01	1.2E-01	1.4E-01	1.6E-01
8	6.6E-01	2.7E-01	7.3E-02	3.5E-02	3.4E-02	4.5E-02	6.1E-02	8.0E-02	1.0E-01	1.1E-01
9	5.9E-01	1.9E-01	3.8E-02	1.6E-02	1.5E-02	2.2E-02	3.3E-02	4.5E-02	5.6E-02	6.6E-02
10	5.1E-01	1.3E-01	1.8E-02	6.5E-03	5.9E-03	9.1E-03	1.3E-02	1.9E-02	2.4E-02	2.8E-02

#### 4.8 Effect of the Width Factor of Super Gaussian Filter on the Resolution of the Optical System Contains Spherical Aberration ( $W_{40}=0.1, 0.3, 0.5, 0.7, \& 0.9$ ) $\lambda$

Figures (4-12-16) represent PSF for optical systems contain spherical aberration with the values ( $W_{40}=0.1, 0.3, 0.5, 0.7, \& 0.9$ )  $\lambda$ . The figures have been drawn by using the data that are calculated from equation (3-10). From these figures we notice that any increase in spherical aberration effected clearly with the increase of the band width of these figures and the decrease in the width factor of the super Gaussian

filter has the same effect which is seen in all figures (4-12-16), where the less band width when the value of the super Gaussian filter ( $a=1$ ).

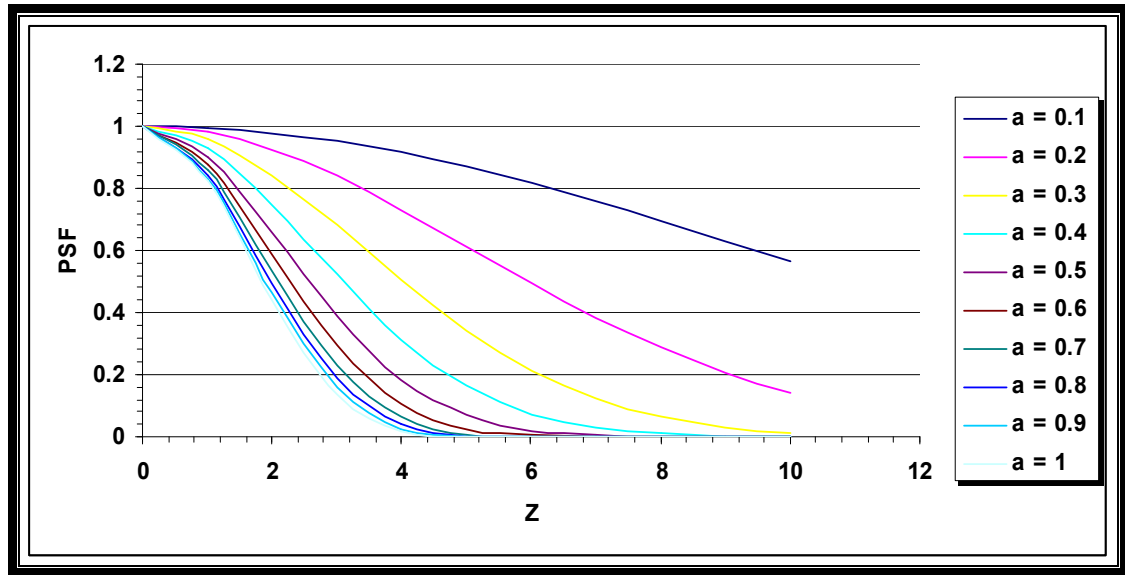


Figure (4 - 12): Point spread function for the optical system contains spherical aberration ( $W_{40} = 0.1 \lambda$ ) with super Gaussian filter & ( $\varepsilon = 0$ ).

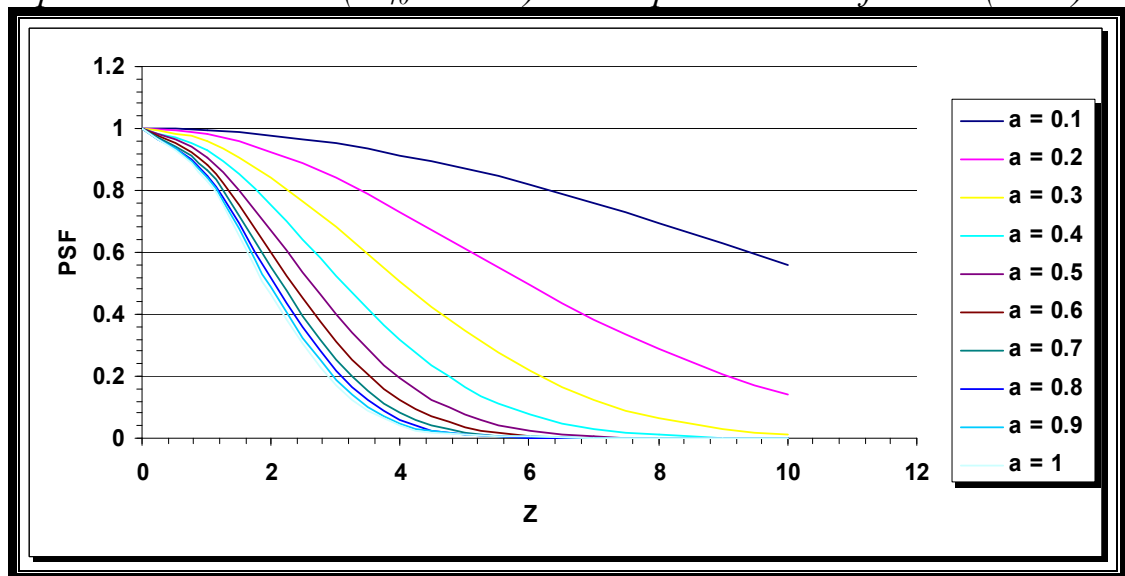


Figure (4 - 13): Point spread function for the optical system contains spherical aberration ( $W_{40} = 0.3 \lambda$ ) with super Gaussian filter & ( $\varepsilon = 0$ ).

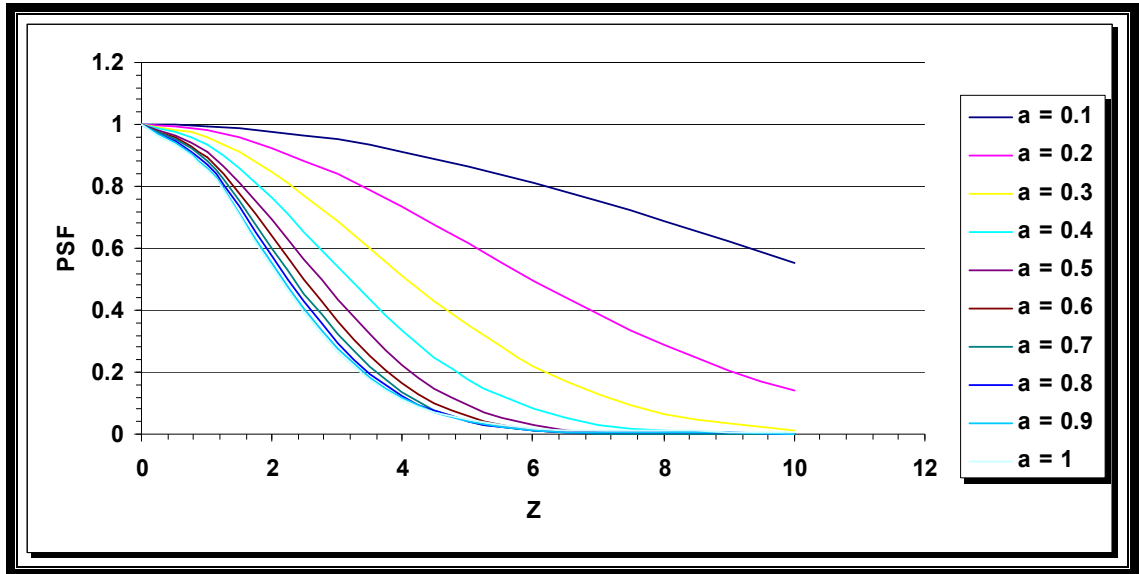


Figure (4-14): Point spread function for the optical system contains spherical aberration ( $W_{40} = 0.5 \lambda$ ) with super Gaussian filter & ( $\varepsilon = 0$ ).

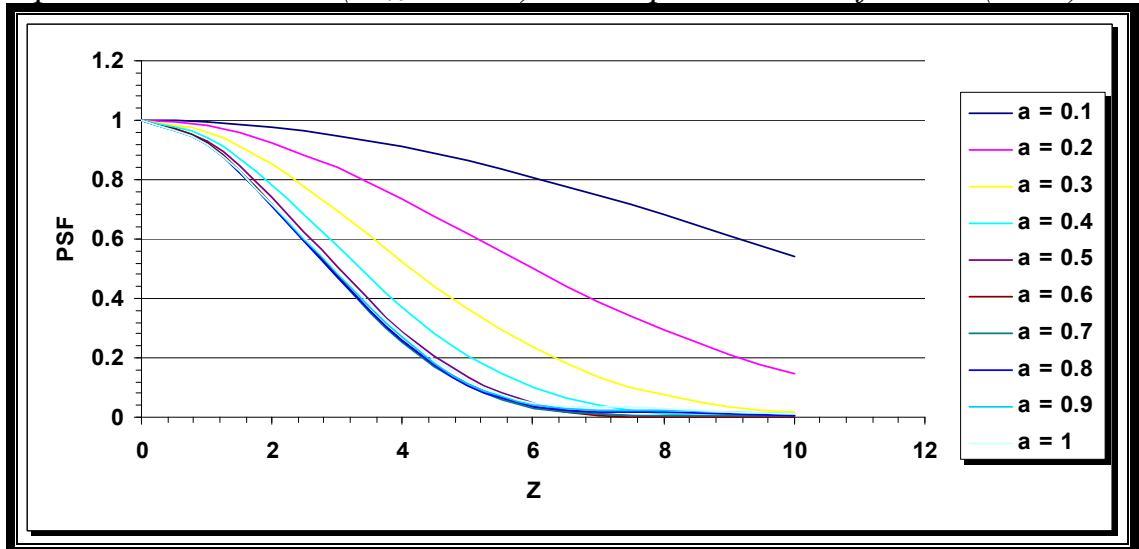


Figure (4 - 15): Point spread function for the optical system contains spherical aberration ( $W_{40} = 0.7 \lambda$ ) with super Gaussian filter & ( $\varepsilon = 0$ ).

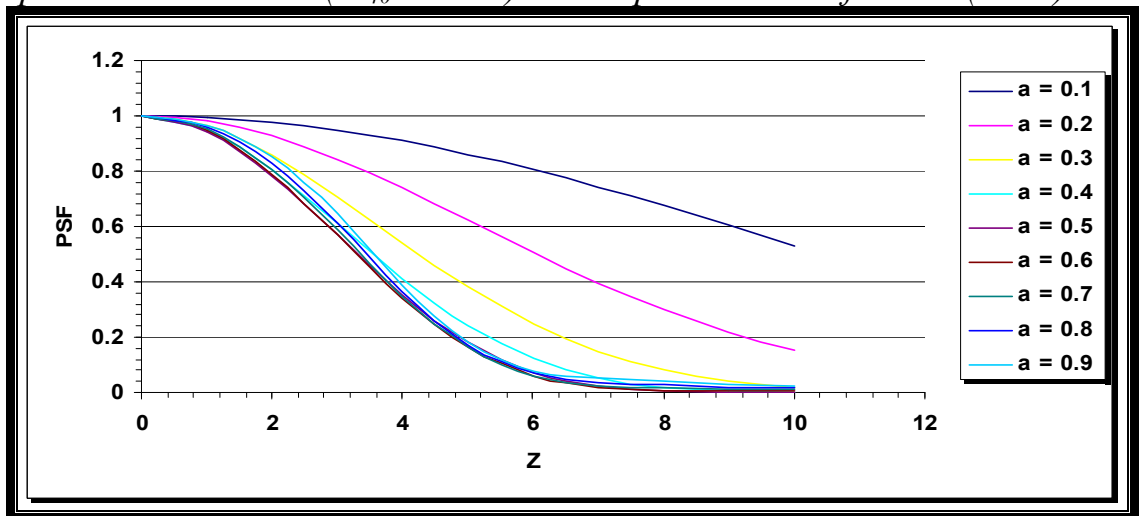


Figure (4 - 16): Point spread function for the optical system contains spherical aberration ( $W_{40} = 0.9 \lambda$ ) with super Gaussian filter & ( $\varepsilon = 0$ ).

#### 4.9 Effect of the Width Factor of Super Gaussian Filter on Strehl Ratio for the Optical System Contains Spherical Aberration ( $W_{40}=0.1, 0.3, 0.5, 0.7, \& 0.9) \lambda$ .

Figures (4-17-21) represent **Strehl** ratio for the optical systems contain spherical aberration with the values ( $W_{40}=0.1, 0.3, 0.5, 0.7, \& 0.9) \lambda$ . These figures have been drawn by using the data that are calculated from equation (3-10). From these figures we notice that any increase in spherical aberration is affected clearly with the decrease of the **Strehl** ratio also the decrease in the width factor of the super Gaussian filter has the same effect which is seen in all figures (4-17-21). We conclude that any increase in spherical aberration with the decrease in the width factor will affect in negative form on **Strehl** ratio.

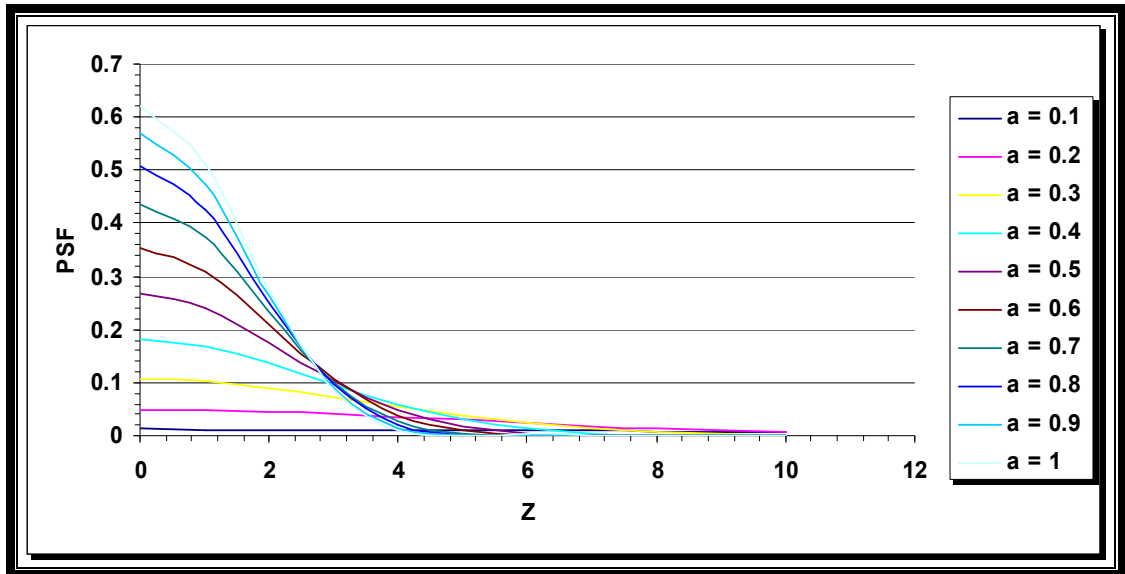


Figure (4 -1 7): Strehl ratio for the optical system contains spherical aberration ( $W_{40} = 0.1 \lambda$ ) with super Gaussian filter & ( $\epsilon = 0$ ).

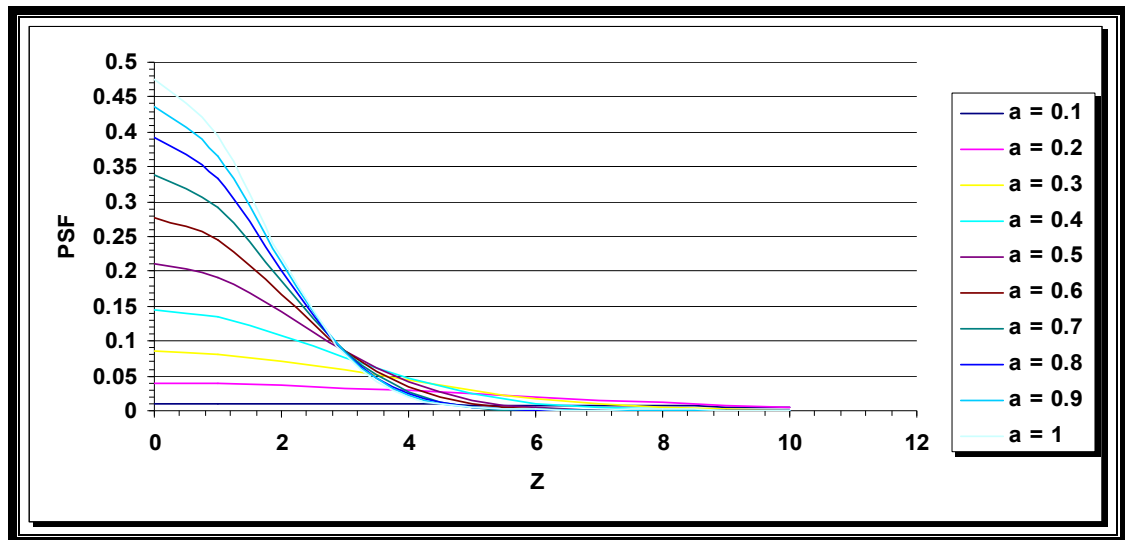


Figure (4 -1 8): Strehl ratio for the optical system contains spherical aberration ( $W_{40} = 0.3 \lambda$ ) with super Gaussian filter & ( $\varepsilon = 0$ ).

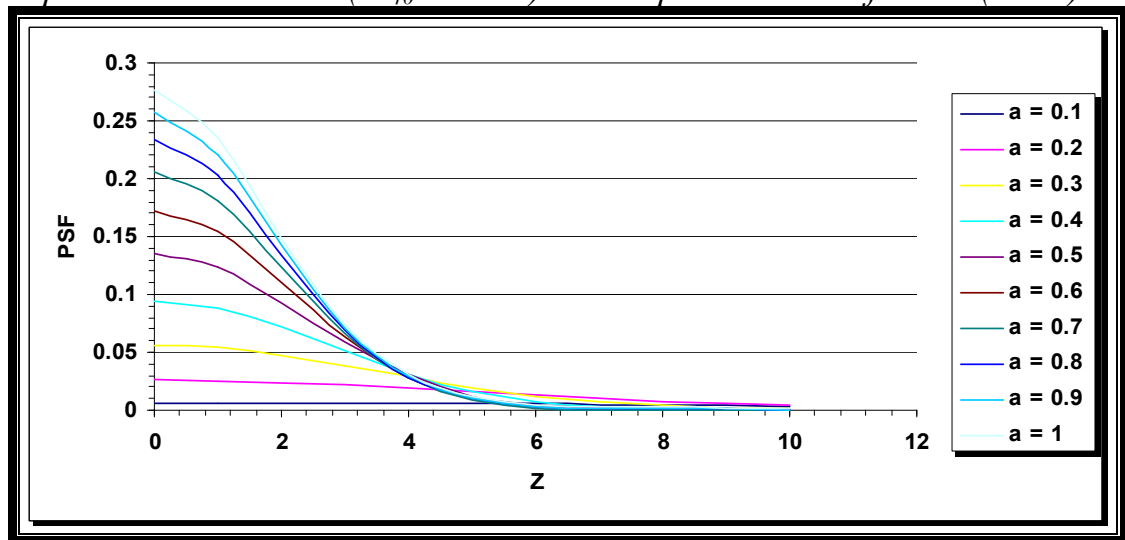


Figure (4 -1 9): Strehl ratio for the optical system contains spherical aberration ( $W_{40} = 0.5 \lambda$ ) with super Gaussian filter & ( $\varepsilon = 0$ ).

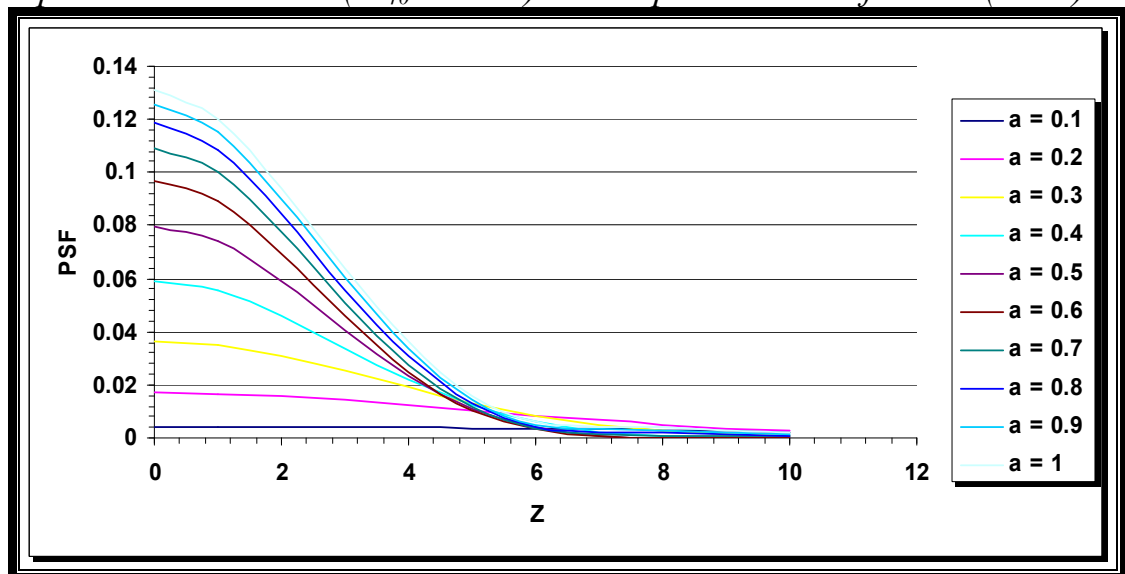


Figure (4 -20): Strehl ratio for the optical system contains spherical aberration ( $W_{40} = 0.7 \lambda$ ) with super Gaussian filter & ( $\varepsilon = 0$ ).

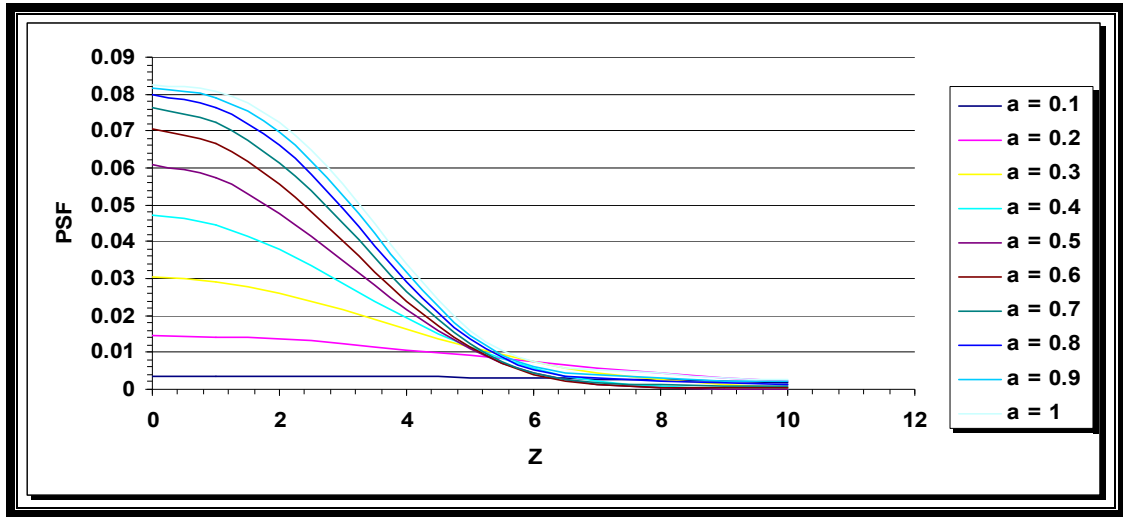


Figure (4 -21): Strehl ratio for the optical system contains spherical aberration ( $W_{40} = 0.9 \lambda$ ) with super Gaussian filter & ( $\varepsilon = 0$ ).

#### 4.10 Effect of the Width Factor of Super Gaussian Filter on Strehl Ratio for the Optical System Contains Optimum Balance Values ( $W_{20}=-1$ , $W_{40}=1$ ) $\lambda$

Figure (4-22) which is drawn from the data given in table (4-12) and calculated from equation (3-10) shows the optical system that contains third order spherical aberration ( $W_{40}=1\lambda$ ), and focus error ( $W_{20}=-1\lambda$ ). This optical system is of high correction and symmetric for the optical system contains focus error ( $W_{20}=0.25\lambda$ ) from the values of *Strehl* ratio with the same effect of the width factor of the super Gaussian filter. Where this ratio decreases when width factor values decrease.

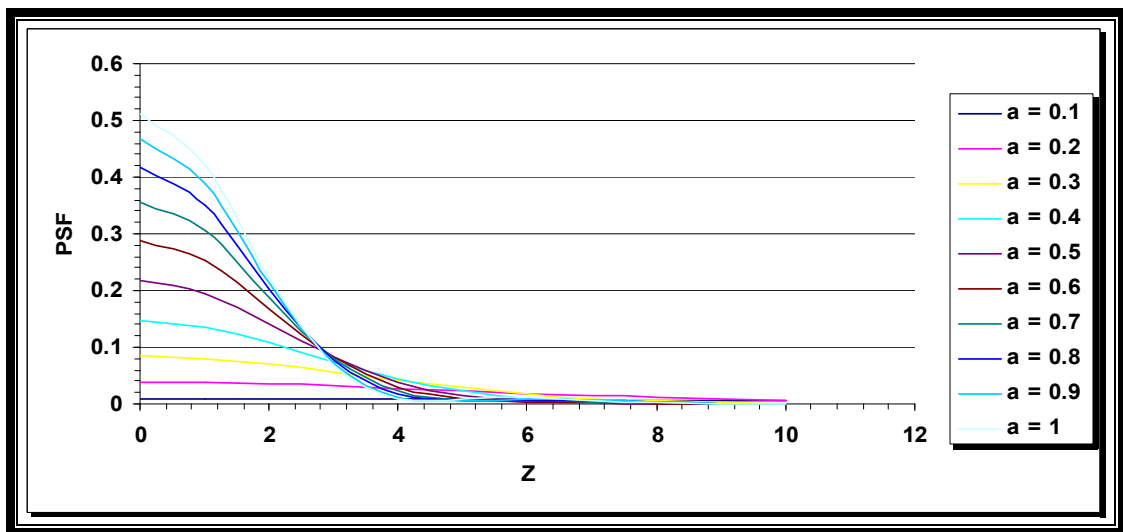


Figure (4-22): Strehl ratio for the optical system contains optimum balance value ( $W_{20}=-1$ ,  $W_{40}=1$ )  $\lambda$  with super Gaussian filter & ( $\varepsilon = 0$ ).



Table (4-12): *Strehl ratio for the optical system contains optimum balance value ( $W_{20}=-1$ ,  $W_{40}=1$ )  $\lambda$  with super Gaussian filter & ( $\varepsilon = 0$ ).*

$z$	$\varepsilon = 0$	$\varepsilon = 0.1$	$\varepsilon = 0.2$	$\varepsilon = 0.3$	$\varepsilon = 0.4$	$\varepsilon = 0.5$	$\varepsilon = 0.6$	$\varepsilon = 0.7$	$\varepsilon = 0.8$	$\varepsilon = 0.9$
0	9.2E-03	3.7E-02	8.4E-02	0.14585	0.21635	0.28859	0.35654	0.41698	0.46904	0.51311
1	9.1E-03	0.03703	8.0E-02	0.13549	0.19477	0.2526	0.30496	0.35026	0.38848	0.42035
2	8.9E-03	3.4E-02	7.0E-02	0.10857	0.14175	0.16811	0.18813	0.20315	0.21446	0.22310
3	8.7E-03	3.1E-02	5.6E-02	7.5E-02	8.2E-02	8.3E-02	8.0E-02	7.5E-02	7.0E-02	6.6E-02
4	8.4E-03	2.7E-02	4.1E-02	4.4E-02	3.8E-02	3.0E-02	2.2E-02	1.6E-02	0.01214	9.2E-03
5	8.0E-03	2.2E-02	2.8E-02	2.2E-02	1.4E-02	9.0E-03	6.2E-03	5.6E-03	6.3E-03	7.6E-03
6	7.5E-03	1.8E-02	1.7E-02	1.0E-02	5.3E-03	4.0E-03	4.8E-03	6.6E-03	8.5E-03	1.0E-02
7	6.9E-03	1.4E-02	9.7E-03	4.1E-03	2.2E-03	2.6E-03	3.6E-03	4.6E-03	5.3E-03	6.0E-03
8	6.4E-03	1.0E-02	5.0E-03	1.5E-03	1.1E-03	1.3E-03	1.4E-03	1.5E-03	1.5E-03	1.5E-03
9	5.8E-03	7.4E-03	2.3E-03	5.8E-04	4.5E-04	3.6E-04	2.1E-04	9.3E-05	5.2E-05	7.3E-05
10	5.1E-03	5.0E-03	1.0E-03	2.2E-04	1.4E-04	6.7E-05	5.0E-05	1.1E-04	2.3E-04	3.9E-04

#### 4.11 Effect of the Width Factor of Super Gaussian Filter on Strehl Ratio for the Obstructed Optical System Contains Optimum Balance Values

Figure (4-23) drawn from the data of equation (3-10). This figure shows the state of the optical system contains optimum balance values ( $W_{20}=-1.04$ ,  $W_{40}=1$ )  $\lambda$  with obstruction ratio ( $\varepsilon=0.2$ ). Figure (4-24) drawn from the data of equation (3-10) for obstructed optical system ( $\varepsilon=0.5$ ) which contains optimum balance values ( $W_{20}=-1.25$ ,  $W_{40}=1$ )  $\lambda$ . Figure (4-25) drawn from the data of equation (3-10). This figure shows the state of the optical system contains optimum balance values

( $W_{20}=-1.64$ ,  $W_{40}=1$ )  $\lambda$  with obstruction ratio ( $\varepsilon=0.8$ ). Figures (4-23-25) show that **Strehl** ratio will reduce by the decrease of the width factor of the super Gaussian filter also show that obstruction ratios and the super Gaussian filter work on deleting the secondary tops. The optimum balance values for obstructed optical systems contain spherical aberration giving in table (1-4) which calculated from equation (1-31):

Table (1-4): The optimum balance values for obstructed optical systems contain spherical aberration

$\epsilon$	$W_{20}$	$W_{40}$
0	-1	1
0.1	-1.01	1
0.2	-1.04	1
0.3	-1.09	1
0.4	-1.01	1
0.5	-1.25	1
0.6	-1.36	1
0.7	-1.49	1
0.8	-1.64	1
0.9	-1.81	1
1	0	0

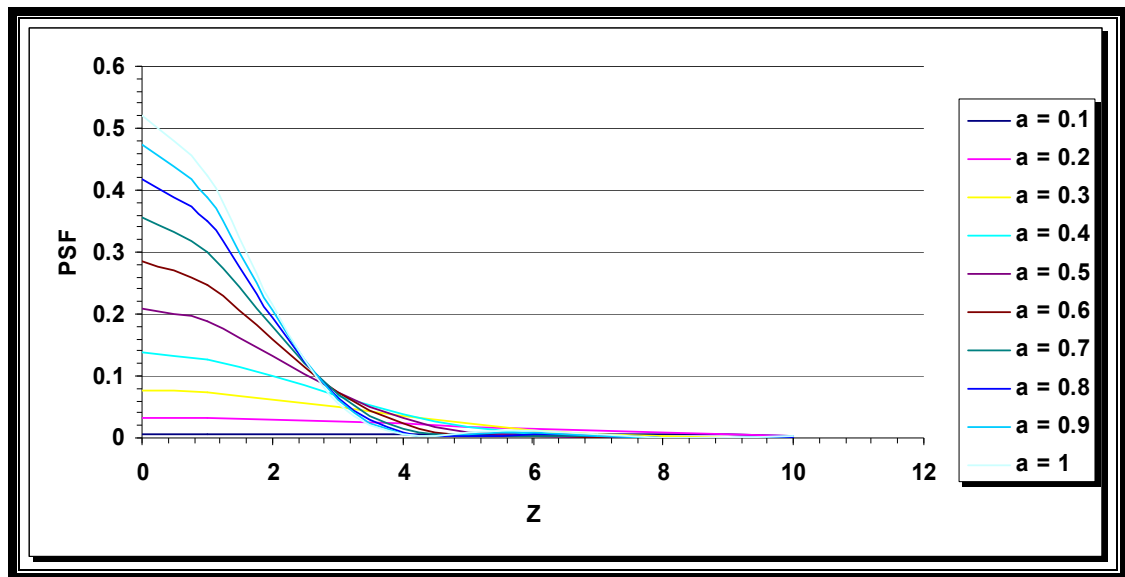


Figure (4-23): Strehl ratio for optical system contains optimum balance value ( $W_{20} = -1.04$ ,  $W_{40} = 1$ )  $\lambda$  with super Gaussian filter & ( $\epsilon = 0.2$ ).  
Figure (4-23), agreement with figure (4-29).

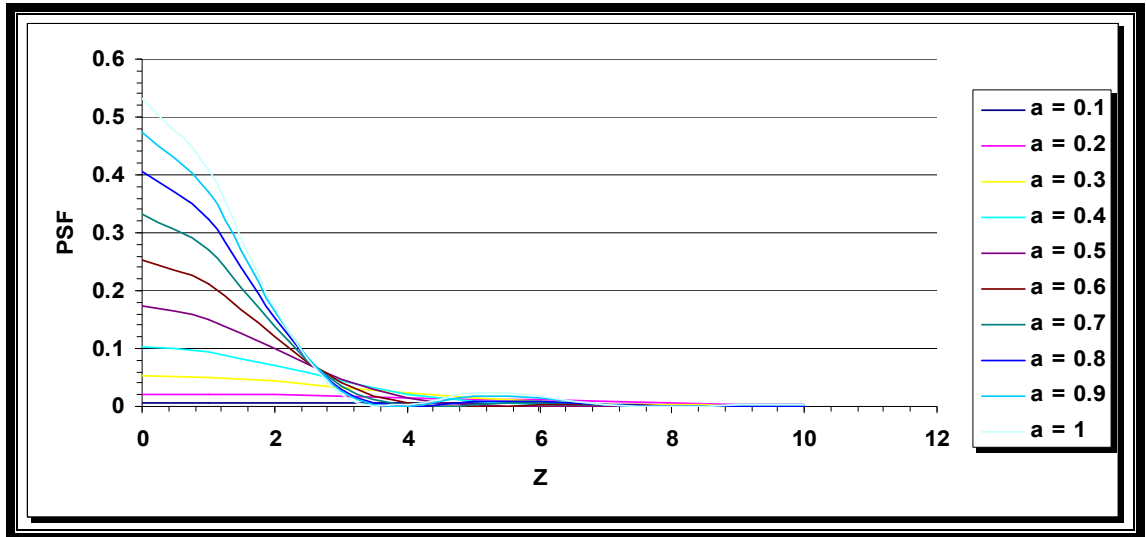


Figure (4-24): *Strehl ratio for the optical system contains optimum balance value ( $W_{20}=-1.25$ ,  $W_{40}=1$ )  $\lambda$  with super Gaussian filter & ( $\epsilon = 0.5$ ).*

Figure (4-24), agreement with figure (4-32)

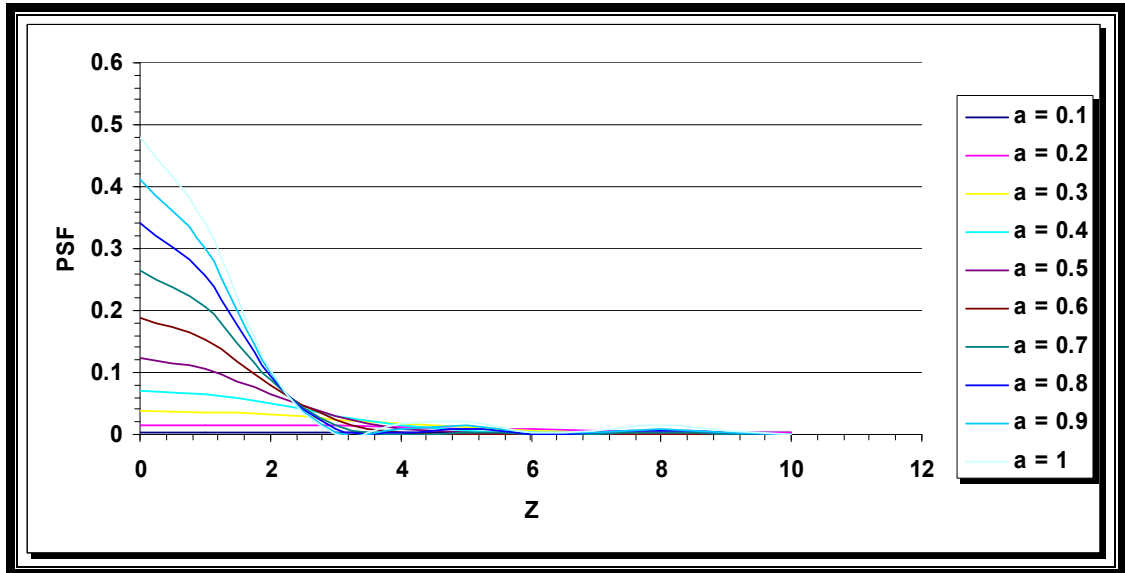


Figure (4-25): *Strehl ratio for the optical system contains optimum balance value ( $W_{20}=-1.64$ ,  $W_{40}=1$ )  $\lambda$  with super Gaussian filter & ( $\epsilon = 0.8$ ).*

Figure (4-25), agreement with figure (4-35).

#### 4.12 Effect of the Width Factor of the Super Gaussian Filter on Strehl Ratio for the Free Optical System Contains Obstruction Ratio with Different Values ( $\epsilon=0.2$ , 0.5, and 0.8)

Figure (4-26) represents *Strehl* ratio for the free optical system. The maximum *Strehl* ratio equals to (0.629815) for the free optical system contains obstruction ratio ( $\epsilon=0.2$ ) where *Strehl* ratio decreases with the decrease of the width factor of the super Gaussian

filter. Figure (4-27) represents *Strehl* ratio for the free optical system contains obstruction ( $\varepsilon=0.5$ ), the maximum *Strehl* ratio equals to (0.5698534). In figure (4-28) the maximum *Strehl* ratio for the free optical system contains obstruction ratio ( $\varepsilon=0.8$ ) and equals to (0.4800972). *Strehl* ratio decreased with the decrease of the width factor likewise for the other curves.

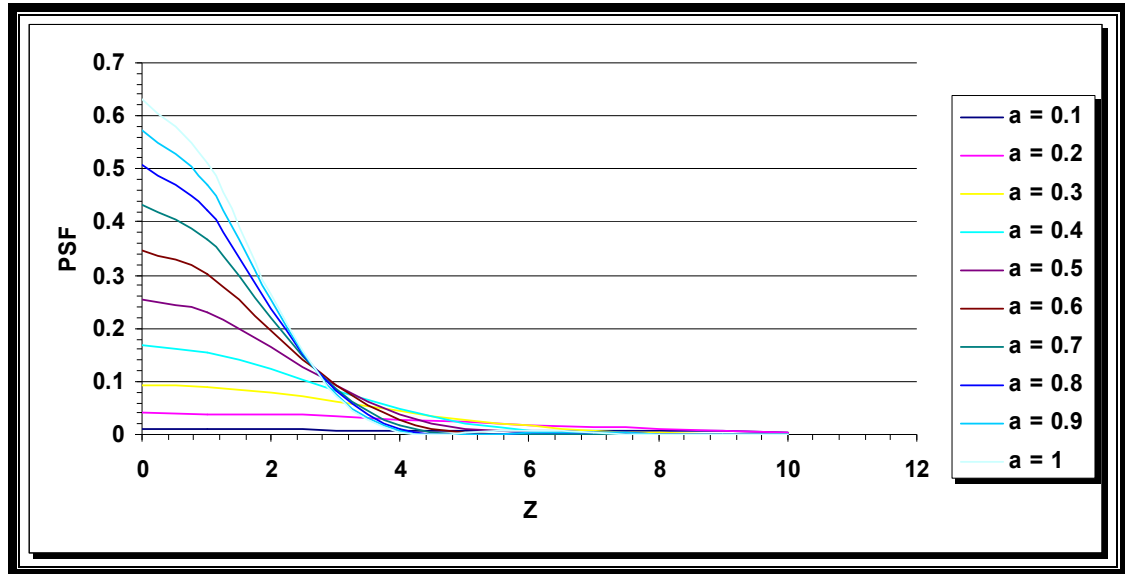


Figure (4 - 26): *Strehl* ratio for the free optical system contains super Gaussian filter & ( $\varepsilon = 0.2$ ).

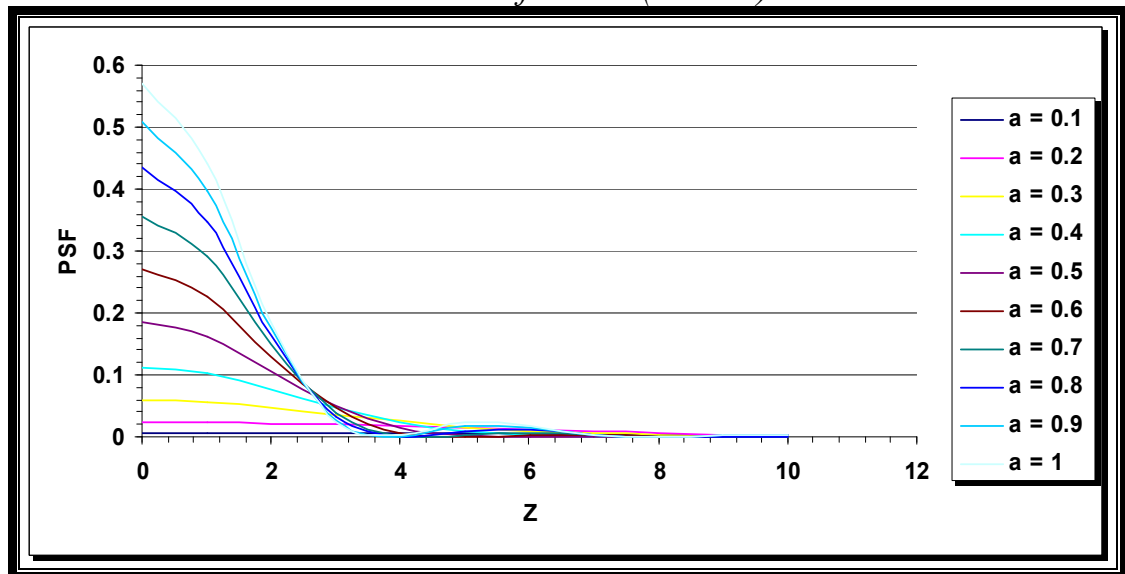


Figure (4 - 27): *Strehl* ratio for the free optical system contains super Gaussian filter & ( $\varepsilon = 0.5$ ).

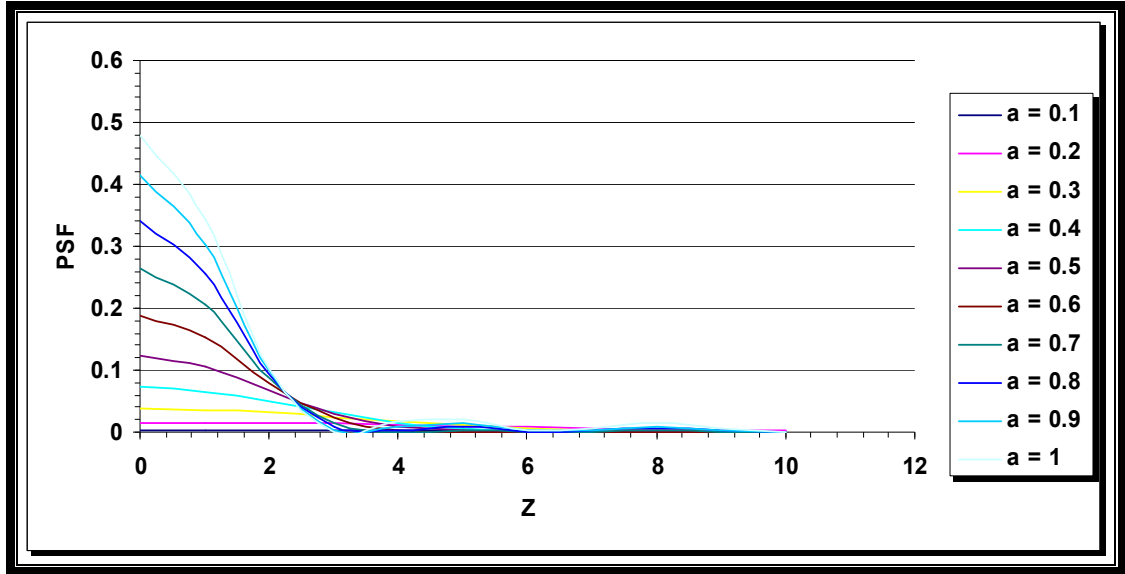


Figure (4 - 28): *Strehl ratio for the free optical system contains super Gaussian filter & ( $\epsilon = 0.8$ ).*

#### **4.13 Effect of the Width Factor of Super Gaussian Filter on Strehl Ratio for the Obstructed Optical System ( $\epsilon=0.2$ ) Contains Focus Error ( $W_{20}=0.25, 0.5, \& 0.75$ ) $\lambda$**

The presence of the different values of focus error in the optical system performs to decrease **Strehl** ratio and also the decrease in the width factor of the super Gaussian filter, that appears in figures (4-29-31) which represent an obstructed optical system ( $\epsilon=0.2$ ) with different values of focus error ( $W_{20}=0.25, 0.5, \& 0.75$ )  $\lambda$ . For the first figure (4-29) maximum **Strehl** ratio equals (0.519695) when the focus error equals to ( $W_{20}=0.25 \lambda$ ). When the focus error increases to ( $W_{20}=0.5 \lambda$ ) **Strehl** ratio decreases to (0.2776234) as shown in figure (4-25). If the optical system contains high amount of focus error, **Strehl** ratio decreases to (0.07581605) as shown in figure (4-26). In all figures **Strehl** ratio decreases with the increase of the width factor and focus error.

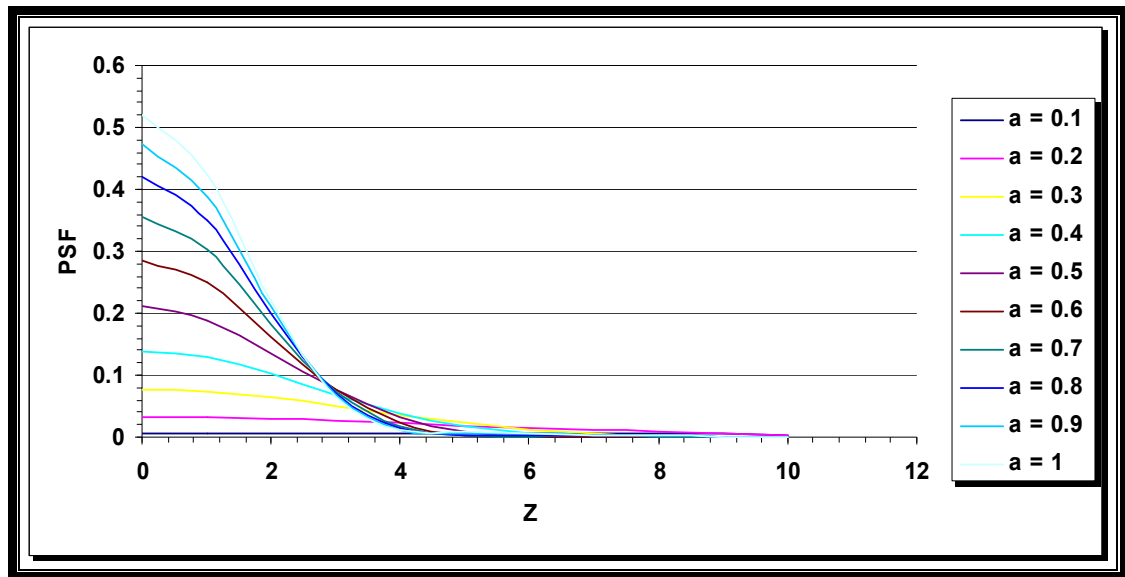


Figure (4 - 29): Strehl ratio for the optical system contains focus error ( $W_{20} = 0.25 \lambda$ ) with super Gaussian filter & ( $\varepsilon = 0.2$ ).

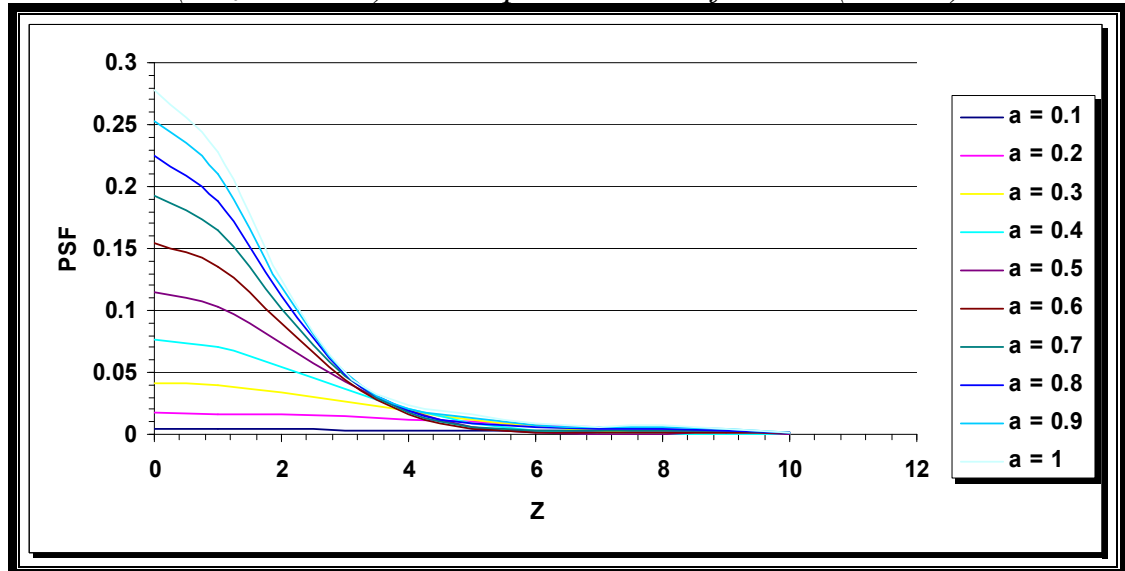


Figure (4 - 30): Strehl ratio for the optical system contains focus error ( $W_{20} = 0.5 \lambda$ ) with super Gaussian filter & ( $\varepsilon = 0.2$ ).

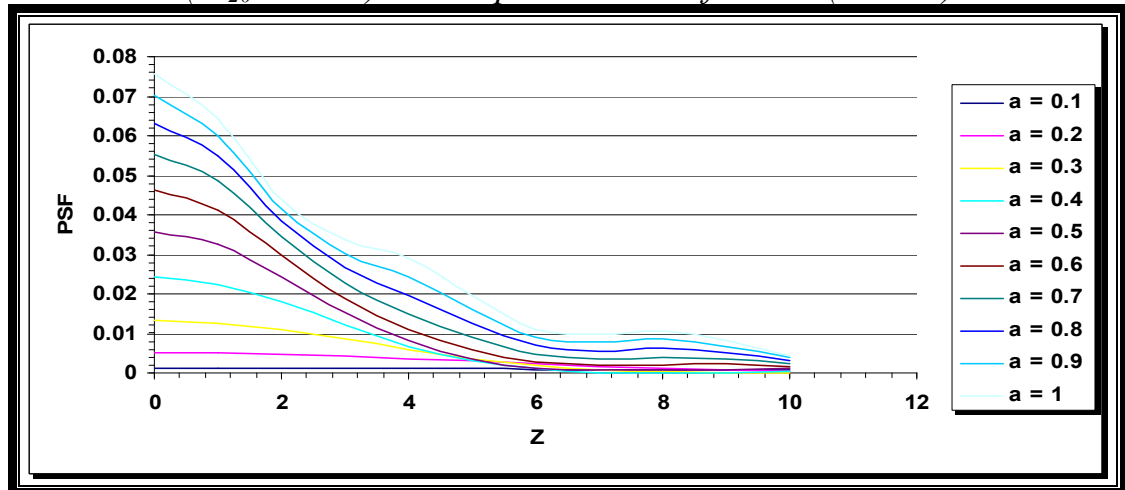


Figure (4 - 31): Strehl ratio for the optical system contains focus error ( $W_{20} = 0.75 \lambda$ ) with super Gaussian filter & ( $\varepsilon = 0.2$ ).

#### 4.14 Effect of the Width Factor of Super Gaussian Filter on *Strehl* Ratio for the Obstructed Optical System ( $\varepsilon=0.5$ ) Contains Focus Error ( $W_{20}=0.25, 0.5, \& 0.75$ ) $\lambda$

Figures (4-32-34) represent *Strehl* ratio for the optical systems with different values of focus error ( $W_{20}=0.25, 0.5, \& 0.75$ )  $\lambda$  and contain obstruction ratio ( $\varepsilon=0.5$ ). Curves of these figures drawn from the data that are extracted by calculating equation (3-9) of PSF for the optical system contain obstruction and focus error. We notice from the first figure (4-32) that *Strehl* ratio starts in (0.507082) when the width factor of the super Gaussian filter ( $a=1$ ) and the focus error ( $W_{20}=0.25 \lambda$ ). This ratio starts to decrease when the width factor decrease. In the second figure (4-33) *Strehl* ratio starts in (0.3510338) when the focus error ( $W_{20}=0.5 \lambda$ ) and the width factor of the super Gaussian filter ( $a=1$ ). Also for the third figure (4-34) *Strehl* ratio starts in (0.1766028) when the width factor ( $a=1$ ) and the focus error ( $W_{20}=0.75 \lambda$ ). We notice that the *Strehl* ratio will start to decrease if the width factors of the super Gaussian filter decrease and focus error increase, and there are distortions in curves appear with the increase of the focus error.

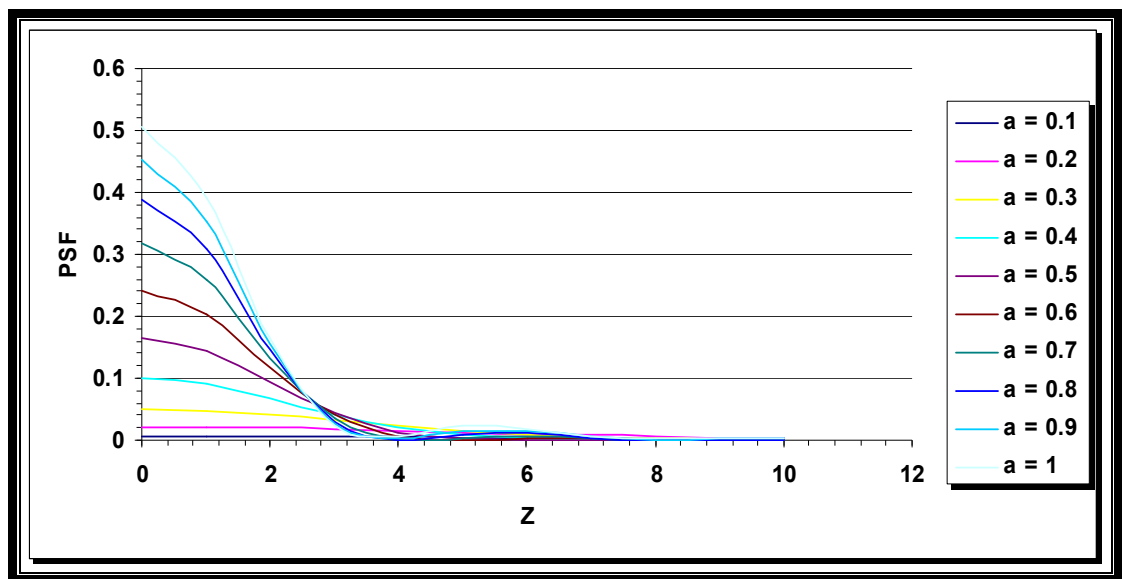


Figure (4 - 32): *Strehl* ratio for the optical system contains focus error ( $W_{20} = 0.25 \lambda$ ) with super Gaussian filter & ( $\varepsilon = 0.5$ ).

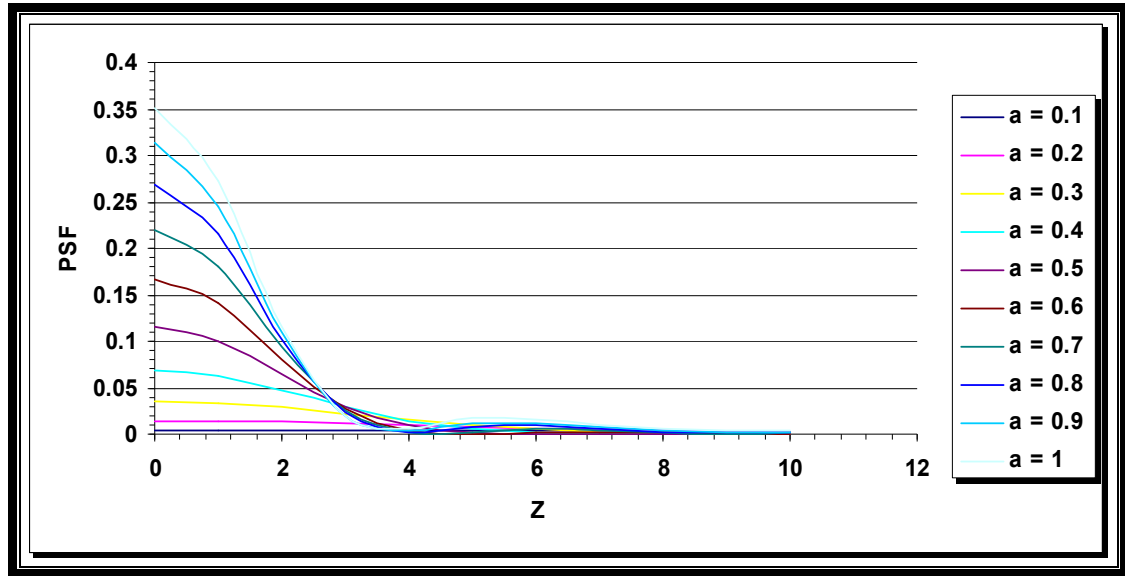


Figure (4 - 33): *Strehl ratio for the optical system contains focus error ( $W_{20} = 0.5 \lambda$ ) with super Gaussian filter & ( $\epsilon = 0.5$ ).*

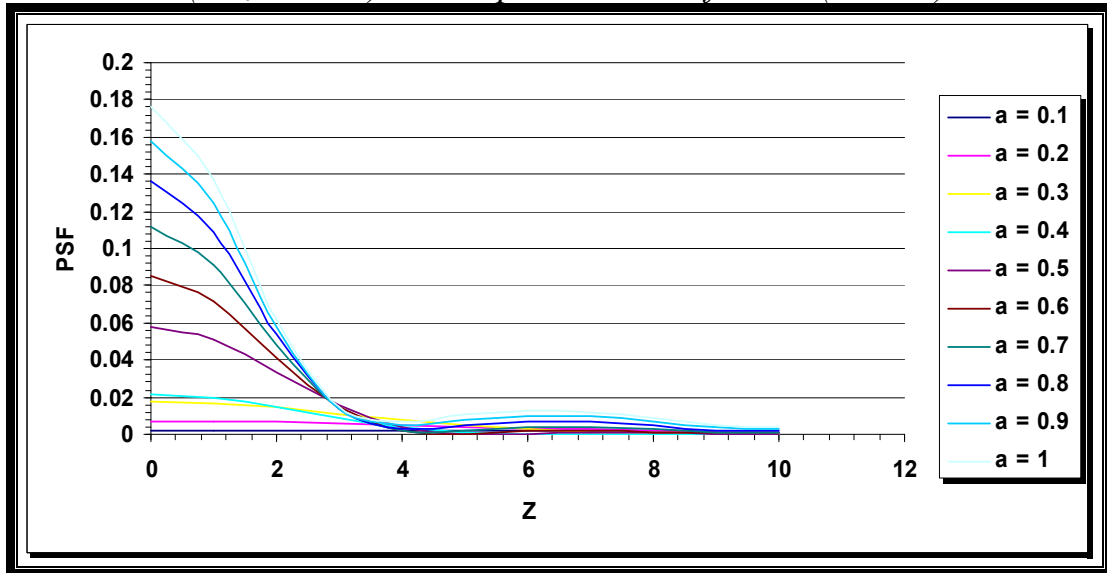


Figure (4 - 34): *Strehl ratio for the optical system contains focus error ( $W_{20} = 0.75 \lambda$ ) with super Gaussian filter & ( $\epsilon = 0.5$ ).*

#### 4.15 Effect of the Width Factor of Super Gaussian Filter on Strehl Ratio for the Obstructed Optical System ( $\epsilon=0.8$ ) Contains Focus Error ( $W_{20}=0.25, 0.5, \& 0.75$ ) $\lambda$

Figures (4-35-37) represent *Strehl* ratio for the obstructed optical system ( $\epsilon=0.8$ ) and contain different values of focus error ( $W_{20}=0.25, 0.5, \& 0.75$ )  $\lambda$ . The first figure (4-35) contains focus error ( $W_{20}=0.25\lambda$ ). The second figure (4-36) contains focus error ( $W_{20}=0.5\lambda$ ). The third figure (4-37) contains focus error ( $W_{20}=0.75\lambda$ ), where there is the high level of



obstruction and focus error and the presence of the super Gaussian filter effect on *Strehl* ratio, in the first figure (4-35) *Strehl* ratio starts at (0.4674417) when the width factor of the super Gaussian filter equals to ( $a=1$ ), in the second figure(4-36) *Strehl* ratio starts at (0.4310673) and ( $a=1$ ), in the third figure(4-37) *Strehl* ratio starts at (0.3754787) and  $a=1$ . The decrease in tops of *Strehl* ratio curves in all figures because of the presence of the focus error and the reduce in width factor of the super Gaussian filter.

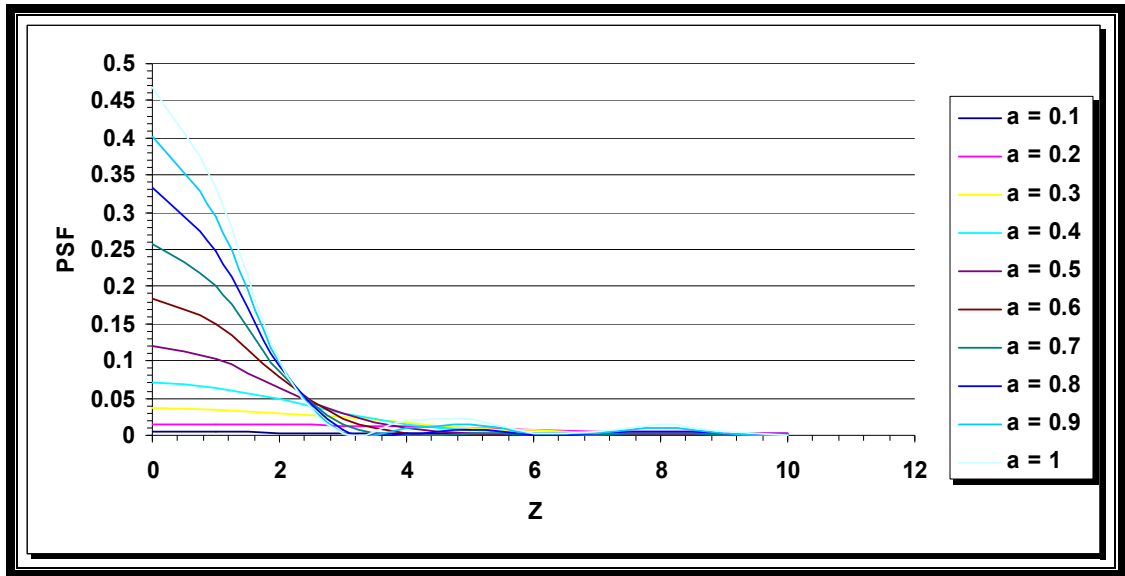


Figure (4 - 35): *Strehl* ratio for the optical system contains focus error ( $W_{20} = 0.25 \lambda$ ) with super Gaussian filter & ( $\varepsilon = 0.8$ ).

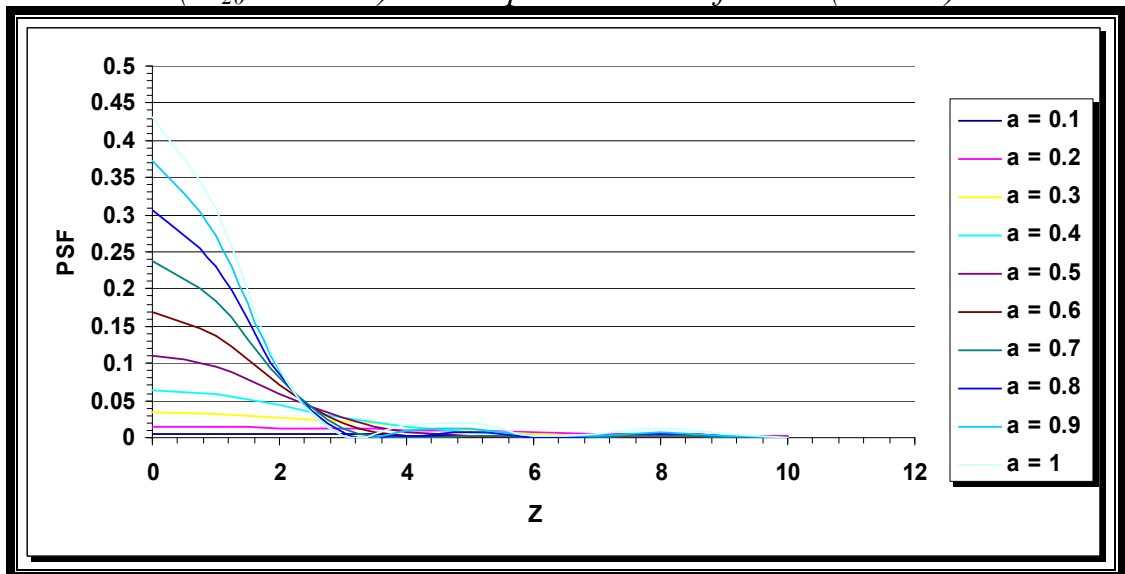


Figure (4 - 36): *Strehl* ratio for the optical system contains focus error ( $W_{20} = 0.5 \lambda$ ) with super Gaussian filter & ( $\varepsilon = 0.8$ ).

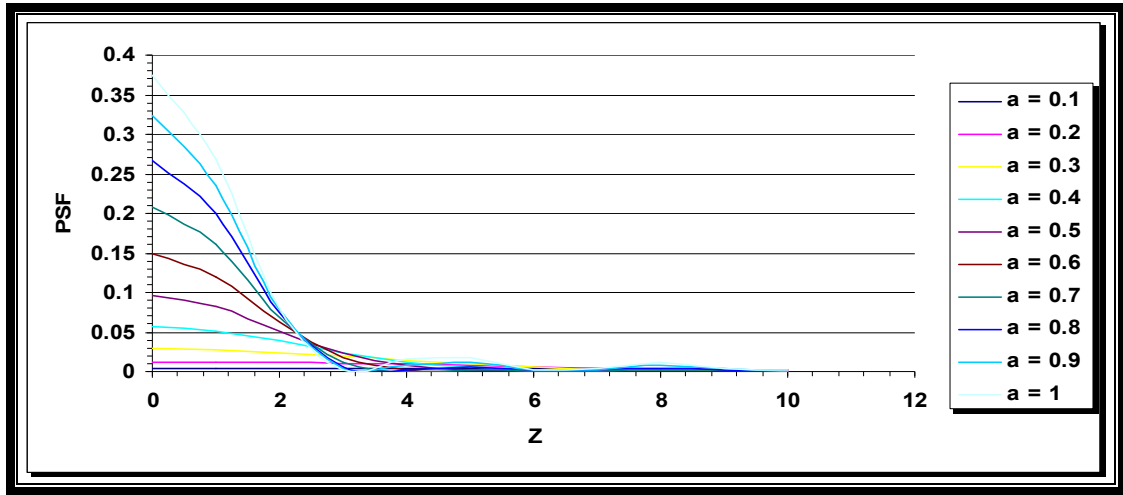


Figure (4 - 37): *Strehl ratio for the optical system contains focus error ( $W_{20} = 0.75$ )  $\lambda$  with super Gaussian filter & ( $\epsilon = 0.8$ ).*

#### 4.16 Effect of the Width Factor of Super Gaussian Filter on *Strehl Ratio for the Obstructed Optical System ( $\epsilon=0.2$ ) Contains Spherical Aberration ( $W_{40}=0.1, 0.3, 0.5, 0.7, \& 0.9$ ) $\lambda$*

Figures (4-38-42), which are drawn from the data that are extracted from equation (3-10) represent *Strehl* ratio for the obstructed optical system ( $\epsilon=0.2$ ) and contains spherical aberration ( $W_{40}=0.1, 0.3, 0.5, 0.7, \& 0.9$ )  $\lambda$ . *Strehl* ratio is maximum in all figures when the width factor ( $a=1$ ) and is the minimum value when  $a=0.1$ . The presence of spherical aberration reduces *Strehl* ratio, and the reduction in the width factor of the super Gaussian filter also reduces *Strehl* ratio.

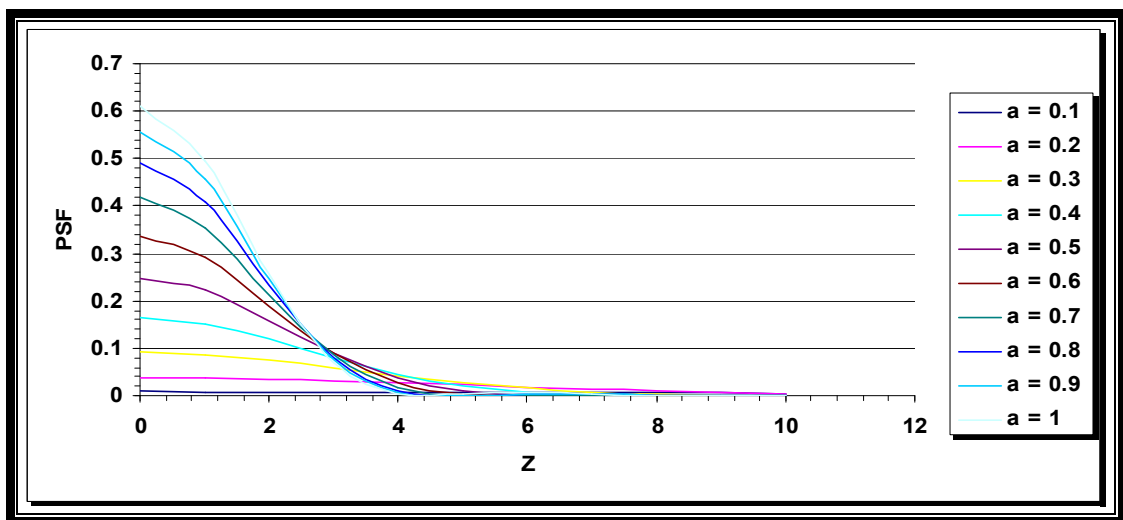


Figure (4 - 38): *Strehl ratio for the optical system contains spherical aberration ( $W_{40} = 0.1$ )  $\lambda$  with super Gaussian filter & ( $\epsilon = 0.2$ ).*

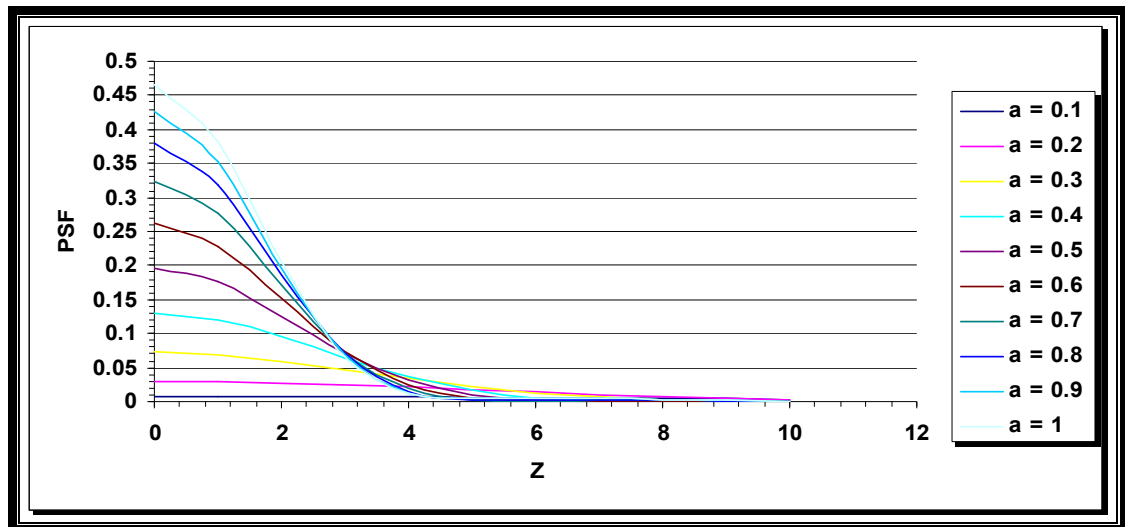


Figure (4 - 39): Strehl ratio for the optical system contains spherical aberration ( $W_{40} = 0.3 \lambda$ ) with super Gaussian filter &  $(\epsilon = 0.2)$ .

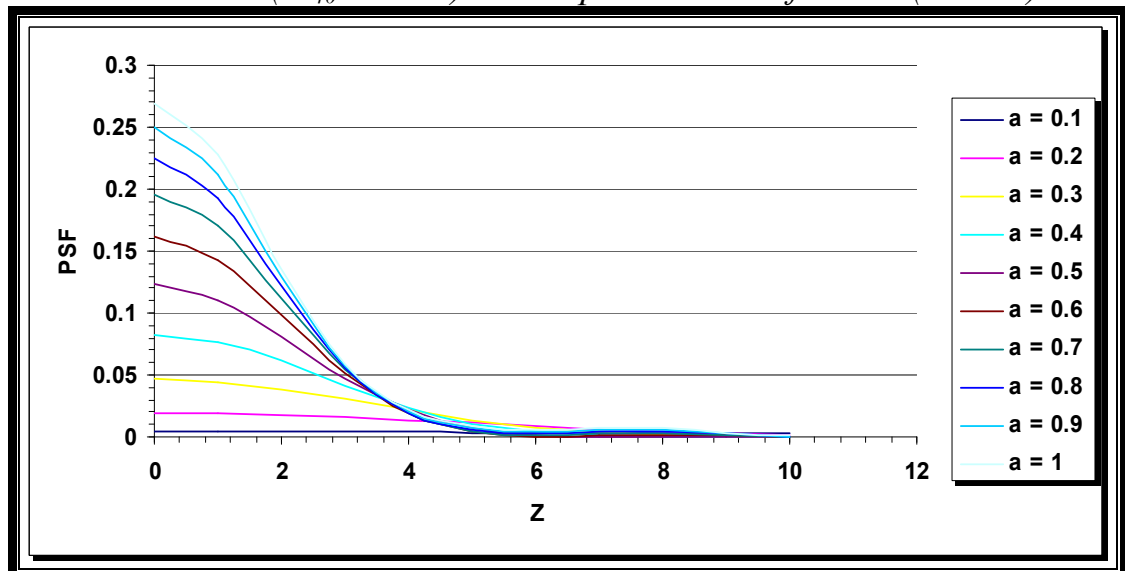


Figure (4 - 40): Strehl ratio for the optical system contains spherical aberration ( $W_{40} = 0.5 \lambda$ ) with super Gaussian filter &  $(\epsilon = 0.2)$ .

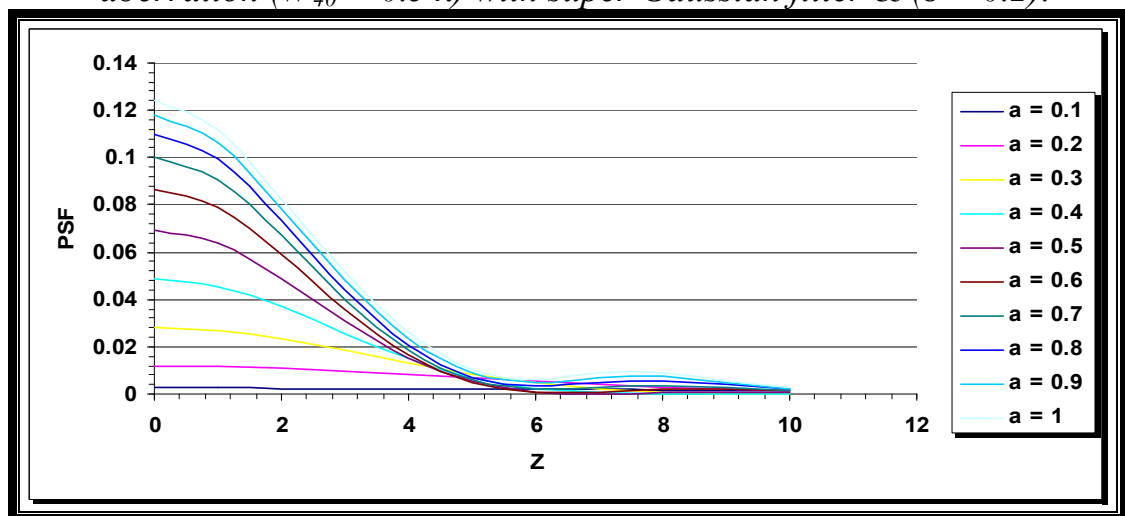


Figure (4 - 41): Strehl ratio for the optical system contains spherical aberration ( $W_{40} = 0.7 \lambda$ ) with super Gaussian filter &  $(\epsilon = 0.2)$ .

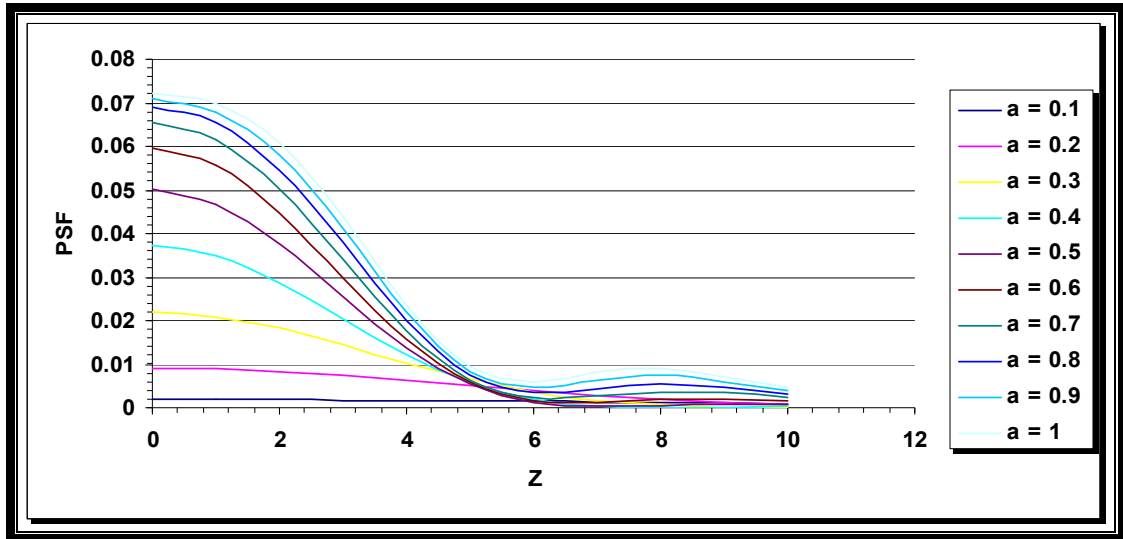


Figure (4 - 42): *Strehl* ratio for the optical system contains spherical aberration ( $W_{40} = 0.9 \lambda$ ) with super Gaussian filter & ( $\varepsilon = 0.2$ ).

#### 4.17 Effect the Width Factor of Super Gaussian Filter on *Strehl* Ratio for Obstructed Optical System ( $\varepsilon=0.5$ ) Contained Spherical Aberration ( $W_{40}=0.1, 0.3, 0.5, 0.7, \& 0.9$ ) $\lambda$

Figures (4-43-47), which are drawn from the data that are extracted from equation (3-10) represent ***Strehl*** ratio for the obstructed optical system ( $\varepsilon=0.5$ ) and contains spherical aberration ( $W_{40}=0.1, 0.3, 0.5, 0.7$ , and  $0.9$ )  $\lambda$ . ***Strehl*** ratio is maximum in all figures when  $a=1$  and is the minimum value when  $a=0.1$ . The presence of spherical aberration reduces ***Strehl*** ratio, and the reduction in the width factor of the super Gaussian filter also reduces ***Strehl*** ratio.

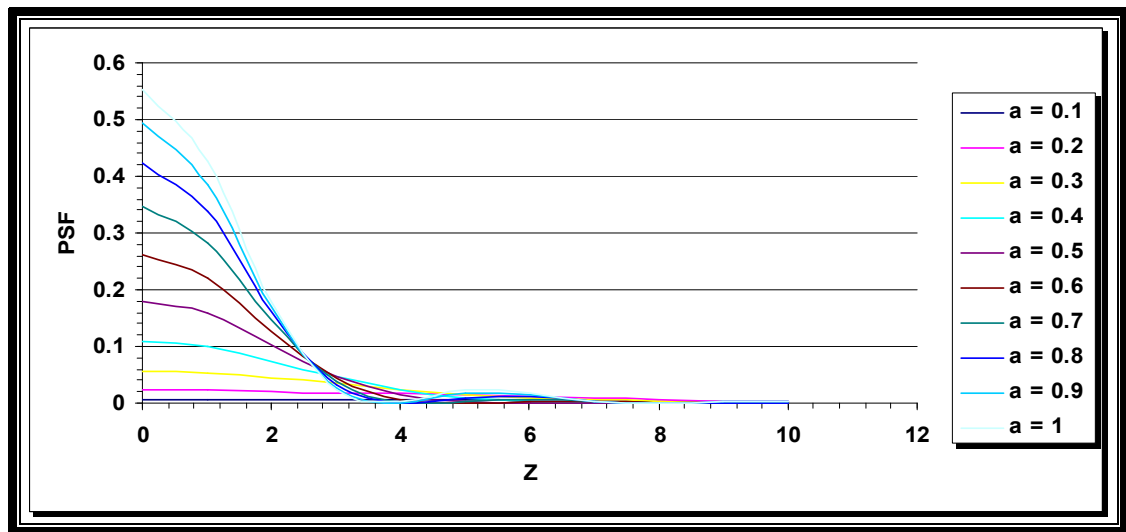


Figure (4 - 43): *Strehl* ratio for the optical system contains spherical aberration ( $W_{40} = 0.1 \lambda$ ) with super Gaussian filter & ( $\varepsilon = 0.5$ ).

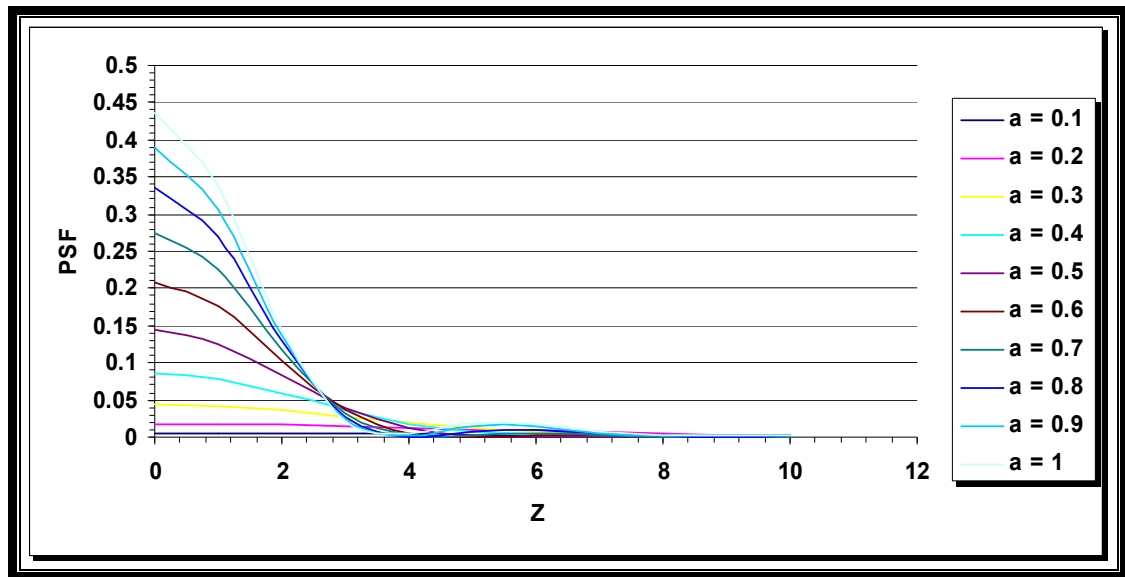


Figure (4 - 44): Strehl ratio for the optical system contains spherical aberration ( $W_{40} = 0.3 \lambda$ ) with super Gaussian filter & ( $\varepsilon = 0.5$ ).

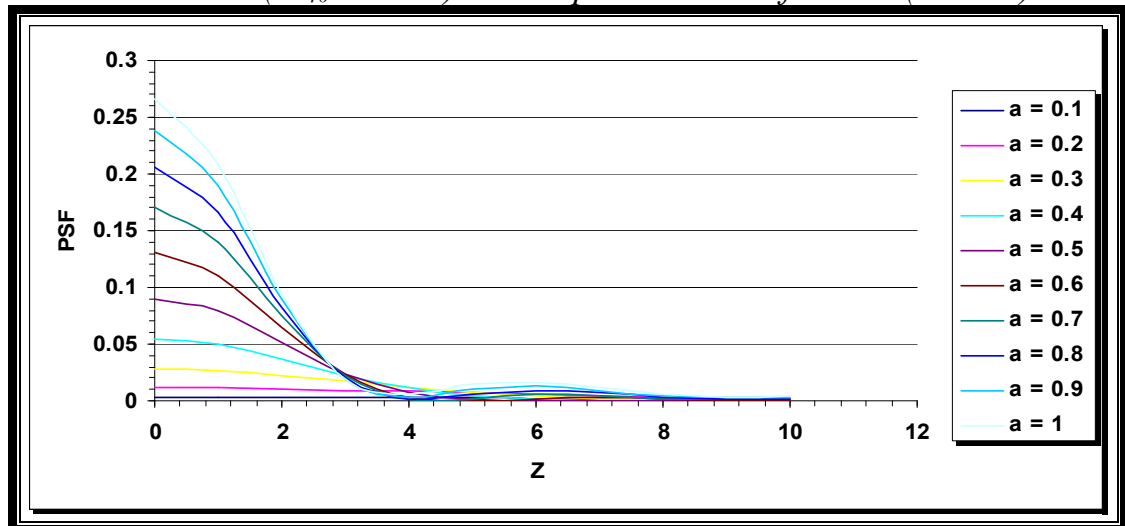


Figure (4 - 45): Strehl ratio for the optical system contains spherical aberration ( $W_{40} = 0.5 \lambda$ ) with super Gaussian filter & ( $\varepsilon = 0.5$ ).

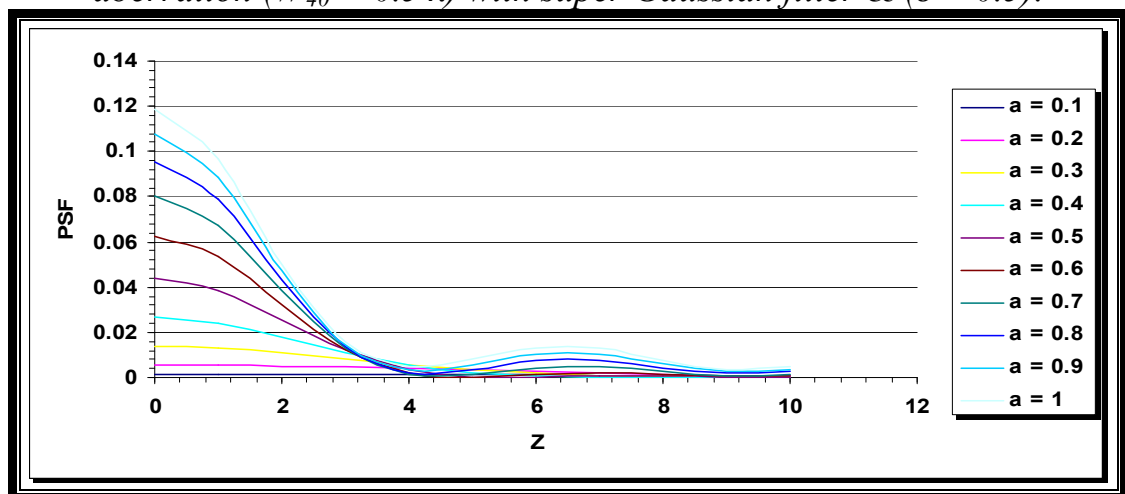


Figure (4 - 46): Strehl ratio for the optical system contain spherical aberration ( $W_{40} = 0.7 \lambda$ ) with super Gaussian filter & ( $\varepsilon = 0.5$ ).

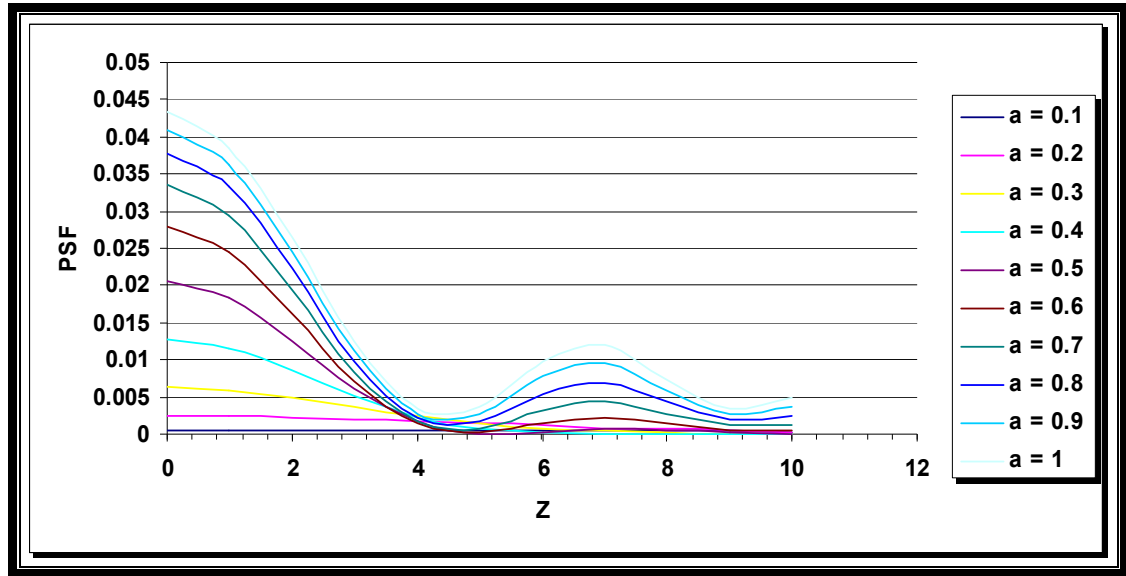


Figure (4 - 47): *Strehl ratio for the optical system contains spherical aberration ( $W_{40} = 0.9 \lambda$ ) with super Gaussian filter & ( $\epsilon = 0.5$ ).*

#### 4.18 Effect of the Width Factor of Super Gaussian Filter on Strehl Ratio for the Obstructed Optical System ( $\epsilon=0.8$ ) Contains Spherical Aberration ( $W_{40}=0.1, 0.3, 0.5, 0.7, \& 0.9 \lambda$ )

Figures (4-48-52) which are drawn from the data that are extracted from equation (3-10) represented **Strehl** ratio for the obstructed optical system ( $\epsilon=0.8$ ) and contain spherical aberration ( $W_{40}=0.1, 0.3, 0.5, 0.7$ , and  $0.9 \lambda$ ). **Strehl** ratio is maximum in all figures when the width factor ( $a=1$ ) and is the minimum value when the width factor ( $a=0.1$ ). The presence of spherical aberration reduces **Strehl** ratio, and the reduction in the width factor of the super Gaussian filter also reduces **Strehl** ratio.

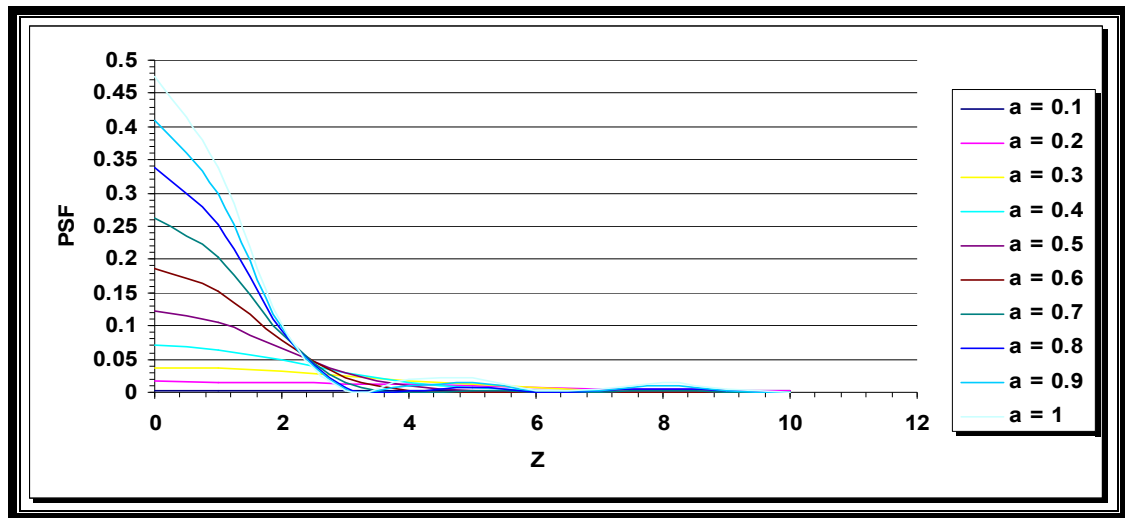


Figure (4 - 48): Strehl ratio for the optical system contains spherical aberration ( $W_{40} = 0.1 \lambda$ ) with super Gaussian filter & ( $\varepsilon = 0.8$ )

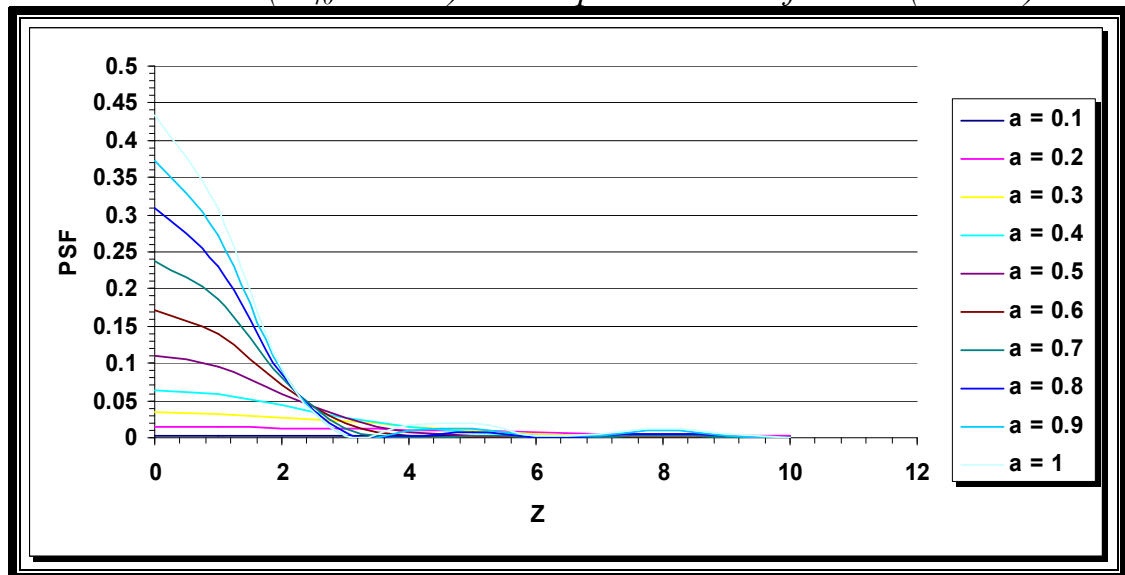


Figure (4 - 49): Strehl ratio for the optical system contains spherical aberration ( $W_{40} = 0.3 \lambda$ ) with super Gaussian filter & ( $\varepsilon = 0.8$ ).

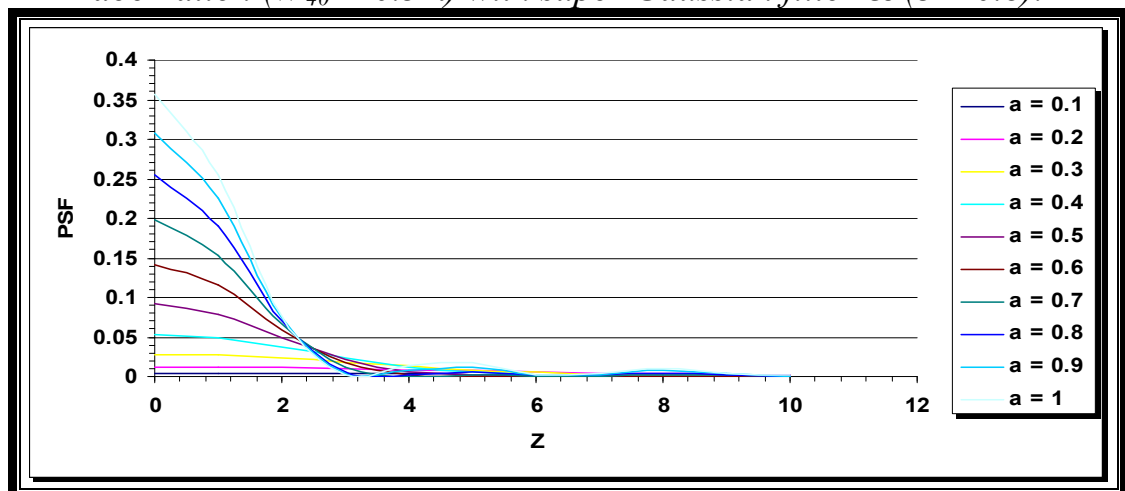


Figure (4 - 50): Strehl ratio for the optical system contains spherical aberration ( $W_{40} = 0.5 \lambda$ ) with super Gaussian filter & ( $\varepsilon = 0.8$ ).

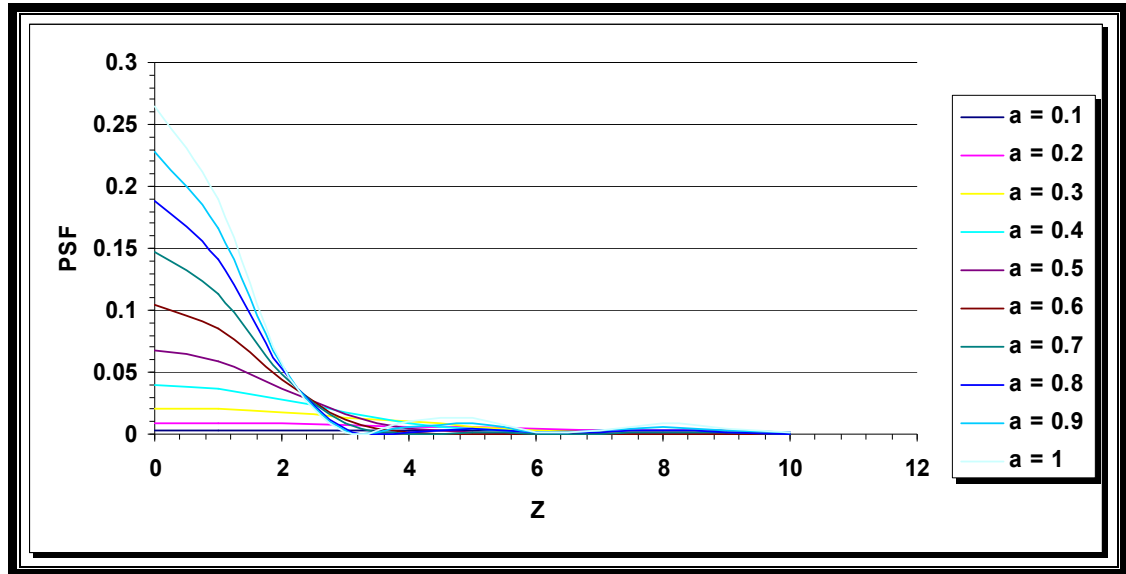


Figure (4 - 51): Strehl ratio for the optical system contains spherical aberration ( $W_{40} = 0.7 \lambda$ ) with super Gaussian filter & ( $\varepsilon = 0.8$ ).

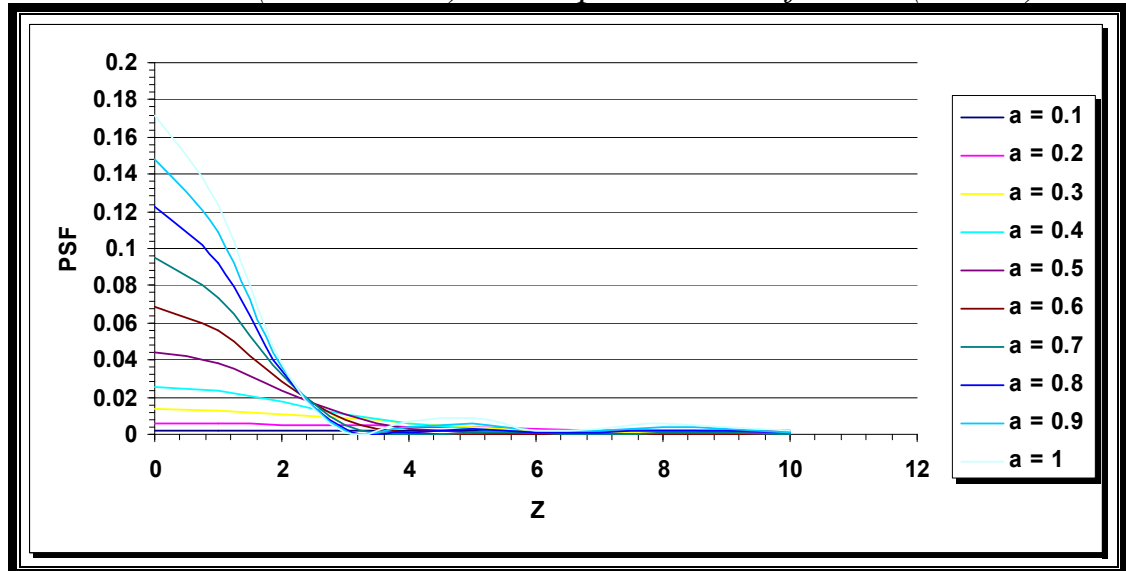


Figure (4 - 52): Strehl ratio for the optical system contains spherical aberration ( $W_{40} = 0.9 \lambda$ ) with super Gaussian filter & ( $\varepsilon = 0.8$ ).



#### 4.19 Conclusions

1. The programs that are used to compute the PSF were correct because the values of free aberration PSF of annular aperture were in agreement with the numerical analytical values.
2. The presence of aberration causes the peak of the PSF to be less, and when the amount of aberration is increased the peak is decreased.
3. The resolution of the optical system increased with the increased of the value of the width factor of the super Gaussian filter, and the value of width factor between ( $a=0.5$  to  $1$ ) considers as best values in comparison with width factor ( $a=0.1$  Or  $0.2$ ).
4. *Strehl* ration decreases with the decrease of the width factor and with the increase of value of the focus error and spherical aberration.
5. The obstruction ratio ( $\epsilon=0.5$ ) is acceptable from the practical state when the optical system contains annular aperture because the intensity in the secondary peak is increased with the increased of the obstruction ratio which means the loss in a central intensity and which appears in the secondary tops.
6. Role of the Gaussian filter for improving the diffraction pattern and for different obstruction ratio depends on the amount and quantity of the aberration existing in the optical system.
7. The band width of PSF in all the figures increases with the decrease of width factor and with the increased of focus error and spherical aberration.

#### ***4.20 Suggestions for Future Work***

For future work, we suggest the following research:

- 1.*** Studying the present work with different amount of aberrations.
- 2.*** Studying the present work with another filter.
- 3.*** Studying the present work with non centering obstruction.

## *Creek symbols*

<i>symbol</i>	<i>Meaning</i>
$\beta$	<i>Depth of modulation</i>
$\delta$	<i>Depth of focus</i>
$\varepsilon$	<i>Obstruction</i>
$\lambda$	<i>Wavelength</i>
$(\xi, \eta)$	<i>Cartesian coordinates in the object plane</i>
$(\xi', \eta')$	<i>Cartesian coordinates in the image plane</i>
$\tau(x, y)$	<i>Transmission function</i>
$\theta$	<i>Phase difference in the pupil plane due to aberration</i>
$\Psi$	<i>the angle in polar coordinates</i>

# List of Figures

Figure	List of Figures	Page
<b>Chapter One</b>		
Figure(1-1)	Star test	3
Figure (1-2)	Twyman-Green interferometer	4
Figure (1-3)	The optical transfer function	5
Figure (1-4)	Airy disk, energy distribution and appearance	6
Figure (1-5)	The original coordinates and rotational coordinates	7
Figure (1-6)	Spherical aberration	9
Figure (1-7)	Coma aberration.	10
Figure (1-8)	Astigmatism aberration.	12
Figure (1-9)	Field curvature	12
Figure (1-10)	Distortion aberration.	13
Figure (1-11)	Chromatic aberration.	14
Figure (1-12)	Raleigh's and Dawes criterions	20
<b>Chapter Two</b>		
Figure (2-1)	Optical axes, object plane, entrance pupil, exit pupil, image plane	25
Figure (2-2)	Diffraction image of a point source	25
Figure (2-3)	The intensity in image plane	33
Figure (2-4)	Annular aperture.	35
Figure (2-5)	Super Gaussian filter with various widths.	41
<b>Chapter Three</b>		
Figure (3-1)	Integral limits for circular aperture with optimal Gauss points distribution in exit pupil	48
<b>Chapter Four</b>		
Figure (4-1)	Effect of the obscuration ratio on the free optical system.	56

<b>Figure (4-2)</b>	<b><i>Effect of the obscuration on the optical system contains focus error (<math>W_{20}=0.25 \lambda</math>).</i></b>	<b>57</b>
<b>Figure (4-3)</b>	<b><i>Effect of the obscuration on the optical system contains focus error (<math>W_{20}=0.5 \lambda</math>).</i></b>	<b>57</b>
<b>Figure (4-4)</b>	<b><i>Strehl ratio for the free optical system contains super Gaussian filter &amp; (<math>\epsilon = 0</math>).</i></b>	<b>58</b>
<b>Figure (4-5)</b>	<b><i>Point spread function for the free optical system contains super Gaussian filter&amp; (<math>\epsilon = 0</math>).</i></b>	<b>59</b>
<b>Figure (4-6)</b>	<b><i>Strehl ratio for the optical system contains focus error (<math>W_{20} = 0.25 \lambda</math>) with super Gaussian filter &amp; (<math>\epsilon = 0</math>).</i></b>	<b>61</b>
<b>Figure (4 - 7)</b>	<b><i>Strehl ratio for the optical system contains focus error (<math>W_{20} = 0.5 \lambda</math>) with super Gaussian filter &amp; (<math>\epsilon = 0</math>).</i></b>	<b>61</b>
<b>Figure (4 - 8)</b>	<b><i>Strehl ratio for the optical system contains focus error (<math>W_{20} = 0.75 \lambda</math>) with super Gaussian filter &amp; (<math>\epsilon = 0</math>).</i></b>	<b>62</b>
<b>Figure (4 - 9)</b>	<b><i>Point spread function for the optical system contains focus error (<math>W_{20} = 0.25 \lambda</math>) with super Gaussian filter &amp; (<math>\epsilon = 0</math>).</i></b>	<b>64</b>
<b>Figure (4-10)</b>	<b><i>Point spread function for the optical system contains focus error (<math>W_{20} = 0.5 \lambda</math>) with super Gaussian filter &amp; (<math>\epsilon = 0</math>).</i></b>	<b>64</b>
<b>Figure(4-11)</b>	<b><i>Point spread function for the optical system contains focus error (<math>W_{20} = 0.75 \lambda</math>) with super Gaussian filter &amp; (<math>\epsilon = 0</math>).</i></b>	<b>64</b>
<b>Figure(4-12)</b>	<b><i>Point spread function for the optical system contains spherical aberration (<math>W_{40} = 0.1 \lambda</math>) with super Gaussian filter &amp; (<math>\epsilon = 0</math>).</i></b>	<b>66</b>
<b>Figure(4-13)</b>	<b><i>Point spread function for the optical system contains spherical aberration (<math>W_{40} = 0.3 \lambda</math>) with super Gaussian filter &amp; (<math>\epsilon = 0</math>).</i></b>	<b>67</b>
<b>Figure(4-14)</b>	<b><i>Point spread function for the optical system contains spherical aberration (<math>W_{40} = 0.5 \lambda</math>) with super Gaussian filter &amp; (<math>\epsilon = 0</math>).</i></b>	<b>67</b>
<b>Figure(4-15)</b>	<b><i>Point spread function for the optical system contains spherical aberration (<math>W_{40} = 0.7 \lambda</math>) with super Gaussian filter &amp; (<math>\epsilon = 0</math>).</i></b>	<b>67</b>

<b>Figure(4-16)</b>	<b><i>Point spread function for the optical system contains spherical aberration (<math>W_{40} = 0.9 \lambda</math>) with super Gaussian filter &amp; (<math>\epsilon = 0</math>).</i></b>	<b>68</b>
<b>Figure(4-17)</b>	<b><i>Strehl ratio for the optical system contains spherical aberration (<math>W_{40} = 0.1 \lambda</math>) with super Gaussian filter &amp; (<math>\epsilon = 0</math>).</i></b>	<b>69</b>
<b>Figure(4-18)</b>	<b><i>Strehl ratio for the optical system contains spherical aberration (<math>W_{40} = 0.3 \lambda</math>) with super Gaussian filter &amp; (<math>\epsilon = 0</math>)</i></b>	<b>69</b>
<b>Figure(4-19)</b>	<b><i>Strehl ratio for the optical system contains spherical aberration (<math>W_{40} = 0.5 \lambda</math>) with super Gaussian filter&amp; (<math>\epsilon = 0</math>).</i></b>	<b>69</b>
<b>Figure(4-20)</b>	<b><i>Strehl ratio for the optical system contains spherical aberration (<math>W_{40} = 0.7 \lambda</math>) with super Gaussian filter &amp; (<math>\epsilon = 0</math>).</i></b>	<b>70</b>
<b>Figure(4-21)</b>	<b><i>Strehl ratio for the optical system contains spherical aberration (<math>W_{40} = 0.9 \lambda</math>) with super Gaussian filter&amp; (<math>\epsilon = 0</math>).</i></b>	<b>70</b>
<b>Figure(4-22)</b>	<b><i>Strehl ratio for the optical system contains optimum balance value (<math>W_{20}=-1, W_{40}=1</math>) <math>\lambda</math> with super Gaussian filter&amp; (<math>\epsilon = 0</math>).</i></b>	<b>71</b>
<b>Figure(4-23)</b>	<b><i>Strehl ratio for the optical system contains optimum balance value (<math>W_{20}=-1.04 W_{40}=1</math>) <math>\lambda</math> with super Gaussian filter&amp; (<math>\epsilon = 0.2</math>).</i></b>	<b>72</b>
<b>Figure(4-24)</b>	<b><i>Strehl ratio for the optical system contains optimum balance value (<math>W_{20}=-1.25, W_{40}=1</math>) <math>\lambda</math> with super Gaussian filter &amp; (<math>\epsilon = 0.5</math>).</i></b>	<b>72</b>
<b>Figure(4-25)</b>	<b><i>Strehl ratio for the optical system contains optimum balance value (<math>W_{20}=-1.64, W_{40}=1</math>) <math>\lambda</math> with super Gaussian filter&amp; (<math>\epsilon = 0.8</math>).</i></b>	<b>73</b>
<b>Figure(4-26)</b>	<b><i>Strehl ratio for free optical system contains super Gaussian filter &amp; (<math>\epsilon = 0.2</math>).</i></b>	<b>74</b>
<b>Figure(4-27)</b>	<b><i>Strehl ratio for the free optical system contains super Gaussian filter &amp; (<math>\epsilon = 0.5</math>).</i></b>	<b>74</b>
<b>Figure(4-28)</b>	<b><i>Strehl ratio for the free optical system contains super Gaussian filter &amp; (<math>\epsilon = 0.8</math>).</i></b>	<b>74</b>
<b>Figure(4-29)</b>	<b><i>Strehl ratio for the optical system contains focus error (<math>W_{20} = 0.25 \lambda</math>) with super Gaussian filter &amp; (<math>\epsilon = 0.2</math>).</i></b>	<b>75</b>

<b>Figure(4-30)</b>	<b><i>Strehl ratio for the optical system contains focus error (<math>W_{20} = 0.5 \lambda</math>) with super Gaussian filter &amp; (<math>\epsilon = 0.2</math>).</i></b>	<b>76</b>
<b>Figure(4-31)</b>	<b><i>Strehl ratio for the optical system contains focus error (<math>W_{20} = 0.75 \lambda</math>) with super Gaussian filter &amp; (<math>\epsilon = 0.2</math>).</i></b>	<b>76</b>
<b>Figure(4-32)</b>	<b><i>Strehl ratio for the optical system contains focus error (<math>W_{20} = 0.25 \lambda</math>) with super Gaussian filter &amp; (<math>\epsilon = 0.5</math>).</i></b>	<b>77</b>
<b>Figure(4-33)</b>	<b><i>Strehl ratio for the optical system contains focus error (<math>W_{20} = 0.5 \lambda</math>) with super Gaussian filter &amp; (<math>\epsilon = 0.5</math>).</i></b>	<b>77</b>
<b>Figure(4-34)</b>	<b><i>Strehl ratio for the optical system contains focus error (<math>W_{20} = 0.75 \lambda</math>) with super Gaussian filter &amp; (<math>\epsilon = 0.5</math>).</i></b>	<b>78</b>
<b>Figure(4-35)</b>	<b><i>Strehl ratio for the optical system contains focus error (<math>W_{20} = 0.25 \lambda</math>) with super Gaussian filter &amp; (<math>\epsilon = 0.8</math>).</i></b>	<b>79</b>
<b>Figure(4-36)</b>	<b><i>Strehl ratio for the optical system contains focus error (<math>W_{20} = 0.5 \lambda</math>) with super Gaussian filter &amp; (<math>\epsilon = 0.8</math>).</i></b>	<b>79</b>
<b>Figure(4-37)</b>	<b><i>Strehl ratio for the optical system contains focus error (<math>W_{20} = 0.75 \lambda</math>) with super Gaussian filter &amp; (<math>\epsilon = 0.8</math>).</i></b>	<b>79</b>
<b>Figure(4-38)</b>	<b><i>Strehl ratio for the optical system contains spherical aberration (<math>W_{40} = 0.1 \lambda</math>) with super Gaussian filter &amp; (<math>\epsilon = 0.2</math>).</i></b>	<b>80</b>
<b>Figure(4-39)</b>	<b><i>Strehl ratio for the optical system contains spherical aberration (<math>W_{40} = 0.3 \lambda</math>) with super Gaussian filter &amp; (<math>\epsilon = 0.2</math>).</i></b>	<b>80</b>
<b>Figure(4-40)</b>	<b><i>Strehl ratio for the optical system contains spherical aberration (<math>W_{40} = 0.5 \lambda</math>) with super Gaussian filter &amp; (<math>\epsilon = 0.2</math>).</i></b>	<b>81</b>
<b>Figure(4-41)</b>	<b><i>Strehl ratio for the optical system contains spherical aberration (<math>W_{40} = 0.7 \lambda</math>) with super Gaussian filter &amp; (<math>\epsilon = 0.2</math>).</i></b>	<b>81</b>
<b>Figure(4-42)</b>	<b><i>Strehl ratio for the optical system contains spherical aberration (<math>W_{40} = 0.9 \lambda</math>) with super Gaussian filter &amp; (<math>\epsilon = 0.2</math>).</i></b>	<b>81</b>

<b>Figure(4-43)</b>	<b><i>Strehl ratio for the optical system contains spherical aberration (<math>W_{40} = 0.1 \lambda</math>) with super Gaussian filter &amp; (<math>\epsilon = 0.5</math>).</i></b>	<b>82</b>
<b>Figure(4-44)</b>	<b><i>Strehl ratio for the optical system contains spherical aberration (<math>W_{40} = 0.3 \lambda</math>) with super Gaussian filter &amp; (<math>\epsilon = 0.5</math>).</i></b>	<b>82</b>
<b>Figure(4-45)</b>	<b><i>Strehl ratio for the optical system contain spherical aberration (<math>W_{40} = 0.5 \lambda</math>) with super Gaussian filter &amp; (<math>\epsilon = 0.5</math>).</i></b>	<b>83</b>
<b>Figure(4-46)</b>	<b><i>Strehl ratio for the optical system contain spherical aberration (<math>W_{40} = 0.7 \lambda</math>) with super Gaussian filter &amp; (<math>\epsilon = 0.5</math>).</i></b>	<b>83</b>
<b>Figure(4-47)</b>	<b><i>Strehl ratio for the optical system contains spherical aberration (<math>W_{40} = 0.9 \lambda</math>) with super Gaussian filter &amp; (<math>\epsilon = 0.5</math>).</i></b>	<b>83</b>
<b>Figure(4-48)</b>	<b><i>Strehl ratio for the optical system contains spherical aberration (<math>W_{40} = 0.1 \lambda</math>) with super Gaussian filter &amp; (<math>\epsilon = 0.8</math>).</i></b>	<b>84</b>
<b>Figure(4-49)</b>	<b><i>Strehl ratio for the optical system contains spherical aberration (<math>W_{40} = 0.3 \lambda</math>) with super Gaussian filter &amp; (<math>\epsilon = 0.8</math>).</i></b>	<b>85</b>
<b>Figure(4-50)</b>	<b><i>Strehl ratio for the optical system contains spherical aberration (<math>W_{40} = 0.5 \lambda</math>) with super Gaussian filter &amp; (<math>\epsilon = 0.8</math>).</i></b>	<b>85</b>
<b>Figure(4-51)</b>	<b><i>Strehl ratio for the optical system contains spherical aberration (<math>W_{40} = 0.7 \lambda</math>) with super Gaussian filter &amp; (<math>\epsilon = 0.8</math>).</i></b>	<b>85</b>
<b>Figure(4-52)</b>	<b><i>Strehl ratio for the optical system contains spherical aberration (<math>W_{40} = 0.7 \lambda</math>) with super Gaussian filter &amp; (<math>\epsilon = 0.8</math>).</i></b>	<b>86</b>



1. V.Gerbic , A.W.Lohman . Applied. Optics, Vol.28, No.24, P.5198, (1989)
2. R. Kingslake. Applied. Optics and Optical Engineering, Vol.3, P.183, (1965) .
3. K.S. Kapany, J .J. Burke. J. Optics .Soc. Am., Vol.52, No.12, P.1351, (1962).
4. Ali H. Al-Hamdani.,Ph.D.Thesis "*Numerical Evaluation of lenses Quality Using Computer Software*" Al-Mustansiriyah University"(1997).
5. M.J. Riedl, "*Optical Design Fundamentals for Infrared Systems*", 2nd ed., SPIE, the International Society for Optical Engineering, Bellingham, Washington, USA, (2001).
6. F. Twyman. Phil. Mag. Opt .Soc.(6)35,49,(1923).
7. M. Daniel, Optical shop testing, (Johnwileg and sons, (1978).
8. J. Woznick. M.,T. Henri, "*Motional Effect in Retardation Plates and Mode Locking in Ring Lasers*",J. Modren Optics, Vol.46, No.6,p.1031,(1999)
9. R.E. Fischer and B.Tadic-Galeb, "*Optical System Design*", McGraw - Hill,(2000).
- 10.R.D. Hudson, "*Infrared System Engineering*", John Wiley and Sons, (1969).
11. L.F. Pau, "*An Introduction to Infrared Imaging Acquisition and Classification Systems*", Research Studies Press LTD,(1983).
- 12.E.Hecht .Optics,3ed,Addition-sley Publishing company,(1998).
- 13.S.A. Habbana, "*Design and Evaluation of Image Quality for IR Scanner* ", Ph.D. Thesis, Military Collage of Engineering, Baghdad, Iraq, (2001).
14. C. S. Williams. O. A. Bechlund, Optics, short course for engineers & Scientists, John wilcy and Sons, Inc (1972).

- 
15. J.W. Blaker, "*Geometric Optics*", The Matrix Theory, Macel Dekker, Inc. New York, (1971).
  16. A.F. Jenkins. "*Fundamentals of Optics*" 4<sup>th</sup> ed. McGraw- Hill, (1957).
  17. B. Michael "*Hand Book of Optics*", 2nd ed. Vol.3. Mc-Graw Hill, (2000).
  18. J. M. Skjajlund, Applied. Optics. , Vol. 27, No. 12, P. 2580, (1988).
  19. L. Levi, Applied optics, A guide to Optical System Design Vol.1 (New York, John Willey & Sons Inc. ), (1968).
  20. R.R. Shannon, SPIE Vol.531, Geometrical optics p.27, (1985).
  21. J. Ojeda-Castaneda, L.B. Berriel-Valdos, and E-Montes, "*Spatial Filter for Increasing the Depth of Focus*" optic letters, Vol.10, pp520-522, (1985).
  22. A. Kourakos. "*Extended Depth-of-Focus in Laser Scanning System Employing a Synthesized Difference-of-Gaussians Pupil*" Msc. Thesis, Virginia Polytechnic Institute and State University, (1999).
  23. Lord Rayleigh, Scientific papers 1, 432 -435 (1899).
  24. A. Marechal, Rev.Opt. Vol.26, p. 257 (1947).
  25. V.N. Mahajan. Applied.Optics, Vol.22, No.19, p.3035, (1983).
  26. B. Michael, "*Hand Book of Optics*", 2nd ed. Vol.1. Mc-Graw Hill, (2000).
  27. W. Smith. "*Modern Optical Engineering*", McGraw- Hill, (2000).
  28. M. Born, E. Wolf, "*Principle of Optics*", 6th ed., Pergman, London, (1970).
  29. D.E. Stoltzman, Applied Optic and Optical Engineering, ed. By R.R. Shannon, (New York. Academic Press), Vol.9, (1983).
  30. R.E. Fischer and B. Tadic-Galeb, "*Optical System Design*", McGraw- Hill, (2000).
  31. S. Longhurs, "*Geometrical and Physics Optics*", 3rd ed, p.254, (1973).

- 
32. Lord Rayleigh, scientific papers (1899).
  33. R. Barakat, J. Am. Opt. Soc., "*Symmetry properties with pupil phase-filters*", Opt. Soc. Vol. 69, No. 9, p. 1311 (1979).
  34. E. L. O'Neill, J. Opt. Soc. Am. p. 285, (1956).
  35. H. H. Hopkins, J. Modern Optics, Vol. 34, No. 3, p. 371, (1987).
  36. R. E. Stephens, L. E. Sutton, J. Opt. Soc. Am. p. 1001, (1968).
  37. V. N. Mahajan, Applied Optics, Vol. 22, No. 19, p. 3035, (1983).
  38. E. H. Linfoot, E. Wolf, Proc. Phys. Soc. (London), P. 145, (1953).
  39. V. Mahajan, "*Internal reflections in balance reflection holograms*", J. Opt. Soc. Am. Vol. 71, No. 1, p. 75 (1981).
  40. E. L. O'Neill & Walther, "Total Absorption of Light by a Sinusoidal Grating Near Grazing Incidence" A, J. Opt. Soc. Am, (1977).
  41. T. C. Poon, "*Deflection of Barium Atoms by a Standing-Wave Light Field Article*", Optics Communications, Vol. 65, No. 6, P. 401, (1988).
  42. V. Gerbig, A. Lohman, W., Applied Optics is a custom manufacturer of laser quality optical lenses Applied Optics, Vol. 28, No. 24, p. 5198, (1989).
  43. K. Strehl, "*Theoretical Diffraction*", (1894).
  44. H. H. Hopkins, Jpn. J. Appl. Phys. 4, suppl. P. 31-35 (1965).
  45. R. Barakat, and M. V. Morello, "*Intensity Extreme in Optically Injected Fabry-Perot Cavities with Saturable Gain*", J. Opt. Soc. Am., (1964).
  46. R. Barakat, "*Imaging Performance of Annular Apertures Apodization and Point Spread Function*" J. Opt. Soc. Am, Vol. 55, No. 7, p. 878, (1966).
  47. A. Marechal, Rev. Opt, (1947).
  48. R. K. Luneburg, "*Mathematical Theory of Optics*", U. California press, Berkeley, 2nd ed, p. 349, (1966).

- 
- 49.R. Barakat, "*Solution of the Luneburg Apodization Programs*", J.Opt.Soc.Am. Vol.52, p.264, (1962).
- 50.J.J .Stamne. , "*Focusing of a Perfect wave and the Airy Pattern Formula*", submitted to opt.Comm,(1988).
- 51.Forskin, "*Luneburg Apodization Problem in the non Paraxial Domain Central Institute for Industrial*", Vol.11, No.26, p.2230 (1980).
- 52.R. BRM. , "*Indian Journal of Pure and Applied System*", Vol.31, No.11, (1993).
- 53.K. L. Reddy, "*Resolution Studies of Apodized Optical System in Coherent Illumination*", Indian Journal of Pure and Applied Physics Vol.33, No.7, p.380 (1995).
- 54.V.L .RAO, "*Effect of Apodization on the Peak Intensity Ratio in the Images of 2-Point Objects*", Indian Journal of Pure and Applied Physics Vol.33, No.2, p.97 (1995).
- 55.R. BRM. , "*Modulation of Rectangular and Triangular Bar Targets by Optical System Using Humming Filters*", Defense science journal, Vol.47, 2, p.217, (1997).
- 56.J .Camps, J.C .Escalera and M.J .Yzuel, "*Symmetry Properties with Pupil Phase-Filter*", optics express, Vol.12, No11
- 57.V.N. Mahajan. Applied. Optics, Vol.17, No.6, p.964, (1978).
- 58.W.H. Steel Rev. Opt., Vol. 32, No. 4, p.143, (1953).
- 59.W.T. Wellford, Josa, Vol.50, No.8, p. 749, (1960).
- 60.H.F.A. Tschunko. Applied Optics, Vol.22, No.9, p.1413, (1983).
- 61.J. Ojeda-castaneda. Applied Optics, Vol.27, No.24, p. 5140, (1992).
- 62.F.Al-Jebory.Adnan, Ph.D. Thesis, "*Improvement Resolution Power of Optical System Design by Using Circular Synthetic Aperture*", [Al-Mustansiriyah University], (2004).

- 
- 63.M.Abramowitz, I.A. Stegun, "*Hand Book of Mathematical Functions*"(Dover Pub.,New York,( 1965).

## الخلاصة

تتضمن الانظمة البصرية عموماً فتحة دائرية و العناصر البصرية وهكذا انضمة تحتوي على حدود دائرية . من هنا تمثل هذه الحدود ايضاً فتحة دائرية في التصنيع و الاختبار. لهذا ليس كل مثال لنظام بدون فتحة دائرية هو تلسكوب كاسيكرينين (Cassegrainian telescope) و الذي يحتوي على فتحة دائرية حلقة (Annular pupil).

الزويغ و التباين لنظام يحتوي على فتحة حلقة تختلف عن تلك التي فيها فتحة دائرية ، أيضاً كمية الخطأ البؤري التي توازن الزيغ الكروي، الذي يحدث او يسبب تباين اقل في الفتحة الحلقة تختلف عن تلك التي للفتحة الدائرية.

على الرغم من ان السعة خلال البؤبؤ تكون منتظمة في العديد من التطبيقات البصرية, فإن الحالة ليست هكذا دائماً ومثال على ذلك المنظومة ذات الفتحة المحسنة (Apodized pupil). الفتحة الكاوسية (Gaussian pupil) هي مثال على الفتحة المحسنة عندما تكون السعة عبر البؤبؤ ذات شكل كاوسي وهذا ناتج من اما لوجود مرشح السعة الموضوع عند البؤبؤ او لكون الموجة الساقطة على البؤبؤ كاوسية الشكل كما هي الحالة في الحزم الكاوسية. ايضاً التباين وموازنة الزيغ للفتحة الكاوسية تكون ذات شكل مختلف عن موازنة الزيغ لمقابلة لها للفتحة المنتظمة.

في هذا البحث وضعت مرشحات كاوسية محسنة مختلفة امام الفتحة الحلقة وتم استخدام نسب اعاقه مختلفة للمرأة الثانوية ( $\epsilon = 0, 0.1, 0.2, 0.3, 0.4, 0.5, 0.6, 0.7, 0.8, 0.9$ ).

تم اشتقاق صيغة لدالة الانتشار النقطية لنظام معاق و احتسابها عددياً باستخدام طريقة كاوس التربيعية. وقد تم كتابة برامج بلغة Q.Basic لحساب دالة الانتشار النقطية لنسب اعاقه مختلفة و كميات مختلفة من الزيغ. اظهرت النتائج الاعتماد الكبير لدالة الانتشار النقطية ونسبة ستريل على نوع المرشح الكاوسي و كمية الزيغ في الانظمة البصرية الحلقة.

# *List of Abbreviations*

<i>symbol</i>	<i>Meaning</i>
<b>a</b>	<i>Width of the super Gaussian filter</i>
<b>A'</b>	<i>Area of the exit pupil</i>
<b>A(u,v)</b>	<i>Amplitude point spread function</i>
<b>B<sub>ang</sub></b>	<i>Angular diameter of Airy disk</i>
<b>B<sub>diff</sub></b>	<i>Airy disk diameter</i>
<b>CTF</b>	<i>Contrast transfer function</i>
<b>DSF</b>	<i>Disk spread function</i>
<b>f</b>	<i>Focal length</i>
<b>(f/#)</b>	<i>Focal number</i>
<b>f(x',y')</b>	<i>Pupil function</i>
<b>I<sub>max</sub></b>	<i>Maximum intensity</i>
<b>I<sub>min</sub></b>	<i>Minimum intensity</i>
<b>J<sub>1</sub>( )</b>	<i>Bessel function of the first kind</i>
<b>k</b>	<i>Wave number</i>
<b>LSF</b>	<i>Line spread function</i>
<b>n</b>	<i>Index of refraction</i>
<b>N</b>	<i>Normalization factor</i>
<b>OTF</b>	<i>Optical transfer function</i>
<b>P</b>	<i>polar distance from the plane center</i>
<b>PSF</b>	<i>Point spread function</i>
<b>S</b>	<i>Resolution (Separation of two points in the image plane )</i>
<b>S.R</b>	<i>Strehl ratio</i>
<b>(u,v)</b>	<i>Reduced coordinates in the object plane</i>
<b>(u',v')</b>	<i>Reduced coordinates in the image plane</i>
<b>V</b>	<i>Variance</i>
<b>W(x,y)</b>	<i>Aberration function</i>
<b>W<sub>i</sub></b>	<i>Gaussian weigh values</i>
<b>(x',y')</b>	<i>The coordinates of the exit pupil function</i>